RF-Induced Transport of Resonant Minority Species in ICRF-Heated Tokamaks

by

Luigi Vacca

Submitted to the Department of Nuclear Engineering
in partial fulfillment of the requirements for the degree of

Doctor of Philosophy in Nuclear Engineering

at the

MASSACHUSETTS INSTITUTE OF TECHNOLOGY

March 1996

Author .....
Department of Nuclear Engineering
March 1, 1996

Certified by .....
Abraham Bers
Professor
Thesis Supervisor

Read by .....
Jeff Freidberg
Professor
Thesis Reader

Accepted by .....
Chairman
Chairman Nuclear Engineering Department

RF-Induced Transport of Resonant Minority Species in ICRF-Heated Tokamaks

by

Luigi Vacca

Submitted to the Department of Nuclear Engineering
on March 1, 1996, in partial fulfillment of the
requirements for the degree of
Doctor of Philosophy in Nuclear Engineering

Abstract

This thesis examines wave-induced minority species transport in ion cyclotron radiofrequency heated tokamak plasmas. ICRF heating generates highly energetic non-Maxwellian tails in the resonant minority ion distribution function. Because of the increase in perpendicular energy of minority ions due to cyclotron resonance interaction, most resonant minority particles are trapped with large banana-width orbits. Fast ion orbits are studied in detail using the guiding-center theory formalism. An area-preserving set of guiding-center equations is derived for computational study. Moreover, a new set of coordinates for trapped particles is introduced to examine the phase space distribution of barely confined particles. Diffusion coefficients for resonant particles in full phase space are computed analytically. They show that RF-induced convection due to asymmetric spectrum is usually much larger than the RF-induced diffusion for symmetric spectra. A different mechanism of transport that does not involve change in parallel momentum is also studied for the interesting case of barely confined particles. This type of transport applies mainly to energetic trapped particles whose banana widths are comparable to the minor radius of the tokamak. Phase space diffusion coefficients are used to estimate the radial displacement of the trapped particle orbit. Fluxes that arise from this transport are larger than the neoclassical fluxes and RF-induced fluxes due to ICW asymmetric spectra. This thesis also shows that the particle and energy loss rates are fairly independent of the RF power for peaked RF power profiles and large confinement parameters.

Thesis Supervisor: Abraham Bers
Title: Professor

Acknowledgments

I would like to start by thanking my advisor, Professor Abraham Bers, for his constructive criticism and advice throughout this thesis. He taught me how important it is to be rigorous and precise in a research endeavor. A special thanks goes to Abhay Ram and Steve Schultz for their continuous feedback on the material I have presented in our intensive meetings. I would also like to thank the Nuclear Engineering Department at MIT for enhancing my scientific knowledge. Among professors, I would like to thank Professor J. Freidberg, whose teaching is rivalled only by his personal qualities. In the past, I have enjoyed discussions with Professor B. Coppi, P. Catto, J. Kesner and C. Hsu. During the almost seven years that I have spent at MIT I have had the privilege of meeting wonderful people and making great friends. In particular, I would like to mention Derin Ernst, Riccardo Betti, Chris Texeirera, Eugene Turnow, Eric Cushing, Paul Morin and Ed Miech. I wish to thank my parents for their unconditional love and support in my efforts to survive and prosper in a foreign country. The presence of my girlfriend, Cheryl Grace, was instrumental in helping me overcome the moments of discouragement that I experienced during the last two years. Last but not least, I would like to dedicate this thesis to the memory of my deceased grandfather, Carlo, who loved me in a way that words cannot describe.

Contents

Chapter 1

Introduction

1.1 Theoretical background and motivation

Plasma heating using radio-frequency electromagnetic waves has been proven to be one of the best means of auxiliary heating of tokamak plasmas in JET and TFTR experiments [1, 2]. This method uses waves in the ion cyclotron range of frequencies (ICRF) that resonate with the ion cyclotron frequency of one or two-ion species of the plasma. The energy directly absorbed by the ions is also delivered to the non-resonant particles through collisional damping. In particular, the two-ion hybrid regime is probably the most effective heating mechanism [3]. This regime is based on the resonant interaction of the fast magnetosonic wave with a small concentration of hydrogen (usually called the minority species) in a deuterium plasma. Theoretically, very little cyclotron absorption would be expected due to the right circular polarization of the fast wave in a single ion species plasma. However, the presence of a second ion species leads to an increment of the wave field rotating in the same direction of the ion gyration, namely the left circularly polarized component of the fast wave [4]. The result is that the minority species absorbs energy resonating at its fundamental frequency from the fast wave. It is important to remember that the majority species (deuterium) also absorbs energy, but it does so at a frequency which is twice its fundamental frequency and therefore is less efficient by a factor of $(k_\perp \rho)^2$ [5]. If the relative concentration of the minority species is high, then the fast mode

can convert into a Bernstein wave near the two-ion hybrid layer and eventually deliver its energy through electron Landau damping [6].

There is another scenario where the minority concentration is low and wave absorption is dominated by the ion-cyclotron damping of the minority species. This scenario is assumed in this thesis. Resonant ions generally gain perpendicular energy through cyclotron interaction. By doing so, their orbits become more trapped and their banana widths becomes larger. In a strong RF heating regime collisions are not fast enough to prevent the formation of a minority tail. The very energetic minority ions are subject to transport mechanisms that are qualitatively different from those that govern the bulk ions and electrons. Such mechanisms are not fully understood and are being studied vigorously.

The goal of my thesis is to shed more light on several theoretical aspects of minority transport as well as to examine a different mechanism of transport. To begin, I examine the transport that originates directly from the wave-particle interaction (RF-driven transport). Furthermore, the strong perpendicular anisotropy of the minority distribution function will be taken into account. Lastly, the wide banana orbits also contribute to radial transport in a way that has not been thoroughly investigated before.

This thesis is essentially divided into five chapters. In the first chapter, I provide a general introduction to the problem of RF-induced transport in an ICRF-heated plasma. In the second chapter, I examine fast ion orbits using the guiding-center theory formalism. Their topological features need to be understood in detail before venturing into the realm of transport and confinement. In the third chapter, full phase space quasilinear coefficients are derived from first principles. The advantage of this approach is that the diffusion coefficients are a function of the invariants of motion and lend themselves to treating finite banana width effects. In the fourth chapter, I review the collision operator for fast minority ions. In the last chapter, I compute RF-induced particle and energy fluxes at the edge of the plasma and give suggestions for future research.

I have found that an effective loss of particles and energy is caused by diffusion in both parallel momentum and perpendicular energy in full phase space. Non-neoclassical particle and energy losses due to finite orbit effects and perpendicular velocity diffusion generally outsize neoclassical, parallel momentum diffusion driven transport in the trapped region for a minority species.

Since my reader may not be fully acquainted with some of the theoretical aspects of plasma physics, I wrote this thesis to be self-contained and as clear as possible. Text is accompanied by figures which appear in Appendix N. I hope that this thesis will be helpful and inspirational to researchers developing new ideas outside the usual paths in the challenging field of fusion plasma transport.

Chapter 2

Unperturbed Motion of Fast Ions in a Tokamak

2.1 Guiding center motion and adiabatic invariants

2.1.1 Introduction

The study of the transport and heating of ions requires an understanding of their unperturbed orbits. Charged particle motion can be conveniently studied in the framework of guiding center theory. The Larmor radii of charged particles in a Tokamak plasma are generally smaller than the average radius of curvature of the magnetic field. Hence, the charged particle motion is best described by the motion of its guiding-center position. The guiding-center formalism is based upon the small gyroradius expansion of the equations of motion and their gyrophase averaging. This theory has been developed and refined over the past thirty years. The works of Northrop, Morozov and Solovev deserve particular mention [7, 8]. More recently, Littlejohn [9] proved that the addition of second order terms in the guiding-center equations has the advantage of keeping the Hamiltonian structure intact. This thesis adopts Littlejohn's formalism to study the unperturbed motion of fast ions in a tokamak. It is

important to mention that Littlejohn also developed a guiding-center theory based on Lagrangian theory [10]. The two formulations are perfectly equivalent. We prefer the Hamiltonian formulation since it has been studied more thoroughly, especially with perturbation methods.

2.1.2 Guiding center Hamiltonian

The full unperturbed Hamiltonian for a charged particle in a magnetic field is

$$H = \frac{1}{2m}(\mathbf{p} - q\mathbf{A}(\mathbf{x}))^2 \tag{2.1}$$

where the canonical variables are $\mathbf{p}$ and $\mathbf{x}$, respectively, the particle momentum and the particle position [11].

The vector potential $\mathbf{A}$ refers to the total equilibrium magnetic field. The magnetic field is assumed to be time invariant and axisymmetric around the vertical axis to the equatorial plane of the tokamak. These assumptions are of fundamental importance to our treatment of unperturbed motion. Noether's theorem [11] guarantees the existence of invariants of motion for systems that are endowed with symmetry. Such invariants simplify the particle orbit study tremendously.

The next step is to introduce the particle velocity $\mathbf{v}$ defined as

$$\mathbf{v} = \frac{1}{m}(\mathbf{p} - q\mathbf{A}(\mathbf{x})) \tag{2.2}$$

The Hamiltonian in equation (2.1) is not a guiding-center Hamiltonian yet. To make use of the guiding-center Hamiltonian, new variables need to be introduced

Guiding-center position	parallel velocity	magnetic moment	gyrophase
$\mathbf{X_{gc}}$	$v_{\|\|}$	μ	ϕ_{gc}

These guiding-center variables are related to the particle position $\mathbf{x}$ and velocity $\mathbf{v}$ through a set of invertible transformations (see Appendix A for details). It has been shown [9] that our unperturbed Hamiltonian can be written in guiding-center variables as

$$H_0 = \frac{1}{2}mv_{\|}^2 + \mu B(\mathbf{X_{gc}}) + O(\epsilon^2) \tag{2.3}$$

where ϵ = gyroradius/(magnetic scale length) is a small parameter. In practical calculations, one truncates the Hamiltonian, neglecting terms that are quadratic or higher order in ϵ. The G.C. variables are a mixed combination of canonical and non-canonical variables. In fact, only the magnetic moment and the gyrophase can be regarded as canonical variables. The Poisson brackets for guiding-center variables are listed in Appendix B. Finally, the equations of motion can easily be derived by starting from equation (B.1), given the Hamiltonian in equation (2.3), the Poisson brackets in equations (B.3), (B.4) and (B.5), and making use of the chain differentiation rule. For further details we refer to the guiding-center treatment in Balescu [12].

In Appendix B, we derive the guiding-center equations of motion for a charged particle in a tokamak with circular flux-surfaces using an Hamiltonian method.

2.1.3 Guiding-center equations of motion

The guiding center equations of motion relative to the Hamiltonian in equation (2.3) are

$$\dot{\mathbf{X}}_{\mathbf{gc}} = \frac{1}{B^*}(v_{\|}\mathbf{B}^* + \epsilon\mathbf{b} \times \frac{\mu}{m}\nabla B) \tag{2.4}$$

$$\dot{v}_{\|} = \frac{\mathbf{B}^*}{mB^*} \cdot (-\mu\nabla B) \tag{2.5}$$

$$\dot{\mu} = 0 \tag{2.6}$$

and

$$\dot{\phi} = \frac{qB}{m} \tag{2.7}$$

The vector $\mathbf{B}^*$ has been defined in Appendix B. The full system has three degrees of freedom, and therefore, there are six scalar equations.

As established by previous research [7], the magnetic moment is an adiabatic invariant to all orders, because the gyrophase dependence of the guiding center Hamiltonian has been eliminated by a gyrophase-averaging method. Equations (2.4)-(2.7) satisfy two important properties [10]:

- conservation of an approximate energy $H_0 = \frac{1}{2}mv_{\|}^2 + \mu\mathbf{B}$ from (2.3)
- the existence of a Liouville's theorem for $\mathbf{B}^*$

In addition, the presence of B^* in the equations guarantees that toroidal angular momentum is conserved exactly in axisymmetric systems.

Our goal is to describe and study the motion of fast ions in a tokamak. This can be accomplished through direct integration of the equations of motion. An alternate and more efficient way to compute the full phase-space orbits is to use the Hamiltonian properties of our system. Instead of directly integrating the full set of equations of motion, one can write an algebraic equation that relates the radial coordinate to the poloidal angle starting from the invariants of motion. The solution of the algebraic equation gives the parallel and perpendicular velocities combined with the conservation of momentum, energy, and magnetic moment. Since the fields are assumed to be axisymmetric, the toroidal variable does not enter into the expressions of the velocities. The time dependence as well as the toroidal angle can be obtained by integrating the two respective equations of motion.

2.1.4 Normalized guiding-center equations in a tokamak

The radial and poloidal coordinates of a particle's trajectory in a tokamak can be computed from its constants of motion.

However, to determine the time it takes for a particle to move from one point to another in its path and to recover the toroidal angle position requires integration of the equations of motion for the unperturbed Hamiltonian. Here we derive such equations in a form that is suitable for both computational and analytical work. The equilibrium fields are assumed to be known and given *a priori*. They can be computed by solving the Grad-Shafranov equation for given pressure and current profiles. To make analytical work simpler, we adopt a simple tokamak geometry, where toroidal coordinates are (r, θ, ζ). The equations of motion are written in non-dimensional variables. The radial coordinate is normalized to the minor radius, where $x = r/a$.
The versor in the direction of the magnetic field is a flux-surface function

$$\mathbf{b}(x) = f(x)\mathrm{e}_\zeta + g(x)\mathrm{e}_\theta \tag{2.8}$$

where

$$\sqrt{f^2 + g^2} = 1 \tag{2.9}$$

The magnitude of the total magnetic field is

$$|B| = \frac{B_0}{hf} \tag{2.10}$$

where $h = 1 + x\frac{a}{R_0}cos\theta$ and B_0 is the toroidal magnetic field magnitude at $r = 0$.
Important vectorial identities for the magnetic field versor $\mathbf{b}$ in equation (2.8) in toroidal coordinates are listed in Appendix C.
We normalize time with respect to a standard bounce time defined as $t_b = \frac{R_0}{v_{th}}$.
The thermal velocity $v_{th} = \sqrt{2T/m}$ corresponds to the temperature of the majority ion species.

The normalized guiding-center equations for the poloidal and toroidal angles are respectively

$$\frac{d\theta}{d(t/t_b)} = A + B + C + D \tag{2.11}$$

and

$$\frac{d\zeta}{d(t/t_b)} = \frac{v_{\|th}}{hB^{**}}\frac{\mathbf{B}^* \cdot \mathbf{e}_\zeta}{B_0} + \frac{\mu}{2hB^{**}}\frac{1}{\omega_{c0}t_b}\frac{R_0}{a}\mathbf{b} \times a\frac{\nabla B}{B_0} \cdot \mathbf{e}_\zeta \tag{2.12}$$

where

$$A = v_{\|th}\frac{R_0}{a}\frac{1}{x}\frac{1}{B^{**}}\frac{g}{hf} \tag{2.13}$$

$$B = \frac{v_{\|th}^2}{xB^{**}}\frac{1}{\omega_{c0}t_b}(\frac{R_0}{a})^2[-\frac{fcos\theta}{h}\frac{a}{R_0} - f^*] \tag{2.14}$$

$$C = \frac{v_{\|th}}{x}\frac{\mu}{B^{**}}\frac{1}{4\omega_{c0}^2t_b^2}(\frac{R_0}{a})^3[g(\frac{gg^*}{x} + \frac{ff^*}{h}\frac{a}{R_0}cos\theta) + \tag{2.15}$$
$$-2\frac{f^2g^*}{h}\frac{a}{R_0}cos\theta - 2\frac{g^2g^*}{x} + \frac{\hat{b_0}f}{h}\frac{a}{R_0}cos\theta + f\hat{b_0^*} + f^*\hat{b_0}]$$

$$D = \frac{\mu}{x}\frac{1}{2B^{**}}(\frac{R_0}{a})^2\frac{1}{\omega_{c0}t_b}f[-\frac{cos\theta}{fh^2}\frac{a}{R_0} - \frac{f^*}{hf^2}] \tag{2.16}$$

$$\frac{\mathbf{B}^* \cdot \mathbf{e}_\zeta}{B_0} = \frac{1}{h} + \frac{v_{\|th}}{\omega_{c0} t_b} \frac{R_0}{a} [g^* + \frac{g}{x}] + \tag{2.17}$$
$$+\mu (\frac{1}{2\omega_{c0} t_b} \frac{R_0}{a})^2 [\frac{f g g^*}{x} - \frac{f^2 f^*}{h} \frac{a}{R_0} cos\theta - 2\frac{g^2 f^*}{x} - \frac{g \hat{b_0}}{x} - g^* \hat{b_0} - g \hat{b_0^*}]$$

and finally

$$\mathbf{b} \times a \frac{\nabla B}{B_0} \cdot \mathbf{e}_\zeta = g [\frac{cos\theta}{f h^2} \frac{a}{R_0} + \frac{f^*}{h f^2}] \tag{2.18}$$

The vectorial identities that yield equations (2.11) and (2.12) are listed in Appendices B, C and D. The normalized guiding-center equations for the poloidal and toroidal angles are computed by dotting equation (2.4) for the guiding-center position vector with the poloidal and toroidal unit vectors and dividing the result by the standard bounce time t_b to achieve normalization. This is done in Appendix D. Other normalized quantities such as $B^{**}, c_0, \hat{b_0}, \hat{b_0^*}, f^*, f^{**}, g^*, g^{**}$ are listed in Appendix E. The guiding-center equations for the parallel velocity $v_\|$ and the radial coordinate r are not listed because these variables are recovered through the constants of motion.By doing so we are spared two integrations. This set of equations has all the properties of a Hamiltonian system and therefore can be used for long-time integration of particle orbits.

2.1.5 Guiding-center particle orbits in a tokamak

In order to find the particle orbits, we make use of three guiding-center constants of motion:

- energy E $\equiv \frac{1}{2} m v^2$
- magnetic moment $\mu \equiv \frac{m v_\perp^2}{2B}$

- toroidal angular momentum $p_\zeta \equiv R(mv_\zeta + qA_\zeta)$

These constants will be written in non-dimensional form and customized to a given set of equilibrium fields.

In MKS, the toroidal angular momentum is

$$p_\zeta = hR_0(mv_\zeta + qA_\zeta) \tag{2.19}$$

The toroidal velocity is given by

$$v_\zeta = -v_\parallel \frac{B_\zeta}{B} = -v_\parallel f(x) \tag{2.20}$$

where $f(x)$ is the toroidal component of versor $\mathbf{b}$. By substituting equation (2.20) in equation (2.19) the toroidal angular momentum becomes

$$p_\zeta = -mhR_0 v_\parallel f(x) + qh(x,\theta)R_0 A_\zeta(x) \tag{2.21}$$

The parallel velocity can be written as

$$v_\parallel = \pm\sqrt{\frac{2}{m}[E - \mu\frac{B_0}{hf}]} \tag{2.22}$$

Rationalizing the toroidal momentum we get

$$\bar{p} \equiv \frac{p_\zeta}{mR_0 v_{th}} = -hf\frac{v_\parallel}{v_{th}} + \frac{qA_\zeta R_0 h}{mv_{th}} \tag{2.23}$$

where $x = r/a$.

Furthermore,

$$h = 1 + x\frac{a}{R_0}cos\theta \tag{2.24}$$

The normalized parallel velocity is

$$\bar{v}_{\|} \equiv \frac{v_{\|}}{v_{th}} = \pm\sqrt{\frac{v^2}{v_{th}^2} - \frac{2\mu B_0}{mhv_{th}^2 f}} = \pm\sqrt{\bar{v}^2 - \frac{\bar{\mu}}{hf}} \tag{2.25}$$

where $\bar{v}$ and $\bar{\mu}$ are normalized velocity and magnetic moment which are defined in equations (2.27) and (2.28).

A particle orbit can also be described by its position and velocity at any arbitrary point along the particle trajectory. The following notation is used for initial conditions

$$\frac{v_{\|0}}{v_{th}}, \frac{v_{\perp 0}}{v_{th}}, \frac{r_0}{a} = x_0, \theta_0 \tag{2.26}$$

The non-dimensional constants of motion are

- velocity

$$\bar{v} \equiv v_{norm} = (v_{\|0th}^2 + v_{\perp 0th}^2)^{1/2} \tag{2.27}$$

- magnetic moment

$$\bar{\mu} \equiv \mu_{norm} = h_0 f_0 v_{\perp 0th}^2 = h f v_{\perp th}^2 \tag{2.28}$$

where

$$\mu = \frac{mv_{\perp}^2}{2B} = \frac{mv_{th}^2}{2B_0}\bar{\mu} \tag{2.29}$$

and

$$h_0 = 1 + x_0\frac{a}{R_0}cos\theta_0 \tag{2.30}$$

- toroidal angular momentum

$$\bar{p} = -h_0 f_0 \bar{v}_{\|0} + \frac{qA_\zeta(x_0^2)h_0 R_0}{mv_{th}} = -hf\bar{v}_{\|} + \frac{qA_\zeta(x^2)hR_0}{mv_{th}} \tag{2.31}$$

We will make extensive use of normalized variables throughout this thesis. By convention, these normalized variables are denoted by barred symbols.

2.1.6 A simple toroidal equilibrium and motion invariants

The problem of transport is related to the equilibrium fields of the tokamak. A measure of particle confinement is given by the toroidal momentum as shown in previous research [13, 14, 8, 12, 15]. In turn, the toroidal momentum is a function of the current density through the toroidal component of the vector potential. Equilibrium will now be given to progress toward an understanding of the topology of the particle orbits. The choice of equilibrium fields must be optimized to meet requirements of simplicity and to preserve physical content. The equilibrium pinch [16, 17] is a simple configuration that preserves some of the basic ingredients of the physics of equilibrium confinement. The toroidal field is generated by external currents and has the usual $1/R$ dependence. It is given by

$$B_\zeta = \frac{B_0}{h(x,\theta)} \tag{2.32}$$

where B_0 is the toroidal field intensity at $R = R_0$. We work in cylindrical coordinates (r, ϕ, z). The poloidal field is given by Ampere's law

$$\mu_0 J_z = \frac{1}{r}\frac{d}{dr}(rB_\phi) \tag{2.33}$$

If we make the current density a constant, then Maxwell's equation can be easily integrated to yield the poloidal field inside the plasma

$$B_\phi = \frac{\mu_0 I}{2\pi a^2} r \tag{2.34}$$

where B_ϕ is the poloidal component of the equilibrium magnetic field and I is the total toroidal current inside the plasma. The toroidal vector potential is obtained by integrating $\mathbf{B} = \nabla \times \mathbf{A}$ to give

$$A_z = \frac{\mu_0 I}{4\pi} x^2 \tag{2.35}$$

The absolute value of the total magnetic field is

$$|B| = \frac{B_0}{hf} = \sqrt{(\frac{B_0}{h})^2 + B_\phi^2} \tag{2.36}$$

The toroidal component of the unit versor can be expressed as a function of the fields by solving equation (2.36). This yields

$$f = (1 + (\frac{\mu_0 I}{2\pi a B_0})^2 x^2 h^2)^{-1/2} \tag{2.37}$$

The normalized toroidal momentum can now be written in explicit form

$$\bar{p} = -h(x) f(x) \bar{v_\parallel} + A_c x^2 \tag{2.38}$$

where

$$A_c = \frac{\mu_0 q I}{4\pi m v_{th}} \tag{2.39}$$

Knowing how the constants of motion depend upon the radius and the poloidal angle, in the next chapter we write and solve an algebraic equation for $x = x(\theta)$ and recover the parallel velocity and the perpendicular velocity through equations (2.27), (2.28), and (2.31).

2.1.7 Summary

Guiding center equations have been derived for a tokamak plasma with circular flux surfaces. A simple equilibrium model has been adopted to make equations suitable for quantitative analysis. Constants of motion have been written as functions of particle position and velocity. In the next step, we will use these relationships to study fast ion motion in a tokamak.

2.2 Fast ion orbits in a tokamak

2.2.1 Introduction

Ion cyclotron heating increases the perpendicular energy of resonant minority ions. As these particles gain energy, they become more trapped. Trapped particles are generated when pitch-angle scattering is not fast enough to scatter the particles into the passing region. Resonant ions can become so energetic that their orbits touch the plasma's edge and their banana widths reach dimensions comparable to the minor radius. The banana tips move toward the resonant layer as they gain perpendicular energy crossing the resonant layer, see figure (2.1) [1]. To understand the transport of these energetic particles due to RF and collisions, their orbits need to be understood in detail. A general treatment of particle orbit can be found in books by Balescu [12] and White [15]. Also, Rome [14] studied the topology of tokamak orbits using a set of phase space variables where the toroidal angular momentum is replaced by the maximum value of the particle radial position. More recently, Putvinskii used a reduced set of constants of motion to study alpha particle confinement [18]. In this chapter we focus on barely confined trapped particles that touch the plasma's edge. These particles are labelled by the position of their banana tips. We will also compute the banana widths and their poloidal periods.

2.2.2 An algebraic equation for particle orbits

An algebraic equation for particle orbits can be derived by employing the integrals of motion. These are energy, magnetic moment, and toroidal momentum. We make use of equations (2.27), (2.28), and (2.31). We simplify the orbit equation by letting $f = 1$. This simplification implies that the intensity of the poloidal magnetic field is neglected with respect to the intensity of the toroidal magnetic field, which is a good approximation for tokamaks [18]. By doing so, we obtain

[1] Figures are in Appendix N

$$\bar{v}^2 = \frac{v^2}{v_{th}^2} \tag{2.40}$$

$$\bar{\mu} = h\bar{v}_\perp^2 \tag{2.41}$$

and

$$\bar{p} = -h\bar{v}_\parallel + A_c x^2 \tag{2.42}$$

The parameter A_c has been defined in equation (2.39). Next, solve for $\bar{v}_\parallel$ and substitute it into the expression (2.31) for the toroidal momentum to get an equation in θ and x. The orbit equation is quartic in x [2]

$$ax^4 + c(\theta)x^2 + d(\theta)x + e = 0 \tag{2.43}$$

where

$$a = A_c^2 \; ; \; c = -2\bar{p}A_c - (\frac{a}{R_0})^2\bar{v}^2 cos^2\theta \tag{2.44}$$

and

$$d = cos\theta(-2\frac{a}{R_0}\bar{v}^2 + \frac{a}{R_0}\bar{\mu}) \; ; \; e = \bar{p}^2 - \bar{v}^2 + \bar{\mu} \tag{2.45}$$

Theoretically, a quartic equation can be solved analytically, however, the length of the solutions are such that little information can be extracted from them. Moreover, we

[2]The coefficient a should not be confused with the minor radius a that appears only in the inverse aspect ratio in this section.

are only interested in energetic trapped particles that have large orbits which touch the plasma's edge [19, 20].
We will examine barely confined trapped particles in the next section of this chapter.

2.2.3 Barely confined trapped particles phase space

The orbit equation describes approximately all particle trajectories in a tokamak as functions of the constants of motion. This is more information than required for our study of barely confined particles. We let $cos\theta = 1$ in equation (2.43), which means that we examine the particle orbit intersection with the outer midplane of a tokamak. The algebraic equation becomes

$$ax^4 + c_1x^2 + d_1x + e = 0 \tag{2.46}$$

where the coefficients are

$$c_1 = -2\bar{p}A_c - (\frac{a}{R_0})^2\bar{v}^2 \tag{2.47}$$

$$d_1 = -2\frac{a}{R_0}\bar{v}^2 + \frac{a}{R_0}\bar{\mu} \tag{2.48}$$

We are interested in particles that are barely confined, therefore we let $x = 1$.
This yields an equation for the constants of motion

$$A_c^2 - 2\,\bar{p}A_c - (\frac{a}{R_0})^2\bar{v}^2 - 2\,\bar{v}^2\frac{a}{R_0} + \bar{\mu}\frac{a}{R_0} + \bar{p}^2 - \bar{v}^2 + \bar{\mu} = 0 \tag{2.49}$$

Our choice of the constants of motion is now restricted to a two-dimensional space rather than a three-dimensional one. In addition we assume the inverse-aspect ratio equal $\frac{1}{3}$. Indeed, most tokamaks have inverse-aspect ratios equal or quite close to this value. Besides being physically evident, it can also be computed from equation (2.43)

that $cos\theta = 1$ is either a maximum or a minimum for x.

Since we search for a maximum in x, we will require the second derivative of x, with respect to θ, to be negative

$$\frac{d^2x}{d\theta^2} = -(cos\theta\frac{dx}{d(cos\theta)} - sin^2x\frac{d^2x}{d(cos(\theta))^2}) < 0 \tag{2.50}$$

This leads to the following inequality that has to be satisfied by the constants of motion when $a/R_0 = \frac{1}{3}$

$$\frac{-\frac{8}{9}\bar{v}^2 + \frac{\bar{\mu}}{3}}{4A_c^2 - 4A_c\bar{p} - \frac{8}{9}\bar{v}^2 + \frac{\bar{\mu}}{3}} < 0 \tag{2.51}$$

For a derivation of this inequality, see Appendix F.

Whenever the three constants of motion are given, we need to ensure that this inequality is satisfied.

2.2.4 Trapped particles whose tips are on the resonant layer

We begin by considering minority heating on axis because it is most commonly used in experiments. Energetic trapped particles that interact resonantly with the fast wave eventually end up having their banana tips close to the resonant layer [21]. These particles have a strong resonant wave-particle interaction and, therefore, will be studied carefully.

They can be easily identified in phase space by examining their constants of motion. By setting the parallel velocity to zero at their banana tips, one can easily derive the following relationships for the energy and the momentum from equations (2.25) and (2.38)

$$\bar{p} = A_c x_0^2 \; ; \; \bar{v}^2 = \bar{\mu} \tag{2.52}$$

where x_0 is the radial coordinate of the banana tip of the trapped particle.
By substituting these relations in equation (2.49) we get

$$A_c^2 - 2A_c^2 {x_0}^2 - \frac{4\,\bar{v}^2}{9} + A_c^2 {x_0}^4 = 0 \tag{2.53}$$

This biquadratic equation can easily be solved for x_0^2 to yield the following

$$x_0^2 = \begin{bmatrix} 1.0 + \frac{1}{3A_c/2}\sqrt{\bar{v}^2} \\ 1.0 - \frac{1}{3A_c/2}\sqrt{\bar{v}^2} \end{bmatrix} \tag{2.54}$$

The first root can be discarded because it gives a trajectory that goes beyond the boundaries of the torus on the resonance layer.
Solving equation (2.54) for energy, we obtain

$$\bar{v}^2 = \frac{9}{4} A_c^2 (1 - x_0^2)^2 \tag{2.55}$$

This equation is plotted out in figure (2.2) for a tokamak whose parameters are similar to Alcator, namely $a/R_0 = 1/3$, $B_T \approx 5T$, $I \approx 1MA$, $n_{e0} \approx 1 \times 10^{21} m^{-3}$ and $T_e \approx 3KeV$ [22]. The energy has been normalized to 1 KeV. We are interested in particles whose energies are well above the thermal energy because these are the most representative of the minority tail distribution function. One can see from figure (2.2) that the most energetic trapped particles have their tips close to the center of the plasma, as one can infer from toroidal momentum conservation. As the energy decreases, the tips move radially outward. For instance, the maximum energy that such particles can have while being confined is $1.2MeV$. In general, the maximum energy is determined by the amount of toroidal current flowing within the tokamak. The maximum confined particle energy changes proportionally to the squared toroidal

current

$$(Energy)_{max} \propto I^2 \tag{2.56}$$

Equation (2.56) is derived from equations (2.39) and (2.55).

2.2.5 General expressions for trapped particles

We will generalize the approach used to study the trapped particles whose tips touch the resonant layer and extend it to trapped particles whose banana tips are located anywhere in the torus. We let the parallel velocity be zero at some point and compute the constants of motion as a function of the coordinate of this point. By doing so, we obtain from equations (2.25) and (2.38)

$$\bar{\mu} = (1 + \frac{1}{3} cos\theta_0 x_0)\bar{v}^2 \; ; \; \bar{p} = A_c x_0^2 \tag{2.57}$$

where x_0 and θ_0 are the radial and poloidal angle coordinates of the tip of the banana. By substituting these expressions into equation (2.49) we obtain

$$\bar{v}^2 = \frac{9}{4} A_c^2 \frac{(x_0^2 - 1)^2}{1 - x_0 cos\theta_0} \tag{2.58}$$

These expressions allow us to find the constants of motion when the location of the banana tips is given.

The barely confined particle energy is plotted in figure (2.3). It is clear that highly energetic particles are those whose banana tips are closer to the plasma center. As the trapped particle banana tips move toward the inner part of the torus, their energy decreases. We need to verify whether equation (2.51) holds for these particles. If we substitute for the constants of motion in the second derivative condition we obtain

$$-\frac{a\,(11-15\,x_0\,\cos(\theta_0)-6\,{x_0}^2+14\,{x_0}^3\cos(\theta_0)-5\,{x_0}^4+{x_0}^5\cos(\theta_0))}{-4+4\,x_0\,\cos(\theta_0)}>0 \quad (2.59)$$

A numerical computation for $0 < x_0 < 1$ and $0 < \theta_0 < \pi$ shows that this inequality is indeed satisfied for barely confined particles.

2.2.6 Particle drifts for energetic trapped particles

Trapped particles that touch the plasma edge are very energetic. At the same time, their parallel velocities become smaller as they approach their tip location. In such instances, particle drifts cannot be neglected even at leading order in ϵ. Stringer [23] pointed out that the drift velocities of energetic particles cannot be ignored with respect to their parallel velocities if one wishes to ascertain the domain of the trapping region. Although his treatment was based on a study of alpha particle orbits, it applies to fast minority ions as well. An additional reason for studying the particle drifts is to compute the poloidal period of energetic particles. This can be carried out as follows by computing the integral for trapped particles

$$T_{pol} = 2\int_{-\theta_b}^{\theta_b} \frac{d\theta}{d\theta/dt} \quad (2.60)$$

where the derivative is computed along the unperturbed orbit and θ_b is the poloidal bounce angle.

In Appendix D, the full expression for the poloidal angle velocity is given. Here we keep all the linear terms in ϵ for simplicity. The poloidal angle velocity is obtained from equations (D.1)-(D.3) in Appendix D by letting $f = 1$ and $B^* = B_0/hf$ and neglecting quadratic terms in ϵ

$$\frac{d\theta}{dt} = \frac{1}{a}[\frac{v_{\|}g}{x} - \frac{v_d cos\theta}{x}] \quad (2.61)$$

where a is the minor radius. The particle drift velocity is

$$v_d = \frac{v_\parallel^2 + v_\perp^2/2}{\omega_{c0} R_0} \tag{2.62}$$

and the rotational factor g is

$$g = \frac{A_q x}{(1 + A_q^2 x^2)^{1/2}} \approx A_q x \tag{2.63}$$

where A_q is

$$A_q \approx \frac{2}{aB_0} \frac{\mu_0 I}{4\pi} \tag{2.64}$$

For Alcator parameters we get $A_q \approx 1/5$.

The poloidal velocity is now expressed in terms of the constants of motion. Substituting equation (2.63) and (2.64) into (2.61) yields the following expression for the poloidal velocity

$$\frac{d\theta}{dt} = \frac{1}{a}[A_q v_\parallel - \frac{2E - \mu B}{m\omega_{c0} R_0} \frac{cos\theta}{x}] \tag{2.65}$$

We will work with normalized variables.

We divide the time by a standard bounce time $t_b = (v_\parallel / R_0)^{-1}$ to get

$$\frac{d\theta}{d\bar{t}} = \frac{R_0}{a} \frac{v_{th}}{\omega_{c0} R_0} [\pm \frac{A_q \omega_{c0} R_0}{v_{th}} (\bar{v}^2 - \frac{\bar{\mu}}{h})^{1/2} - \frac{cos\theta}{x} (\bar{v}^2 - \frac{\bar{\mu}}{2h})] \tag{2.66}$$

and we substitute the parallel velocity as a function of $\bar{p}$ from equation (2.42) to get

$$\frac{d\theta}{d\bar{t}} = \frac{R_0}{a} \frac{v_{th}}{\omega_{c0} R_0} [\frac{A_q \omega_{c0} R_0}{v_{th}} \frac{A_c x^2 - \bar{p}}{h} - \frac{cos\theta}{x} (\bar{v}^2 - \frac{\bar{\mu}}{2h})] \tag{2.67}$$

This expression can be simplified when we make use of the relation

$$\frac{A_q \omega_{c0} R_0}{v_{th}} = 2A_c \frac{R_0}{a} \tag{2.68}$$

yielding

$$\frac{d\theta}{d\bar{t}} = \frac{R_0}{a} \frac{v_{th}}{\omega_{c0} R_0} [2A_c \frac{R_0}{a} \frac{A_c x^2 - \bar{p}}{h} - \frac{cos\theta}{x} (\bar{v}^2 - \frac{\bar{\mu}}{2h})] \tag{2.69}$$

Let's substitute Alcator parameters to get an order of magnitude for these velocities. For a 1 KeV thermal plasma in a tokamak where the magnetic field intensity is 5 Tesla, $10 < A_c < 100$. Substituting these numbers into equation (2.69) we obtain

$$\frac{d\theta}{d\bar{t}} \propto 120 \frac{20x^2 - \bar{p}}{h} - \frac{cos\theta}{x} (\bar{v}^2 - \frac{\bar{\mu}}{2h}) \tag{2.70}$$

It is clear that the second term on the R.H.S. is much smaller than the first term on the R.H.S. unless the particle gets very close to the plasma axis ($x \rightarrow 0$) . Another important factor is the $cos\theta$ dependence of the drifts. This means that no matter how close the particle gets to the plasma center, the drifts will be zero as long as the particle moves along the vertical diameter. This explains the topology of certain classes of trapped particles that have very large banana widths and move long distances along the diameter. Some researchers [24] call them potato orbits, because their poloidal projection resembles the contour of a potato.

2.2.7 Approximate analytical expressions for poloidal periods

In this section, poloidal periods are derived in terms of the constants of motion. For a standard derivation, see Balescu [12]. We will begin by evaluating the bounce times T_b. At leading order in ϵ the guiding-center equation for the poloidal angle is

$$\frac{d\theta}{dt} \approx \frac{v_{\|}}{q_s R_0} \tag{2.71}$$

where $q_s = \frac{rB_\zeta}{RB_\theta}$ is the safety factor. The parallel velocity can be written as

$$v_{\|} = \sigma\sqrt{\frac{2}{m}(E - \mu B_0 + \epsilon\mu B_0)}\sqrt{1 - k^2 sin^2\frac{\theta}{2}} \tag{2.72}$$

where

$$k^2 = \frac{2\epsilon\mu B_0}{E - \mu B_0 + \epsilon\mu B_0} \tag{2.73}$$

If the safety factor is a constant along the particle orbit, then the poloidal bounce time for passing particles is given by

$$T_b = \oint dt = \frac{q_s R_0}{\sqrt{\frac{2}{m}(E - \mu B_0 + \epsilon\mu B_0)}} \int_0^{2\pi} \frac{d\theta}{\sqrt{1 - k^2 sin^2\frac{\theta}{2}}} \tag{2.74}$$

Assuming the departure from the flux-surfaces is small, the normalized bounce time can be written as a function of the normalized constants of motion in equations (2.27), (2.28) and (2.38)

$$\hat{T}_{bpass} = \frac{T_b}{R_0} v_{th} = \frac{4q_s(\hat{\epsilon})}{\sqrt{v^2 - (1 - \hat{\epsilon})\bar{\mu}}} K(k_p) \tag{2.75}$$

where the modulus of the complete elliptic integral of the first kind is

$$k_p = \sqrt{\frac{2\hat{\epsilon}\bar{\mu}}{v^2 - (1-\hat{\epsilon})\bar{\mu}}} \tag{2.76}$$

we define a radial position $\hat{\epsilon}$

$$\hat{\epsilon} = \frac{a}{R_0}\sqrt{\frac{1}{A_c}(\bar{p} + \sigma\sqrt{v^2 - \bar{\mu}})} \tag{2.77}$$

and the safety factor is given by

$$q_s(\hat{\epsilon}) = \frac{\hat{\epsilon}}{g(\hat{\epsilon})} \tag{2.78}$$

For trapped particles, the computation of the bounce time is somewhat similar

$$\hat{T}_{btrapp} = \frac{8q_s(\epsilon_t)}{\sqrt{2\epsilon_t\bar{\mu}}}K(\frac{1}{k_t}) \tag{2.79}$$

The only difference is that we take the average radial position from the tip of the banana

$$\epsilon_t = \frac{a}{R_0}\sqrt{\frac{\bar{p}}{A_c}} \tag{2.80}$$

the modulus of the complete integral of the first kind is

$$k_t = \sqrt{\frac{2\epsilon_t\bar{\mu}}{v^2 - (1-\epsilon_t)\bar{\mu}}} \tag{2.81}$$

and the safety factor is evaluated at the banana tip

$$q_s(\epsilon_t) = \frac{\epsilon_t}{g(\epsilon_t)} \tag{2.82}$$

2.2.8 Poloidal period for trapped particles touching the plasma edge

We now estimate the poloidal period for trapped particles whose orbits touch the plasma edge using the results from section (2.2.7). An analytical expression for the normalized poloidal period of thin bananas in the range $x \approx 1$ can be derived from equation (2.79) using equations (2.63) and (2.78) to yield

$$\hat{T}_{tr} \approx \frac{8}{A_q}\left(\frac{a}{2R_0\bar{\mu}}\right)^{1/2} K(1/k_t) \tag{2.83}$$

where the trapping parameter is

$$k_t = \left(\frac{2a}{R_0}\frac{\bar{\mu}}{\bar{v}^2 - (1 - a/R_0)\bar{\mu}}\right)^{1/2} \tag{2.84}$$

The poloidal velocity tends toward zero as the trapped particle approaches the banana tip. All spatial quantities in the expression for the poloidal period will be evaluated at the banana tip location.

The normalized poloidal period can be written as a function of the location of the trapped particle tip

$$\hat{T}_{tr} \approx \frac{8}{A_q}\left(\frac{a}{2R_0\bar{\mu}}\right)^{1/2} \frac{K(sin^2(\theta_0/2))}{\sqrt{x_0}} \tag{2.85}$$

For the normalized magnetic moment we use equations (2.57) and (2.58)

$$\bar{\mu} = \frac{9}{4}A_c^2(1 + \frac{1}{3}cos\theta_0 x_0)\frac{(x_0^2 - 1)^2}{1 - x_0 cos\theta_0} \tag{2.86}$$

This approximation loses its accuracy for trapped particles that have their banana tips close to the plasma axis. Fortunately, this does not change the validity of equation (2.85) because those particles fill only a very small region in phase space. Normalized poloidal periods are plotted as functions of the location of their banana tips. See figure (2.4). The divergent behavior of the elliptic integral can be seen at the passing-trapped region boundary where the poloidal angle of the tip of the banana is π. The time scale of the bouncing motion can be easily obtained by computing t_b. For Alcator parameters [22]

$$t_b = \frac{R_0}{v_{th}} \approx 2 \times 10^{-6} sec. \tag{2.87}$$

2.2.9 Orbital widths for barely confined particles

Because barely confined particles have large orbital widths, they collide with majority ions and electrons along their trajectories. Due to wide orbit effects, collision rates can differ greatly along the orbit. For these reasons, it is important to estimate the orbital widths in phase space. The maximum orbital width is between the two particle intersections at $cos\theta = 1$. One intersection is already known: it takes place at the plasma's edge. The other must be found by solving equation (2.46). Before doing so, we divide equation (2.46) by $(x - 1)$ to simplify it, which yields a cubic equation that can be reduced to the following form

$$x^3 + x^2 + Ax + B = 0 \tag{2.88}$$

where

$$A = (1 + \frac{c_1}{a}) \; ; \; B = (1 + \frac{c_1 + d_1}{a}) \tag{2.89}$$

The coefficients a, c_1 and d_1 have been defined in equations (2.44),(2.47), and (2.48). Equation (2.88) has three solutions, two of which are complex. The real one gives the abscissa of the inner intersection. The real solution can be obtained analytically, but it is better to compute it numerically. By doing so, the maximum orbital width is computed for Alcator parameters. In figure (2.5), we plotted the contour of the maximum width for barely confined trapped particles as a function of the location of their banana tips. There is a large region in phase space where the width is approximately 0.9 times or more than the minor radius. This region is the potato orbit region because of the shape of the orbit. This region becomes larger as the poloidal angle of the tip approaches the inner edge of the torus midplane. The width decreases almost linearly with the increasing radial position of the tip as soon as we leave the potato region.

2.2.10 Summary

We examined barely confined trapped particles in phase space. We showed that the location of their tips is the most logical phase space label for these particles. Poloidal periods were computed at leading order in ϵ. We also showed where these approximations break down. The maximum radial excursions of these particles were computed numerically. The results showed that there is a fairly large region in phase space where barely confined particles have orbital widths comparable to the minor radius: the potato orbit region. We would like to point out that passing particles are of marginal interest in this analysis because only a small fraction of them have barely confined orbits. In the next chapters, we study the effects that the fast wave and collisions have on these particles.

Chapter 3

Resonant wave-particle in ICRF-heated tokamaks

3.1 Introduction

In this chapter we study resonant wave-particle interaction for ICRF-heated tokamaks. In the first section we briefly review the Hamiltonian formulation of charged particle motion in a small amplitude wave. In the second section we list and discuss praises and limitations of past research on quasilinear theory. In the third and fourth sections we derive a quasilinear operator for a resonant particle distribution function along with formal expressions for the quasilinear diffusion coefficients. In the fifth and sixth sections we derive an approximate expression for the diffusion tensor using Hamiltonian perturbation theory. Finally, in the last section we compute the magnitude and the scaling of the diffusion coefficients for standard tokamak parameters. The main goal of this chapter is to derive a simple, analytic expression for the diffusion coefficients of resonant trapped particles which can be used to estimate RF-heated minority transport.

3.2 Hamiltonian formulation of charged particle motion in a small-amplitude electromagnetic wave

Let us consider a static magnetic field $\mathbf{B}$ in a tokamak. We assume that this equilibrium field is given and described by the Grad-Shafranov equation. In addition to the equilibrium field, we have a high frequency electromagnetic wave. Given the two corresponding vector potentials, $\mathbf{A}$ and $\mathbf{A_1}$, the non-relativistic Hamiltonian of a single-charged particle can be written in a straightforward manner as

$$H = \frac{1}{2m}(\mathbf{p} - q\mathbf{A}(\mathbf{x}) - q\mathbf{A_1}(\mathbf{x}, \mathbf{t}))^2 \tag{3.1}$$

where we made use of the Coulomb gauge [8], which is equivalent to letting the electrostatic potential ϕ_1 equal zero. If one has explicit expressions for the vector potentials in terms of space and time, then one can simply write the canonical equations for $(\mathbf{p}, \mathbf{x})$ and solve them. However, we take a more interesting approach that uses the guiding-center theory. To start, let's assume that the wave has a small amplitude with respect to the equilibrium field. This assumption is certainly valid in a tokamak where the equilibrium fields are much larger than any other electromagnetic perturbation. Let's introduce a small parameter λ such that

$$|\frac{\mathbf{A_1}}{\mathbf{A}}| = O(\lambda) \ll 1 \tag{3.2}$$

This ordering allows us to use the approximate guiding-center Hamiltonian instead of the full Hamiltonian given by equation (3.1). To derive the approximate guiding-center Hamiltonian, we start by writing out the Hamiltonian in the following manner

$$H = \underbrace{\frac{1}{2m}(\mathbf{p} - q\mathbf{A})^2}_{\textit{guiding center motion}} - \underbrace{\frac{q}{m}\mathbf{A_1}\cdot(\mathbf{p} - q\mathbf{A})}_{\textit{linear } w-p \textit{ interaction}} + \underbrace{\frac{q^2}{2m}\mathbf{A_1}^2}_{\textit{quadratic term}} \tag{3.3}$$

or more concisely

$$H = H_0 + \lambda H_1 + \lambda^2 H_2 \tag{3.4}$$

The exact Hamiltonian written in this form indicates that the particle motion is described by its leading-order unperturbed motion given by H_0 plus a small wave perturbation given by H_1. The quadratic term H_2 in λ is small and therefore neglected. In addition to being small, the quadratic term H_2 is not needed to derive quasilinear diffusion coefficients because these generally stem from linear wave-particle interaction only. To make further progress, we introduce the velocity $\mathbf{v}$

$$m\mathbf{v} \equiv \mathbf{p} - q\mathbf{A} \tag{3.5}$$

This is the velocity of the particle. Our Hamiltonian can now be written as the sum of two Hamiltonians: the first contains all information concerning the guiding-center motion of a charged particle in a static magnetic field, while the second describes the interaction between the particle and the wave. This can be summarized as

$$H \simeq \frac{1}{2}mv^2 - q\mathbf{v} \cdot \mathbf{A_1} \tag{3.6}$$

The linearization of the full Hamiltonian in equation (3.1) has accomplished the goal of separating the unperturbed motion from the wave particle interaction contribution so that the complete motion is given by the linear superposition of two motions: one due to the static fields and the other, due to the wave. The first Hamiltonian can be written as a guiding center Hamiltonian

$$H_0 \equiv \frac{1}{2}mv^2 = \frac{1}{2}mv_{\parallel}^2 + \mu B(\mathbf{X_{gc}}) + O(\epsilon^2) \tag{3.7}$$

Since this Hamiltonian was examined in the second chapter, we will focus on the linearized Hamiltonian H_1 in this chapter.

3.3 Quasilinear Theory and Diffusion Coefficients in Phase Space

3.3.1 Introduction

A few specialized quasilinear operators have been derived to study the evolution of a minority distribution function heated by the fast Alfven wave. However, little research has been done to include spatial transport in a quasilinear formulation, primarily because present quasilinear-theory formalisms are designed to deal only with diffusion in velocity space. The added complexity of working in the full phase space, instead of just the usual velocity space, makes the formulation of a generalized diffusion equation a difficult task. Before we address the problem of such a formulation, we discuss some advantages and limitations of past and other research regarding quasilinear transport studies of a heated minority. We will also examine past work toward a unified approach.

3.3.2 Quasilinear theories

The first quasilinear operator for a plasma in a homogeneous magnetic field was derived independently by Yakimenko in 1963 [25] and by Kennel and Engelmann in 1966 [26]. This operator was meant to study the temporal and velocity space behavior of a plasma in a homogeneous field under the action of an incoherent wave spectrum due to some turbulent modes. The same operator has also been used to study the

effect of a coherent, externally induced wave, assuming (usually implicitly) that there is some mechanism (chaos or collisions) that makes the wave-particle interaction incoherent. However, as a consequence of the equilibrium magnetic field inhomogeneity in a tokamak, the resonance process is qualitatively different from that which occurs in homogeneous magnetic fields. In a homogeneous magnetic field, the wave-particle cyclotron resonance condition is satisfied at any location, while in an inhomogeneous field, a particle escapes cyclotron resonance through its unperturbed motion. After these resonant mechanisms were understood, it became clear that more sophisticated quasilinear operators were needed to study cyclotron heating in tokamaks.

Stix's quasilinear operator for ion cyclotron heating

In 1975, Stix derived a quasilinear operator [3] by averaging the Kennel-Engelmann operator over a tokamak flux surface. He included the effect of magnetic field inhomogeneity in tokamaks. Using a single-particle approach, he proved that wave-particle resonances take place only at certain locations along the orbit. He then computed the average perpendicular energy gained by a resonating particle. The averaged RF power absorbed by the plasma in the single-particle model was equal to that calculated by using the flux-averaged quasilinear operator.

More recently, Stix also addressed the problem of stochastic interaction between a particle and an ion cyclotron wave. The quasilinear description implies that a resonating particle gets small, random kicks in energy. In this case, Stix showed that collisions can randomize the phase between the particle and the wave if the collision time and the orbital periods satisfy a certain inequality [5]. His operator is remarkable because it can be easily explained in terms of a simple model. However, it has an important limitation: it does not take into account the interaction of trapped particles with the waves.

While the parallel velocity of most passing particles can be considered as a constant of motion in most of their phase space, the parallel velocity of trapped particles ranges from zero at the tip to its maximum value on the low-field side of the tokamak. Hence, the quasilinear operator has to be weighted by the amount of time

that a particle spends at different locations in its orbit. This concept leads to a bounce-averaged quasilinear operator. Incidentally, note that flux-surface averaging and bounce-averaging are equivalent only in the limit of very passing particles. Stix's quasilinear operator is

$$\frac{\partial f}{\partial t}_{quas} = \frac{\pi Z^2 e^2}{2m^2|k_{||}|}|E_+|^2 \sum_n \frac{1}{v_\perp}\frac{\partial}{\partial v_\perp} v_\perp^2 |J_{n-1}(k_\perp \rho)|^2 \delta[v_{||} - \frac{\omega - n\omega_{ci}}{k_{||}}]\frac{1}{v_\perp}\frac{\partial f}{\partial v_\perp} \qquad (3.8)$$

where Z is the electric charge of the resonating species, $k_{||}$ is the parallel component of the wave vector, E_+ is the left-hand circularly polarized component of the electric field, J_n is the Bessel function of order n and δ is the delta function. Moreover, the parallel and the right-handed contributions to the electric field are neglected.

Bounce-averaged quasilinear operators

Several bounce-averaged quasilinear operators are described in the literature [21, 27, 28, 29, 30, 31].

For instance, Hammett derived a simple one in his doctoral thesis [21]. He started from the Kennel-Engelmann operator for an infinite, spatially uniform plasma and bounce-averaged the quasilinear operator using the small banana width approximation. To eliminate the resonant delta function in the quasilinear operator, he transformed the velocity-space operator in the energy and magnetic moment space. Both energy and magnetic moment are constants of motion to leading order in the fields, which simplifies the bounce-average integral. Trapped particles whose banana tips cross the resonance layer were also treated in his single-particle model. This was accomplished by solving the integrable singularity that arises from banana particles whose tips are in the vicinity of the resonance layer. The bounce-averaged quasilinear operator was also written as a function of energy and pitch-angle cosine at the outside midplane as

$$< \frac{\partial f}{\partial t} >_b = \frac{1}{|\xi| E T_b}\left(\frac{\partial \Gamma_E}{\partial E} + \frac{\partial \Gamma_\xi}{\partial \xi}\right) \qquad (3.9)$$

where the velocity-space coordinates are $E = mv^2/2$ and $\xi = (v_\parallel/v)$ at the outer midplane position, T_b is the poloidal bounce time, and the fluxes in velocity space are

$$\Gamma_E = E|\xi| \sum_{k,n} \frac{\pi e^2}{2m} \sum_{res} \left(\frac{v_\perp^2 |\theta_{k,n}|^2}{|v_\parallel \frac{\partial}{\partial l}(k_\parallel v_\parallel + n\omega_{ci})|}\right)_{res} L_{res} f \tag{3.10}$$

$$\Gamma_\xi = -\frac{\xi^2 - \xi_*^2}{2E\xi} \Gamma_E \tag{3.11}$$

where $\frac{\partial}{\partial l}$ is the spatial derivative along the field line and ξ_* is the cosine of a trapped particle's pitch angle whose banana tips lie in the resonance layer. $\theta_{k,n}$ has units of electric field per wavelength and is defined by

$$\theta_{n,k} = E_{\mathbf{k}+} e^{-i\psi} J_{n-1} + E_{\mathbf{k}-} e^{i\psi} J_{n+1} + \frac{v_\parallel}{v_\perp} E_{\mathbf{k}_\parallel} J_n \tag{3.12}$$

where the argument of the Bessel functions is $k_\perp \rho$ and the fields are

$$E_{\mathbf{k}\pm} = \frac{1}{2}(E_x \pm iE_y)_{\mathbf{k}} \tag{3.13}$$

and the wavelength vector components are

$$k_x = k_\perp cos\psi \; ; \; k_y = k_\perp sin\psi \; ; \; k_z = k_\parallel \tag{3.14}$$

The velocity-space operator is

$$L_{res} = m\frac{\partial}{\partial E} - (\xi^2 - \xi_*^2)\frac{m}{2\xi E}\frac{\partial}{\partial \xi} \tag{3.15}$$

It is instructive to examine some aspects of the bounce-averaging procedure more closely. The collision and the quasilinear operators are added in an *ad hoc* fashion to the drift kinetic equation, which is the gyrophase-averaged version of the Vlasov equation [30]

$$\frac{\partial f}{\partial t} + v_{\|}\frac{\partial f}{\partial l} = C(f) + Q(f) \tag{3.16}$$

where C and Q are the collision and the quasilinear operator, respectively.
The drift velocity has been neglected because of the assumption of small drift velocity compared to the parallel velocity. Hammett also made the assumption that the streaming term has the fastest time scale with respect to the collision and quasilinear operators, and $\frac{\partial f}{\partial t}$ by a factor $1/\epsilon$, then he expanded the distribution function in ϵ in the form $f = f_0 + \epsilon f_1 +$ to yield $\frac{\partial f_0}{\partial l} = 0$ at leading order and at next order in ϵ

$$\frac{\partial f_0}{\partial t} + v_{\|}\frac{\partial f_1}{\partial l} = C(f_0) + Q(f_0) \tag{3.17}$$

The spatially-periodic f_1 term can be annihilated by bounce-averaging. The bounce average of a phase-space quantity A is defined by

$$< A > \equiv \frac{1}{T_b}\int \frac{dl}{v_{\|}} A \tag{3.18}$$

Unfortunately, this definition of bounce average is not complete because we neglected drifts in the averaging operation, where $v_{\|} + v_{drift}$ should have been employed in equation (3.18) instead of $v_{\|}$. A more exact bounce average would include the departure of particles from field lines. This correction is substantial for trapped particles that are highly energetic such as those present in minority tails. It is worth noting that a perturbative approach that includes particle drifts in the kinetic equation has been adopted by Chang [32] in his collisional treatment of radial transport. He adopted the Kennel-Engelmann's quasilinear operator to compute the radial particle and energy

flux of tail ions. Chang concluded that the radial particle transport of tail ions by the Coulomb slowing-down collisions on background electrons is of the order of a banana width in a slowing-down time. He also concluded that the radial energy transport by Coulomb slowing-down scattering is composed of convective and diffusive terms and leads to a non-negligible loss of energy due to the strong anisostropy of the tail distribution function.

Another important limitation is that Chang's and Hammett's quasilinear operator do not treat off-axis heating.

An improved quasilinear operator that treats off-axis heating was derived by Catto and Myra [30]. They derived a quasilinear operator for minority heating in a tokamak using the formalism of Bernstein and Baxter [27] to study relativistic electron cyclotron heating in magnetic mirror confinement plasmas. They were able to smooth the transition from correlated to decorrelated interactions by examining collisional decorrelation to obtain diffusion coefficients that include both trapped and passing particles. Their bounce-averaged quasilinear operator is

$$< \frac{\partial f}{\partial t}_{quas} >= \frac{1}{v^2}\frac{\partial}{\partial v}[v^2(D_v\frac{\partial f}{\partial v} + D_x\frac{\partial f}{\partial \lambda})] + \frac{1}{T_b}\frac{\partial}{\partial \lambda}[T_b(D_x\frac{\partial f}{\partial v} + D_\lambda\frac{\partial f}{\partial \lambda})] \qquad (3.19)$$

where the velocity space variable is given by $\lambda = B_0 v_\perp^2/Bv^2$ and the diffusion coefficients are

$$D_v = 4\pi^2\epsilon\omega D\lambda[Ai(z_a)]^2/T_b|\frac{1}{2}\chi'''|^{2/3} \qquad (3.20)$$

$$D_x = \frac{2}{v}(\frac{\omega_{c0}}{\omega} - \lambda)D_v \qquad (3.21)$$

$$D_\lambda = \frac{4}{v^2}(\frac{\omega_{c0}}{\omega} - \lambda)^2 D_v \qquad (3.22)$$

where $\epsilon = r/R_0$, Ai is the Airy function, $z_a = \pm(\omega - \omega_{c0}(1 \pm \epsilon))/|\frac{1}{2} \pm \epsilon\omega_{c0}(v/qR_0)^2(1 - \lambda - \pm\epsilon\lambda)|^{1/3}$, $\lambda = \omega_{c0}/\omega_{ctip}$ and

$$D = (\frac{Ze}{m})^2(\frac{\sum_n |e_n^+|^2}{2\epsilon\omega}) \tag{3.23}$$

where e_n^+ is the left-hand polarized component of the n-th harmonic of the toroidal angle of the electric field and the phase is given by

$$\chi(\tau_*) = \int_0^{\tau_*} d\tau(\omega - l\omega_c) \tag{3.24}$$

where l is the cyclotron harmonic number. The explicit expressions for the third derivative of the phase χ''' are mathematically involved, therefore we refer the interested reader to Myra's and Catto's article [30] for further details. They used a phenomenological collision model to study the effect of decorrelation due to collisions.

Despite all these remarkable operators, further study is required to formulate a more realistic quasilinear operator that accounts for the inclusion of the Doppler shifted cyclotron resonance, finite banana width effects, and radial diffusion.

3.3.3 RF-induced transport of a heated minority

Whang and Morales [33], Riyopoulos et alia [34], and later Chen *et alia* [13] studied the problem of minority ion transport in ICRH tokamak plasmas. Whang and Morales found that confinement improves rapidly with plasma current, which may limit heating in low-current tokamaks with large RF power levels.They also predicted a depletion of heated minority protons from the plasma core due to radial non-uniformity of the diffusion coefficient. Riyopoulos *et alia* found the electric field amplitude E_{nc} at which the induced RF diffusion becomes comparable to the neoclassical.This is given by

$$E_{nc} = (v_{ph}/v_A)B_0(\nu_{ei}/\omega_{ci})^{1/2}\epsilon^{-1/2}q_s \tag{3.25}$$

where v_{ph} is the wave phase velocity, v_A is the Alfven velocity, ν_{ei} is the electron-ion collision rate and q_s is the safety factor. They concluded that for TFTR the directly wave-induced diffusion poses no threat to confinement if the electric field does not exceed a few tens of $V \cdot cm^{-1}$. Chen *et alia* made a distinction between RF driven convection and RF driven diffusion. RF driven diffusion is always negligible compared to RF driven convection. They also estimated RF driven flux with neoclassical flux to obtain

$$\frac{\Gamma_{RF}}{\Gamma_{neo}} \approx N\frac{a^2}{R^2}\frac{1}{q_s}\frac{1}{\tau_s\nu_i} \tag{3.26}$$

where N is the toroidal wavenumber, τ_s is the collisional slowing-down time of minority ions on bulk electrons and ν_{ii} is the ion-ion pitch-angle scattering rate. They concluded that for a highly asymmetric wave spectrum in $k_{\|}$ and large RF power making $\tau_s\nu_i$ smaller , the RF driven convection can dominate over the neoclassical flux. Another source of transport is caused by the presence of energetic ions whose banana widths may become so large that the orbits become unconfined. These effects are not strictly defined as transport, because they can take place even if the particle toroidal momentum is unchanged. They certainly deserve further study. More recently, Core [35] formulated a quasilinear equation that includes radial transport. He added a radial diffusion term to the kinetic equation

$$\frac{df}{dt} = C + Q + D_r \tag{3.27}$$

where C,Q, and D_r are the collision operator, the Kennel-Engelmann's quasilinear operator, and the radial diffusion operator, respectively. The radial diffusion opera-

tor is

$$D_r = \frac{1}{\epsilon_t}\frac{\partial}{\partial \epsilon_t}\epsilon_t D_{RF}\frac{\partial f}{\partial \epsilon_t} \tag{3.28}$$

where $\epsilon_t = r_{tip}/R_0$ gives the radial position of the banana tip of the resonant trapped ion. The diffusion coefficient D_{RF} is

$$D_{RF} = (\frac{q_s k_\parallel v_\perp}{R_0 \epsilon_t \omega_{ci}^2})^2 < \delta v_\perp \delta v_\perp > \tag{3.29}$$

where $< \delta v_\perp \delta v_\perp >$ is the time averaged energy gain by the ions as they pass through the resonant layer. Core bounce-averaged the Fokker-Planck equation to obtain an equation which is two-dimensional in velocity space and one-dimensional in radius. Velocity-space diffusion is known to occur at a faster rate than radial diffusion. This led to the introduction of different time scales. The Fokker-Planck equations for the two different time scales were solved by assuming an ansatz solution for the distribution function. Core concluded that spatial diffusion can have important consequences for heating efficiency.

For the JET experiment in particular, a reduction in the energy content of the resonant ion tail was found to be the most important effect. This work used the transport formalism developed for neoclassical transport, where distribution functions are defined on a single flux surface.

If we deal with trapped particles whose orbits are shifted from flux surfaces, then the radius of a flux surface cannot be considered a constant of motion. Thus, one has to increase the number of phase-space variables by choosing a spatial location for a particle along with its velocity or by adopting a toroidal invariant as a new variable. A completely different approach to the problem of heating and transport is based on the numerical integration of particle orbits and the use of Monte Carlo methods to treat collisions and wave-particle resonance [36, 37]. A more refined version of the

Monte Carlo method is given by the orbital-averaging of the Fokker-Planck equation to obtain a Monte Carlo operator [38]. These techniques have the advantage of including finite-banana width effects, but require intensive numerical work because the computation has to be practically performed in the entire phase space for all particles.

3.4 Quasilinear equation and transport in tokamaks

3.4.1 Introduction

The purpose of this section is to develop a unified approach to heating and transport. Several effects not extensively studied in previous research on transport by ICRF waves in plasmas are: Doppler-shifted resonances, finite banana widths, and current drive. We derive a quasilinear operator in the full phase space that formally retains all of these effects.

The quasilinear diffusion coefficients are usually very complicated functions of velocity and space. The evaluation of the diffusion coefficients in phase space normally requires numerical computation. However, approximate analytical expressions can be obtained for diffusion coefficients in a tokamak by making simplifying assumptions. Guiding-center equations are written to study resonances for energetic particles in any region of phase-space. Among other applications, this formalism can be used to study combined heating and current drive due to the lower-hybrid wave and the fast wave.

Let's consider the problem of a single charged particle motion in a tokamak. We assume that the equilibrium magnetic field is known. Moreover, the given field is static and smooth enough so that a particle's Larmor radius is much smaller than the inhomogeneity scalelength of the magnetic field. These assumptions make guiding-center theory applicable to our problem.

Hamiltonian guiding-center theory has some advantages over other formulations of guiding-center motion, the most significant being the existence of a Liouville's the-

orem in guiding-center space [9]. To examine it further, we must be more specific about the equilibrium field.

In an ideal tokamak, the magnetic field is axisymmetric. Axisymmetry implies the existence of an exact constant of motion: the toroidal angular momentum. However, when we use guiding-center variables, it is not immediately clear that the toroidal angular momentum remains a constant of motion. It is possible in the framework of Hamiltonian guiding-center theory to define a conserved toroidal angular momentum in guiding-center coordinates.

The magnetic moment has opposite properties: in general, it is not a constant of motion because the full equilibrium Hamiltonian is gyrophase-dependent. However, in adiabatic systems [1], it is possible to derive a guiding-center Hamiltonian independent of gyrophase. In such systems, the magnetic moment is a constant of motion to all orders [7]. The guiding-center Hamiltonian is an infinite series expanded in terms of a small parameter $\epsilon = m/q$. For practical purposes, we truncate our Hamiltonian and retain only the leading-order contribution which allows us to make use of a third constant of motion: the Hamiltonian itself. We will call it energy when we refer to it, but we need to keep in mind that this Hamiltonian is only an approximate energy.

To summarize, we have introduced three phase-space variables and pointed out that these are only approximate constants of motion for adiabatic systems. The more spatially homogeneous the magnetic field is, the more accurate these approximate constants are. Furthermore, in an RF-heated tokamak, the changes in the constants of motion due to wave-particle resonance interaction are larger and faster than the higher order terms in ϵ added to the approximate constants of motion. Throughout this study, we will assume these variables are exact constants of motion.

If we introduce collisions and waves into our scenario, then the three integrals of motion are no longer constants of motion. In particular, we are interested in the changes of the three constants due to a wave whose frequency is of the order of the

[1] by adiabatic we mean that the inhomogeneity lengthscale of the static equilibrium field is much larger than the particle's gyroradius

ion cyclotron frequency.

Generally speaking, the wave-particle interaction problem is non-linear. However, the small amplitude wave assumption of equation (3.2) allows us to treat waves as a perturbation on the background fields. This approach simplifies this complex problem considerably and makes it analytically tractable in certain cases. The wave-particle interaction can be of two types: resonant and non-resonant. Here we examine only resonant wave-particle interactions since these are the dominant heating mechanisms for ICRF.

Resonant particles are confined to a region in phase-space where the following relationship is satisfied at least over part of their orbit

$$|\omega - n\omega_c - k_{\|}v_{\|} - \mathbf{k}_{\perp} \cdot \mathbf{v_{drift}}| = 0 \tag{3.30}$$

Resonant interactions by themselves do not lead to particle heating. To obtain heating, the wave-particle interaction must be stochastic. Stochasticity can be caused by collisions or external noise (extrinsic stochasticity) or by the wave-particle interaction itself (intrinsic stochasticity). Conditions for the onset of stochasticity in IC-heated tokamaks have been established in literature [39, 40, 5, 33, 41]. Here, we focus on the intriguing problem of combined heating and transport and point out that the formalism used lends itself to the study of stochastic motion as well.

3.5 Derivation of a quasilinear equation

3.5.1 Guiding-center phase space

We begin with the usual assumptions for the validity of guiding-center theory. To derive our quasilinear equations, we start by defining our constants of motion for three species: passing, counterpassing and trapped particles as

$$\mathbf{J} = (\mu, E, p_\phi) \tag{3.31}$$

The direction of the parallel velocity $\sigma = \frac{v_\parallel}{|v_\parallel|}$ is a given parameter, which takes on the following values depending on the species

$$\begin{aligned} \text{passing particles: } \sigma &= +1 \\ \text{counterpassing particles: } \sigma &= -1 \\ \text{trapped particles: } \sigma &= \pm 1 \end{aligned}$$

We introduce a six-dimensional phase-space $(\mathbf{J}, \Theta)$ which is equivalent to the standard guiding-center phase-space

$$(\mathbf{J}, \Theta) \Longleftrightarrow (\mathbf{X_{gc}}, v_\parallel, \mu, \phi_{gc}) \tag{3.32}$$

We proceed to show that both spaces are equivalent.
First of all, we choose the vector Θ to be

$$\Theta = (\theta, \zeta, \phi_{gc}) \tag{3.33}$$

where we use the toroidal coordinates (r, θ, ζ) in tokamaks with circular flux surfaces. The symbol ϕ_{gc} stands for the gyrophase in guiding-center phase-space.
We also introduce two relations which give the other guiding center variables, namely $v_\parallel$ and r, as functions of the six phase-space variables.
These are

$$p_\phi = -m v_\parallel R(r) + q\psi_p(r) \tag{3.34}$$

where $\psi_p = RA_\zeta$ is the poloidal flux and

$$v_\parallel = \sigma\sqrt{\frac{2}{m}(E - \mu B(r,\theta))} \tag{3.35}$$

If we give initial conditions for a particle, we can compute $\mathbf{J}$ and $\boldsymbol{\Theta}$. Conversely, if $\mathbf{J}$ and $\boldsymbol{\Theta}$ are known, we can in principle compute the parallel velocity and the radial position using the relations in equations (3.34) and (3.35). This shows that every particle is identified by its constants of motion or equivalently by its initial conditions in phase-space.

3.5.2 Hamiltonian and Vlasov equation

To derive a quasilinear equation, equations of motion in phase-space and a Vlasov equation in guiding-center space are required.

The equations of motion are known once we have a Hamiltonian and associated Poisson brackets.

We start by linearizing the Hamiltonian in terms of a small parameter λ

$$H = H_0(\mathbf{J}) + \lambda H_1(\mathbf{J}, \boldsymbol{\Theta}, t) \tag{3.36}$$

The zero-order Hamiltonian H_0 is the same truncated Hamiltonian given in equation (2.3). It yields equations of motion for a charged particle in equilibrium fields. The linear Hamiltonian H_1 is the same linear Hamiltonian that appears in equations (3.3) and (3.4). It accounts for the linear contribution due to the wavefield. Here λ is equivalent to the ratio between the wavefield and the equilibrium field as defined in equation (3.2).

From this point on, every small-amplitude field quantity is assumed to be propor-

tional to λ.

The covariant Vlasov equation can be written as [9]

$$\frac{\partial f}{\partial t} + \dot{\mathbf{J}} \cdot \frac{\partial f}{\partial \mathbf{J}} + \dot{\Theta} \cdot \frac{\partial f}{\partial \Theta} = 0 \tag{3.37}$$

The collision operator has not been included because collisions are assumed to occur at a slower rate than wave-particle resonant interactions. A detailed treatment of the Hamiltonian motion must be carried out whenever we compute the diffusion coefficients. This is described in section (3.6).

3.5.3 The distribution function

A quasilinear equation describes the evolution of a zero order in λ distribution function under the action of waves. The equations of motion are derived from two Hamiltonians ordered in λ. Since they are linear in their Hamiltonians, it follows that they are also ordered in λ just as their respective Hamiltonians. To be consistent with the ordering of the equations of motion, we linearize the distribution function as we did with the Hamiltonian

$$f = f_0(\mathbf{J}, t_{QL}) + \lambda f_1(\mathbf{J}, \Theta, t) \tag{3.38}$$

The result is two time dependences that have different time scales. The quasilinear time present in the zero-order distribution function is the time scale over which diffusion and transport occurs. Its time scale is usually much longer than the average bounce period. The time dependence in the linear part of the distribution function results from the oscillation time of the wave and therefore, is usually much faster than the bounce time by over two orders of magnitude in a tokamak.

We can summarize the relations existing among the different times as

$$T_{wave} << T_{bounce} << T_{QL} \tag{3.39}$$

The equation that governs the time evolution of the constants of motion is given by the following formal equation

$$\dot{\mathbf{J}} = \dot{\mathbf{J}}_{\mathbf{1}} \tag{3.40}$$

In this equation, J changes only in the presence of a wave.
The equation of motion for the angles contains a zero order term in λ in addition to a linear term to yield the following definition

$$\dot{\Theta} = \Omega + \dot{\Theta}_{\mathbf{1}} \tag{3.41}$$

This equation states that the time evolution of Θ is caused by both the unperturbed and the perturbed fields. The zero order term Θ contains all the unperturbed motion frequencies in the poloidal, toroidal and gyrophase angles. We are now seeking an equation where the independent variables are the J's and the characteristic time is the quasilinear time T_{QL}.

3.5.4 Ansatz for linearized variables

To obtain a quasilinear equation, three time-averages are introduced to remove fast-time variables from the equation. Before doing so, we must make a few assumptions about the small-amplitude fields and distribution function. Further progress can be made by adopting an eikonal expression for the perturbed quantities

$$\dot{\mathbf{J}}_1 = \frac{\dot{\mathbf{J}}_1^{|} e^{i\psi_1} + c.c.}{2} \tag{3.42}$$

and

$$f_1 = \frac{f_1^{|} e^{i\psi_1} + c.c.}{2} \tag{3.43}$$

The quantities $\dot{\mathbf{J}}_1^{|}$ and $f_1^{|}$ are slowly varying in time and space with respect to the exponentials.

An alternative and more complex treatment of the fields and the distribution function can be obtained only by solving the self-consistent problem of a wave equation where the source term given by the current is related to the field through a conductivity [42, 43], as a function of the distribution function, although desirable this approach is not needed to pursue our investigation.

The phase for a monochromatic wave in a tokamak is given as

$$\psi_1 \equiv \phi_{gc} - \omega t + N\zeta + M\theta - k_\perp r \tag{3.44}$$

where M and N are, respectively, the poloidal and the toroidal wavenumbers.

3.5.5 Orbit-averaging operators

Here we define the orbit-averaging operators. The first phase-space average is over the wave frequency. The averaging operation is carried out in the following manner

$$< A >_\omega = \frac{2\pi}{\omega} \int_0^{2\pi/\omega} A \, dt \tag{3.45}$$

where A is any phase-space quantity. The next step is gyrophase averaging. Although wave-frequency and gyrophase averaging deal with time scales of the same order of magnitude, they are two distinct operations. Gyrophase averaging is defined as

$$< A >_{\phi_{gc}} = \frac{1}{2\pi} \int_0^{2\pi} A \, d\phi_{gc} \tag{3.46}$$

The last averaging is a multi-dimensional integration along the unperturbed orbit. Here we assume that the motion is periodic in both the poloidal and the toroidal angles. We formally carry out this last averaging

$$< A >_{\theta} \equiv \frac{1}{T_b} \int_0^{T_b} A \, dt_L \tag{3.47}$$

where t_L is the Lagrangian time when we follow the particle along its orbit.
Since we assumed axisymmetric fields, we can treat the toroidal angle as a dummy variable. Its purpose is to eliminate the Θ dependence in the quasilinear equation. This also means that the averaged equation deals with functions varying over timescales certainly longer than the average bounce period.
The poloidal bounce period for passing particles is defined as

$$T_b = \int_0^{2\pi} \frac{d\theta}{\dot{\theta}_0} \tag{3.48}$$

where θ_0 gives the equation of motion for the poloidal angle given in Appendix D. The poloidal bounce period for trapped particles is given by

$$T_b = 2 \int_{-\theta_b}^{\theta_b} \frac{d\theta}{\dot{\theta}_0} \tag{3.49}$$

where θ_b is the poloidal angle of the tip of the banana.

3.5.6 The quasilinear equation

We are ready to derive the quasilinear equation. We substitute the zero-order and linear variables of (3.38), (3.40), (3.41)-(3.43) into the Vlasov equation (3.37). See Appendix H for details. By doing so, we obtain the quasilinear averaged equation

$$\frac{\partial f_0(\mathbf{J})}{\partial t} + \frac{1}{4} < \dot{\mathbf{J}}_1^* \cdot \frac{\partial f_1}{\partial \mathbf{J}} + \dot{\theta}_1^* \frac{\partial f_1}{\partial \theta} + \dot{\zeta}_1^* \frac{\partial f_1}{\partial \zeta} + \dot{\phi}_1^* \frac{\partial f_1}{\partial \phi} + c.c. >_{\omega, \phi_{gc}, \theta} = 0 \tag{3.50}$$

The final result is that only zero order and quadratic terms survive the averaging process, where we used the following identity to average out the linear terms

$$< e^{i\psi_1} >_{\omega, \phi_{gc}, \theta} = 0 \tag{3.51}$$

The next step in the derivation is to neglect the terms that contain derivatives in Θ. This is justified because the poloidal, toroidal and gyrophase angles' diffusion do not directly lead to radial transport. The resulting quasilinear equation becomes

$$\frac{\partial f_0}{\partial t} + \frac{1}{4} < \dot{\mathbf{J}}_1^* \cdot \frac{\partial f_1}{\partial \mathbf{J}} + c.c. >_{\omega, \phi_{gc}, \theta} = 0 \tag{3.52}$$

This quasilinear equation has been averaged over the gyromotion and the bounce motion, therefore it is dependent only on the constants of motion and the quasilinear time. We next use the following vectorial relation for the second term in equation (3.52)

$$\nabla \cdot (f\mathbf{A}) = f \nabla \cdot \mathbf{A} + \mathbf{A} \cdot \nabla f \tag{3.53}$$

In addition, the averaging process does not change the functions of the constants of

motion

$$< g(\mathbf{J}) >_{\omega,\phi_{gc},\theta} = g(\mathbf{J}) \tag{3.54}$$

where g is any phase-space function. The derivative with respect to the constants $\mathbf{J}$ can therefore be taken out of the averaging brackets. By using (3.53) and (3.54) the quasilinear equation (3.52) becomes

$$\frac{\partial f_0}{\partial t} + \frac{1}{4}\frac{\partial}{\partial \mathbf{J}} \cdot < f_1^* \dot{\mathbf{J}}_1 + c.c. >_{\omega,\phi,\theta} - \frac{1}{4} < f_1^* \frac{\partial}{\partial \mathbf{J}} \cdot \dot{\mathbf{J}}_1 + c.c. >_{\omega,\phi,\theta} = 0 \tag{3.55}$$

We write the average of the second term in the quasilinear equation as

$$< f_1 \dot{\mathbf{J}}_1 >_{\omega,\phi,\theta} = \frac{1}{4} < f_1^{|*} \dot{\mathbf{J}}_1^{|} + f_1^{|} \dot{\mathbf{J}}_1^{|*} >_{\omega,\phi,\theta} = \frac{1}{2} Re < f_1^{|*} \dot{\mathbf{J}}_1^{|} >_{\omega,\phi,\theta} \tag{3.56}$$

The second term is the usual diffusion operator, while the last term yields the convective operator. The presence of the convective operator stems from the formalism for particle motion in an inhomogeneous magnetic field. In fact, if we were working with true action-angle variables in a homogeneous magnetic field, it is easy to show that the convective term would not be present in equation (3.55). In this instance, the Vlasov equation [10, 39] can be written as

$$\frac{\partial f}{\partial t} + \frac{\partial}{\partial \mathbf{J}} \cdot (f \dot{\mathbf{J}}) + \frac{\partial}{\partial \Theta} \cdot (f \dot{\Theta}) = 0 \tag{3.57}$$

When we angle-average out the last term in (3.57), the only term left is the diffusion operator term. Equation (3.57) is valid only if

$$\nabla \cdot \dot{\mathbf{z}} = 0 \tag{3.58}$$

where the vector $\mathbf{z}$ stands for the guiding-center variables $(\mathbf{J}, \Theta)$. Unfortunately, as shown by Littlejohn [9], the correct relationship for the divergence contains an extra term B^*, which is the Jacobian of the transformation from $(\mathbf{x}, \mathbf{v})$ to $\mathbf{z}$

$$\nabla \cdot (B^* \dot{\mathbf{z}}) = 0 \tag{3.59}$$

The comforting news is that B^* is approximately a constant for a small inverse aspect-ratio tokamak [2]. In a sense, the appearance of a convective term resulted because we adopted guiding center variables, which exhibit a Jacobian as a function of the guiding-center phase space. We conclude that a quasilinear equation in a inhomogeneous magnetic field contains both diffusive and convective terms.

To find the perturbed distribution function, the linearized Vlasov equation is

$$\frac{\partial f_1}{\partial t} + \dot{\mathbf{J}}_1 \cdot \frac{\partial f_0}{\partial \mathbf{J}} + \Omega \cdot \frac{\partial f_1}{\partial \Theta} = 0 \tag{3.60}$$

This equation is formally solved by applying the method of characteristics [44]. The slowly varying term of the perturbed distribution function is

$$f_1^{|} = -e^{-i\psi_L} \dot{\mathbf{J}}_1^{|} \cdot \frac{\partial f_0}{\partial \mathbf{J}} \int_0^\infty e^{i\psi_L} dt_L \tag{3.61}$$

where the phase ψ_L is

$$\psi_L(0, t_L) = \int_0^{t_L} (\omega - \omega_c - N\omega_\zeta - M\omega_\theta) dt_L' \tag{3.62}$$

[2] At leading order $B^* \approx B \approx B_0 - \frac{r}{R_0} B_0 cos(\theta)$

when the integrand set to zero yields the generalized cyclotron resonance condition. See Appendix H for a detailed derivation. To be exact, the perturbed distribution function should have included an extra term that represents the solution to the homogeneous differential equation. This term, called the "ballistic term", decays in time by phase mixing [44, 5]. The phase is periodic because the orbital motion is periodic at leading order, which allows us to write the following relation for the phase

$$\psi_L(0, t_L + T_b) = \psi_L(0, t_L) + \psi_L(t_L, t_L + T_b) = \psi_L(0, t_L) + \psi_0 \tag{3.63}$$

Since the motion is periodic the integral $\int_0^\infty e^{i\psi_L} dt_L$ can be written as an infinite series in the following manner [5]

$$\int_0^\infty = \int_0^{T_b} + \int_{T_b}^{2T_b} + ... = \sum_{n=0}^{\infty} I_n \tag{3.64}$$

where

$$I_n = \int_{nT_b}^{(n+1)T_b} e^{i\psi_L(0,t_L)} dt_L \tag{3.65}$$

The following relations hold as a consequence of periodicity

$$I_{n+1} = e^{-i\psi_0} I_n \tag{3.66}$$

and

$$I_n = e^{-in\psi_0} I_0 \tag{3.67}$$

By using equations (3.64), (3.65), (3.66) and (3.67) the phase integral results in a converging series

$$\int_0^\infty e^{i\psi_L} dt = \frac{I_0}{1 - e^{-i\psi_0}} = \frac{\int_0^{T_b} e^{i\psi_L} dt_L}{1 - e^{-i\psi_0}} \tag{3.68}$$

We assume that the initial phase is a random variable [44].

We average equation (3.68) over the initial phase ψ_0, assuming the probability distribution of the initial phase to be uniform. We take the real part of this average

$$Real(\frac{1}{2\pi}\int_0^{2\pi} d\psi_0 \frac{1}{1 - e^{-i\psi_0}}) = \frac{1}{2} \tag{3.69}$$

If we substitute equation (3.68) in the distribution function of equation (3.61) and take the complex conjugate of it, the result is

$$f_1^{|*} = \frac{-e^{i\psi_L} \dot{\mathbf{J}}_1^{|*} \cdot \frac{\partial f_0}{\partial \mathbf{J}} \int_0^{T_b} e^{-i\psi_L} dt_L}{2} \tag{3.70}$$

The averaged second term in equation (3.55) becomes

$$\frac{1}{2} < f_1^{|*} \dot{\mathbf{J}}_1^{|} >_\theta = -\frac{< e^{i\psi_L} >_\theta \dot{\mathbf{J}}_1^{|} \dot{\mathbf{J}}_1^{|*} \cdot \frac{\partial f_0}{\partial \mathbf{J}} \int_0^{T_b} e^{-i\psi_L} dt_L}{4} = \tag{3.71}$$

$$= -\frac{\dot{\mathbf{J}}_1^{|} \dot{\mathbf{J}}_1^{|*} \cdot \frac{\partial f_0}{\partial \mathbf{J}} | \int_0^{T_b} e^{-i\psi_L} dt_L|^2}{4T_b} \tag{3.72}$$

The quasilinear operator can be written as a divergence of a vector $\mathbf{Q}$ in the $\mathbf{J}$ space, where $\mathbf{Q}$ is given by

$$\mathbf{Q} = -\frac{1}{4T_b} | \int_0^{T_b} e^{-i\psi_L} dt_L|^2 (\dot{\mathbf{J}}_1^{|} \dot{\mathbf{J}}_1^{|*}) \cdot \frac{\partial f_0}{\partial \mathbf{J}} \tag{3.73}$$

The convective term can be derived as well. By using the perturbed distribution function obtained in equation (3.61) we find

$$- < f_1 \frac{\partial}{\partial \mathbf{J}} \cdot \mathbf{J_1} >_{\omega,\theta} = \frac{|\int_0^{T_b} e^{i\psi_L} dt_L|^2}{4T_b} (\frac{\partial}{\partial \mathbf{J}} \cdot \dot{\mathbf{J}}_1^{|*}) \dot{\mathbf{J}}_1^{|} \cdot \frac{\partial f_0}{\partial \mathbf{J}} \tag{3.74}$$

Appendix H contains a derivation of equation (3.74).
The quasilinear equation finally becomes

$$\frac{\partial f_0}{\partial t} = \frac{\partial}{\partial J_i} D_{ij} \frac{\partial f_0}{\partial J_j} - \frac{|\int_0^{T_b} e^{i\psi_L} dt_L|^2}{4T_b} (\frac{\partial}{\partial \mathbf{J}} \cdot \dot{\mathbf{J}}_1^{|*}) \dot{\mathbf{J}}_1^{|} \cdot \frac{\partial f_0}{\partial \mathbf{J}} \tag{3.75}$$

where the diffusion tensor is given by

$$D_{ij}(\mathbf{J}) = \frac{1}{T_b} \frac{|\int_0^{T_b} e^{i\psi_L} dt_L|^2 \dot{J}_i^{|} \dot{J}_j^{|*}}{4} \tag{3.76}$$

The normalized diffusion equation is written in terms of normalized variables

$$\frac{\partial f_0}{\partial \hat{t}} = \frac{\partial}{\partial \bar{J}_i} \hat{D}_{ij} \frac{\partial f_0}{\partial \bar{J}_j} - \frac{|\int_0^{T_b} e^{i\psi_L} / t_b dt_L|^2}{4\hat{T}_b} (\frac{\partial}{\partial \mathbf{J}} \cdot \dot{\bar{\mathbf{J}}}_1^{|*}) \dot{\bar{\mathbf{J}}}_1^{|} \cdot \frac{\partial f_0}{\partial \mathbf{J}} \tag{3.77}$$

where the normalized diffusion tensor is

$$\hat{D}_{ij}(\bar{\mathbf{J}}) = \frac{1}{\hat{T}_b} \frac{|\int_0^{T_b} e^{i\psi_L} / t_b dt_L|^2 \dot{\bar{J}}|_i \dot{\bar{J}}|^*_j}{4} \tag{3.78}$$

and the normalized quantities are defined as

$$\hat{t} = \frac{t_L}{t_b}; \hat{T}_b = \frac{T_b}{t_b}; \dot{\bar{J}}|_i = t_b \dot{J}|_i \tag{3.79}$$

where $t_b = v_{th}/R_0$.

The normalized constants of motion were defined in Chapter 2. The tensor is normalized to J_{i0}^2/t_b where the three normalizing constants are

$$\mathbf{J_0} = (\frac{1}{2}mv_{th}^2, \frac{mv_{th}^2}{2B_0}, mR_0v_{th}) \tag{3.80}$$

The next task is to compute the diffusion tensor of equation (3.78). The complex diffusion tensor can be computed numerically. However, for the purposes of this thesis we need only to find an approximation for the tensor in the limit of large aspect-ratio and for tokamaks with circular flux surfaces, a task that will be carried out in the next sections.

3.5.7 Wave Hamiltonian H_1 and relative equations of motion

The wave Hamiltonian in guiding-center coordinates is derived in Appendix G. The derivation is based on the following assumptions for the fast Alfven-wave

- the parallel electric field component is set to zero
- the eikonal form for the electric field has two different space scales
- the amplitude of the electric field varies slowly in a gyroradius length
- $k_\perp \rho << 1$; $k_\perp \simeq k_r$
- $|k_\perp| >> |k_\parallel|$

Since we are interested in particle motion in a tokamak geometry, the wavevector is written as a Fourier harmonic in poloidal and toroidal angles

$$\mathbf{k} = \frac{N}{R}\mathbf{e}_\zeta + \frac{M}{r}\mathbf{e}_\theta - k_\perp \mathbf{e}_\mathbf{r} \tag{3.81}$$

where N and M are the toroidal and poloidal numbers, respectively. We also decide to investigate the problem of fundamental harmonic, therefore we let $n = 1$ in the resonance relationship given by (3.30). The final form of our Hamiltonian is

$$H_1 = \hat{H}_1 e^{i\psi_1} \tag{3.82}$$

where the phase is

$$\psi_1(\mathbf{k}) = N\zeta + M\theta - k_\perp r - \omega t + \phi + \alpha + \pi/2 \tag{3.83}$$

and

$$\hat{H}_1 = \frac{iq}{2\omega}\sqrt{2B\mu/m}[J_0 e^{-i\alpha} E_{+k} + J_2 e^{i\alpha} E_{-k}] \tag{3.84}$$

For a complete derivation of (3.82) see Appendix G. The toroidal harmonics N and M are given by the antenna and reactor parameters, while the perpendicular wavevector $k_\perp$ is computed by solving the wave dispersion relation [5].

Once the wave Hamiltonian is computed, the linear equations of motion can be calculated using the Poisson brackets in Appendix B. These are

$$\dot{\mathbf{X}}^{\mathbf{1}}_{\mathbf{gc}} = \frac{i}{qB^*}\mathbf{b} \times \nabla\psi_1(k) H_1 \tag{3.85}$$

$$\dot{\mu}^1 = -\frac{iq}{m} H_1 \tag{3.86}$$

$$\dot{\phi}_{gc}^{1} = \frac{q}{m}\frac{\partial H_1}{\partial \mu} \tag{3.87}$$

$$\dot{v_{\|}}^{1} = -\frac{i\mathbf{B}^*}{mB^*} \cdot \nabla\psi_1(k) H_1 \tag{3.88}$$

where the phase gradient is expressed in toroidal coordinates

$$\nabla\psi_1(k) = \frac{N}{R}\mathbf{e}_\zeta + \frac{M}{r}\mathbf{e}_\theta - k_\perp \mathbf{e}_\mathbf{r} \tag{3.89}$$

Equation (3.89) is derived by taking the partial derivatives of the phase in equation (3.83) over the spatial coordinates ζ, θ and r.

3.6 Hamiltonian perturbation theory

The equation of motion in Hamiltonian theory is given by the Poisson bracket of the dynamical variable. If A is any variable in phase space, then the equation of motion can be formally written as

$$\dot{A} = [[A, H]] \tag{3.90}$$

The superscript 1 in the linear equations of motion means that they are linearly proportional to λ. A derivation of the linear equations of motion is given in Appendix I. where the Poisson brackets for guiding center variables are defined in Appendix B. Using our linearized Hamiltonian we can write the equation of motion as

$$\dot{A} = [[A, H_0 + H_1]] \tag{3.91}$$

At zero order in λ an operator $\frac{d}{dt_L}$ is defined as

$$\frac{dA}{dt_L} \equiv \dot{A} - [[A, H_0]] \tag{3.92}$$

This operator is equivalent to a Lagrangian time derivative along the unperturbed motion. The equation of motion can be rewritten as

$$\frac{dA}{dt_L} = [[A, H_1]] \tag{3.93}$$

To evaluate the change in the phase space variable that a particle undergoes through a resonance, equation (3.93) must be integrated along the unperturbed orbit

$$\delta A_{res} = \int_{res} [[A, H_1]] dt_L \tag{3.94}$$

where the integral includes every resonance along the unperturbed motion. Since we assumed an eikonal form for the linear Hamiltonian in equation (3.82), the resonance integral can be approximated

$$\delta A_{res} \approx [[A, \hat{H}_1]]_{res} \int_{res} e^{i\psi_L} dt_L \tag{3.95}$$

where $\hat{H}_1$ is given by equation (3.84) and ψ_L is the phase along the unperturbed orbit as defined by equation (3.62). This approximation is valid as long as the slowly varying part of the Hamiltonian is constant with respect to the change in phase. In a tokamak, resonances due to the fast-Alfven wave are localized, hence the approximation used above is valid.

3.6.1 Guiding-center variable changes caused by wave-particle resonance

We calculate the resonant changes in guiding-center variables by integrating (3.85)-(3.88) and using the approximate relation of (3.95). They are evaluated by stationary-phase integration, using the following vectorial relation applied to equation (3.89)

$$\mathbf{b} \times \nabla\psi_1 = (\frac{gN}{R} - \frac{fM}{r})\mathbf{e_r} - fk_\perp \mathbf{e}_\theta + gk_\perp \mathbf{e}_\zeta \tag{3.96}$$

The phase integral that occurs in these calculations is denoted by

$$I = \int_{res} e^{i\psi_L} dt_L \tag{3.97}$$

The change in radial coordinate due to resonance is

$$(\delta r)_{res} \approx [(\frac{fM}{r} - \frac{gN}{R})\frac{1}{\omega}\sqrt{\mu/(2mB)}(J_0 e^{-i\alpha}E_+ + J_2 e^{i\alpha}E_-)]_{res} I \tag{3.98}$$

The change in poloidal angle is

$$(\delta\theta)_{res} \approx [\frac{fk_\perp}{r\omega}\sqrt{\mu/(2mB)}(J_0 e^{-i\alpha}E_+ + J_2 e^{i\alpha}E_-)]_{res} I \tag{3.99}$$

The change in toroidal angle is

$$(\delta\zeta)_{res} \approx [-\frac{gk_\perp}{R}\sqrt{\mu/(2mB)}(J_0 e^{-i\alpha}E_+ + J_2 e^{i\alpha}E_-)]_{res} I \tag{3.100}$$

The change in magnetic moment is

$$(\delta\mu)_{res} \approx [(\frac{q}{m})^2 \frac{1}{\omega}\sqrt{(mB\mu/2)}(J_0 e^{-i\alpha}E_+ + J_2 e^{i\alpha}E_-)]_{res} I \tag{3.101}$$

The change in parallel velocity is

$$(\delta v_\parallel)_{res} \approx [(\frac{fN}{R} + \frac{gM}{r} + \frac{k_\perp v_\parallel}{\omega_c R} f sin\theta)\frac{q}{2m\omega}\sqrt{\frac{2\mu B}{m}}(J_0 e^{-i\alpha}E_+ + J_2 e^{i\alpha}E_-)]_{res} I \tag{3.102}$$

where we used the following approximation for the magnetic field

$$\frac{\mathbf{B}^*}{B} \approx \mathbf{b} - \frac{v_\parallel}{\omega_c}\frac{f sin\theta}{R_0}\mathbf{e_r} \tag{3.103}$$

The change in gyrophase is:

$$(\delta\phi)_{res} \approx (\frac{iq}{2m\omega}(2B\mu/m)^{1/2}(J_0 e^{-i\alpha}E_+ + J_2 e^{i\alpha}E_-))_{res}\frac{\partial I}{\partial \mu} \tag{3.104}$$

Equations (3.98)-(3.104) are derived in Appendix J. The changes in the guiding-center variables are computed for a single resonance, while in general, a particle can have multiple resonant interactions in one poloidal period. Extending the calculation of the changes to multiple resonances requires an accurate study of the stochasticity of the wave-particle interaction. In the next sections we will make use of the random-phase approximation [44].

3.6.2 Analytical evaluation of resonance integrals

This section focuses on localized wave-particle resonances in a tokamak. For a given equilibrium, the three constants of motion determine the magnitude of the interaction. For instance, passing particles interact less with the wave than trapped particles because they spend less time near the interaction region. The calculation of the changes in particle variables from a resonance involves the solution of a complex integral. We evaluate resonance integrals by using the stationary-phase approximation. The changes in particle variables are given by applying equation (3.95) to an eikonal quantity

$$\Delta A = \int_{res} \hat{A}_1 e^{i\psi_L} dt_L \approx \hat{A}_1|_{res} \int_{res} e^{i\psi_L} dt_L \tag{3.105}$$

where A is any phase-space quantity and ψ_L is given by equation (3.62). A phase integral in the resonance region is all that must be determined. To do so, the phase integral is written as

$$I = \int_{res} e^{i\psi_L} dt_L = t_b \int_{res} e^{i\psi_L} \frac{d\hat{t}}{d\theta} d\theta \tag{3.106}$$

where $t_b = R_0/v_\parallel$ and $\hat{t_L} = t_L/t_b$. The phase integral is evaluated along the unperturbed orbit in the resonance region. This integral will be calculated for both passing and trapped particles for a particular equilibrium in the next section.

3.7 Diffusion tensor for ICRF-heated tokamaks

3.7.1 Resonance integrals for passing particles

The resonance integral for passing particles is easy to compute. This is intuitive since passing particles have simple trajectories that follow the field lines at zero order in $\epsilon = m/q$.

For these particles, the parallel velocity is fairly constant throughout their orbits in most of the phase-space region. We ignore the Doppler shift for these particles by letting $M = N = 0$ in ψ_L given by equation (3.62) and evaluate the resonance integral (3.106) as

$$\frac{I}{t_b} \approx \int e^{i\psi_L(\theta)} \frac{a}{R_0} \frac{x(\theta)}{g} \frac{1}{\bar{v}_{\|th}(\theta)} d\theta \tag{3.107}$$

We used the leading order guiding-center term for the derivative of the poloidal angle from equation (D.2) and (D.3). We expand the phase ψ_L in θ around the resonance angle θ_r

$$\psi_L(\theta) \simeq \psi_L(\theta = \theta_r) + \frac{d\psi_L}{d\theta}|_{\theta=\theta_r} \cdot (\theta - \theta_r) + \frac{d^2\psi_L}{d\theta^2}|_{\theta=\theta_r} \cdot \frac{(\theta - \theta_r)^2}{2} + ... \tag{3.108}$$

The resonance condition is derived by the first derivative of the phase set to zero. This also yields the resonance poloidal angle

$$\omega = \frac{qB}{m} = \frac{qB_0}{m} \frac{1}{hf} \tag{3.109}$$

where the equilibrium quantities f and g are given by equations (2.9) and (2.37). The second derivative of the phase is

$$(\frac{d^2\psi_L}{d\theta^2})_{res} = (\frac{d}{d\theta}(\omega - \omega_c)t_b\frac{d\hat{t}}{d\theta})_{res} \approx -[(\frac{a}{R_0})^2\frac{\omega_{c0}t_b}{\bar{v}_{\|th}}\frac{x^2 sin\theta}{g}]_{\theta=\theta_r} \tag{3.110}$$

where we used

$$\frac{d\omega_c}{d\theta} \simeq \dot{\omega}_{c0}\frac{a}{R_0}xsin\theta \tag{3.111}$$

and $\frac{d\theta}{d\hat{t}} \simeq \bar{v}_{\|th}\frac{R_0}{a}\frac{g}{x}$. The stationary-phase method for the resonance integral yields the following result

$$\frac{I}{t_b} \approx \left(\frac{a}{R_0}\frac{x}{g}\frac{1}{\bar{v}_{\|th}}e^{i\psi_L}\right)_{res}\int e^{i\frac{\psi''_{Lres}}{2}(\theta-\theta_r)^2}d\theta \tag{3.112}$$

Taking the limits of the integral to be $+\infty$ and $-\infty$ in (3.112), we obtain

$$\frac{I}{t_b} \approx \sqrt{\frac{2\pi}{\omega_{c0}t_b}}\left(\frac{e^{i\psi_L}}{\sqrt{g|\bar{v}_{\|th}|sin\theta}}\right)_{res} e^{\pm i\pi/4} \tag{3.113}$$

where there is a + sign in the exponential when $(\psi''_L)_{res} < 0$ and vice versa. The resonance integral can be written as a function of the constants of the motion

$$\frac{I}{t_b} \approx \sqrt{\frac{2\pi}{\omega_{c0}t_b}}e^{i\psi_{Lres}}e^{\pm i\pi/4}\frac{1}{\sqrt{g(x_{res})\sqrt{\bar{v}^2 - \bar{\mu}}}} \tag{3.114}$$

where $x_{res} = \sqrt{\frac{1}{A_c}(\bar{p} + \sigma\sqrt{\bar{v}^2 - \bar{\mu}})}$.

3.7.2 Doppler-shifted resonance integrals for passing particles

We turn our attention to integrals that include Doppler-shift. The phase integral is analytically more complex than (3.107). The inclusion of the parallel velocity as well as drifts in the resonance relation is important when treating highly energetic particles. This section is restricted to the case of a passing particle interacting with a monochromatic spectrum wave (1 poloidal and 1 toroidal harmonic), while the general case of multichromatic waves is beyond the scope of this thesis. The resonance integral (3.106) is approximately given by

$$\frac{I}{t_b} \approx \int e^{i\psi_L} \frac{a}{R_0} \frac{x(\theta)}{g} \frac{1}{\bar{v}_{\|th}(\theta)} d\theta \tag{3.115}$$

where we included only the parallel velocity term in the poloidal angle derivative from (D.2) and (D.3) but the toroidal and poloidal wavenumbers M and N are different from zero. Drifts cannot be neglected when the particle resonates near $x = 0$ because the parallel velocity does not contribute to the poloidal angle motion. We expand the phase around a resonant point defined by the particle position where the phase does not change. At leading order in ϵ, the resonance condition is equivalent to

$$(\frac{d\psi_L}{d\theta})_{res} \approx (\omega_{tb} - \omega_{cb}) \frac{1}{\bar{v}_{\|th}} \frac{a}{R_0} \frac{x}{g} - M - N \frac{f}{gh} \frac{a}{R_0} x = 0 \tag{3.116}$$

where $\omega_{tb} = \omega t_b$,$\omega_{cb} = \omega_c t_b$ and we made use of $\frac{d\zeta}{dt} = \frac{\bar{v}_{\|th} f}{h}$.

To estimate the second derivative, we assume that the derivative of x with respect to θ is negligible. The second derivative of the phase is then given by

$$\frac{d^2\psi_L}{d\theta^2} \approx -\frac{d\omega_{cb}}{d\theta} (\frac{1}{\bar{v}_{\|th}} \frac{a}{R_0} \frac{x}{g}) - \omega_{cb} \frac{a}{R_0} \frac{x}{g} \frac{1}{d\theta} (\frac{1}{\bar{v}_{\|th}}) - N \frac{f}{g} \frac{a}{R_0} x \frac{d}{d\theta} (\frac{1}{h}) \tag{3.117}$$

Other important relations are

$$\frac{d\bar{v}_{\|}}{dt} \approx -\frac{\mu}{m}\frac{g}{r}\frac{B_0}{f}\frac{d}{d\theta}(\frac{1}{h}) \tag{3.118}$$

and

$$\frac{d}{d\theta}(\frac{1}{\bar{v}_{\|/th}}) = -\frac{t_b}{\bar{v}^3_{\|th}}\frac{a}{R_0}\frac{x}{g}\frac{d\bar{v}_{\|th}}{dt} \approx \frac{1}{2\bar{v}^3_{\|th}}\frac{xsin\theta}{f}\frac{a}{R_0}\bar{\mu} \tag{3.119}$$

where we made use of the following relation for the magnetic moment

$$\mu = \bar{\mu}\frac{m\bar{v}^2_{th}}{2B_0} \tag{3.120}$$

At leading order in ϵ, the second derivative of the phase is

$$\frac{d^2\psi_L}{d\theta^2} \approx -x^2 sin\theta(\frac{a}{R_0})^2[\frac{\omega_{cob}}{fg}\frac{1}{\bar{v}_{\|th}} + \frac{\omega_{cob}}{hgf^2}\frac{\bar{\mu}}{2\bar{v}^3_{\|th}} + N\frac{f}{g}] \tag{3.121}$$

where $\omega_{cb} = \omega_{cob}/(hf)$. The resonance integral can be evaluated asymptotically as done in equation (3.112)

$$\frac{I}{t_b} \approx [\frac{a}{R_0}\frac{x}{g}\frac{1}{\bar{v}_{\|th}}e^{-i\psi_L}]_{res}\sqrt{\frac{2\pi}{|\psi''_{res}|}}e^{\mp i\pi/4} \tag{3.122}$$

Equation (3.122) reduces to (3.113) if we neglect the last two terms on the right-hand side of equation (3.121). Moreover, equations (3.122) and (3.113) state that the larger the parallel velocity at resonance, the smaller the resonant interaction. This result can also be understood in terms of an effective resonance time spent by the particle

in the resonance vicinity [45].

3.7.3 Resonance integrals for trapped particles

We treat the case of resonance integrals for trapped particles without the Doppler shift. The integral can be written as

$$I = t_b \int_{res} e^{i(\omega_{tb}\hat{t}-\hat{\phi})} d\hat{t} \tag{3.123}$$

where $\hat{t} = t_L/t_b$,$\hat{\phi} = \int \omega_{cb} d\hat{t}$, $\omega_{tb} = \omega t_b$ and $\omega_{cb} = \omega_c t_b$.
Next, we consider the case of trapped particles whose tips are near the resonant layer. Heating on axis is also assumed, which means $\omega_{cb0} = \omega_{tb}$, where the normalized ion cyclotron frequency is approximated by $\omega_{cb} \approx \omega_{cb0}(1 - \epsilon cos\theta)$.

To solve the integral, we expand the phase between the two resonances where $\psi_L'' = 0$. This is possible because ψ_L' has two zeroes at its resonances. This entails the existence of a zero for the second derivative in the interval included between the two. Incidentally, the expansion point is roughly located near the tip because when neglecting drifts, the relationship $\psi_L'' = 0$ is equivalent to $d\theta/dt = 0$ which yields the location of the tip.
The resonance integral can be written as

$$I \approx t_b e^{-i\psi_t} \int e^{i(\psi_t'\hat{t} + \frac{\hat{t}^3}{6}\psi_t''')} d\hat{t} \tag{3.124}$$

where the phase time derivatives are given by

$$\psi_t = (\omega_{tb}\hat{t} - \int \omega_{cb} d\hat{t})_{tip} \tag{3.125}$$

$$\psi_t^{'} = \omega_{cb0}(\epsilon cos\theta)_{tip} \tag{3.126}$$

$$\psi_t^{''} = \omega_{cb0}(\epsilon^{'} cos\theta - sin\theta\theta^{'}\epsilon)_{tip} = 0 \tag{3.127}$$

$$\psi_t^{'''} = \omega_{cb0}(\epsilon^{''} cos\theta - 2sin\theta\theta^{'}\epsilon^{'} - cos\theta(\theta^{'})^2\epsilon - sin\theta\theta^{''}\epsilon)_{tip} \tag{3.128}$$

To find an analytic expression for the resonance integral, we transform the independent variable

$$\frac{\hat{t}^3}{2}\psi_t^{'''} = z^3 \tag{3.129}$$

and take the asymptotic integral by letting the limits of integration be $-\infty$ and $+\infty$. The solution is the well-known Airy function [45, 21]

$$Ai(y) = \frac{1}{2\pi}\int dx e^{i(yx+\frac{x^3}{3})} \tag{3.130}$$

The resonance integral becomes

$$I = t_b e^{i\psi_t}\frac{2\pi}{|\psi_t^{'''}/2|^{1/3}} Ai(\pm\frac{\psi_t^{'}}{|\psi_t^{'''}/2|^{1/3}}) \tag{3.131}$$

where the + is for $\psi_t^{'''} > 0$ and vice versa. This integral will now be written as a function of the constants of the motion, using the normalized constants. The first derivative of the phase is

$$\psi_t^{'} \approx \omega_{cb0}\frac{\bar{\mu} - \bar{v}^2}{\bar{\mu}} \tag{3.132}$$

$$\theta_t^{'} \approx \frac{\bar{v}_{\|th}}{q_s} \approx \pm\frac{\sqrt{\bar{v}^2 - \bar{\mu}}}{q_s} = 0 \tag{3.133}$$

$$\epsilon^{'} \approx -v_{dth} \approx -(\bar{v}^2 - \bar{\mu}/2)\frac{1}{\omega_{cb0}} \tag{3.134}$$

$$\theta^{''} \approx -\frac{\bar{\mu}}{2q_s} \tag{3.135}$$

where the safety factor is given by

$$q(\epsilon_{tip})_s = \frac{\epsilon_{tip}}{g(\epsilon_{tip})} \tag{3.136}$$

The third derivative of the phase can be further simplified to

$$\psi_t^{'''} \approx -\omega_{cb0}\theta^{''}\epsilon \approx \frac{\omega_{cb0}\bar{\mu}g}{2} \tag{3.137}$$

The argument of the Airy [21, 45] function becomes

$$y = \omega_{cb0}^{2/3}\frac{\bar{\mu} - \bar{v}^2}{\bar{\mu}^{4/3}}\frac{1}{(g/4)^{1/3}} \tag{3.138}$$

We can also approximate the Airy function with its asymptotic limit when $y < -0.3079$ as

$$Ai(y) \approx \frac{1}{\sqrt{2\pi}}\frac{1}{|y|^{1/4}} \tag{3.139}$$

Using this approximation yields a simple form for our resonance integral

$$I_t \approx t_b[e^{i\psi_L}\sqrt{\frac{2\pi}{\omega_{cb0}}}\frac{1}{(g/4)^{1/4}}\frac{1}{|\bar{\mu} - \bar{v}^2|^{1/4}}]_{tip} \tag{3.140}$$

When $-0.3 < y < 0$ we can approximate the Airy function as a constant: $Ai(y) \approx 0.28683$. The effect of a finite Doppler shift is not important for trapped particles

since most trapped particles ultimately have their banana tips on the resonance layer without Doppler-shift as shown by Hammett [21].

3.7.4 Analytical estimate of diffusion coefficients for passing particles

Next, we will derive an analytical approximation for the diffusion coefficient tensor of equation (3.78) for passing particles. To simplify this task, we neglect Doppler-shift and assume that the heating occurs on axis. The Doppler-shifted resonance integral can be computed following the procedure in section (3.6.2), however, we will not carry this out because it is not essential in finding the RF-driven fluxes.

The phase integral of equation (3.78) is given by equation (3.114). In evaluating the resonance integral over one bounce period, one must take into account the fact that there are two separate resonances occurring at $\theta = \pi/2$ and $\theta = 3\pi/2$ on the resonance layer. We assume these resonances are decorrelated by collision or wave stochasticity and hence we add them in the following manner

$$Real(\int_0^{T_b} \frac{e^{i\psi_L}}{t_b} dt) = Real(\frac{I_1 + I_2}{t_b}) = Real(\frac{\sqrt{2}|I_1|}{t_b}) \tag{3.141}$$

Equation (3.114) yields

$$|\int_0^{T_b} \frac{e^{i\psi}}{t_b} dt|^2 = \frac{4\pi}{\omega_{c0} t_b} \frac{1}{g(x_{res})\sqrt{\bar{v}^2 - \bar{\mu}}} \tag{3.142}$$

where $x_{res} = \sqrt{\frac{1}{A_c}(\bar{p} + \sigma\sqrt{\bar{v}^2 - \bar{\mu}})}$.

The bounce period for passing particles is given by equation (2.75) in Chapter 2.

The next step is to compute the $\bar{J}_i^{|}$'s for the energy, magnetic moment, and toroidal momentum.

The change $\delta\bar{J}_i^{|}$ in normalized magnetic moment is from equation (3.101)

$$|\delta\bar{\mu}| = \frac{t_b B_0 E_0}{\bar{v}_{th}\omega} \frac{q^2}{m^2} \sqrt{\bar{\mu}} (J_0(k_\perp \rho) e^{-i\alpha} \bar{E}_+(x_{res}) + J_2 e^{i\alpha} \bar{E}_-(x_{res})) \tag{3.143}$$

where the argument of the Bessel functions J_0 and J_2 at leading order in ϵ is given by

$$k_\perp \rho \approx k_\perp a \frac{R_0}{a} \frac{1}{\omega_{co} t_b} \tag{3.144}$$

and the fields are normalized to a spatial average of the electric field E_0. The change in normalized energy is given by

$$\delta \bar{v}^2 \simeq \delta \bar{\mu} \tag{3.145}$$

where the parallel energy change $\delta \bar{v}_\parallel$ has been neglected in equation (3.145). The change in parallel and perpendicular energy are compared when we derive the following relationship derived by differentiating the energy conservation relationship in the wave frame $v_\perp^2 + (v_\parallel - \omega/k_\parallel)^2 = constant$

$$\delta v_\perp / \delta v_\parallel \approx \omega / k_\parallel v_{th} >> 1 \tag{3.146}$$

The change in the toroidal momentum p_ϕ is primarily due to resonant changes in parallel velocity space $\delta v_\parallel$, therefore we differentiate equation (2.23) with respect to the parallel velocity to obtain

$$\delta \bar{p}_\phi \approx h f \delta \bar{v}_{\parallel th} \tag{3.147}$$

The change δx in the guiding-center radial position is neglected in deriving equation (3.147). δx is due to the diamagnetic drift, which is small compared to the parallel

energy drifts in Tokamaks for frequencies of the order of the ion cyclotron frequency [46]. We assume a monochromatic wave having a toroidal wavenumber N, then the change in absolute value of the toroidal momentum is approximately given by

$$|\delta\bar{p}_\phi| \approx \frac{qE_0}{m\omega v_{th}} \frac{f^2 N}{2} \sqrt{\bar{\mu}} (J_0 e^{-i\alpha} \bar{E}_+(x_{res}) + J_2 e^{i\alpha} \bar{E}_-(x_{res})) \tag{3.148}$$

where we kept only the first term on the right-hand side of (3.102) for $\delta v_{||}$, divided equation (3.102) by v_{th} and substituted t_b for I for normalization. The diffusion coefficient tensor for passing particles can be obtained from the diffusion tensor of (3.78), using the poloidal period of (2.75), the phase integral of (3.142) and the changes $\delta\bar{J}_i^{\dagger}$ given by (3.143), (3.145) and (3.148)

$$\hat{\mathbf{D}}_{\mathbf{pass}} = A_{pass} \begin{pmatrix} D_{\bar{\mu}\bar{\mu}} & D_{\bar{\mu}\bar{v}^2} & D_{\bar{\mu}\bar{p}_\phi} \\ D_{\bar{v}^2\bar{\mu}} & D_{\bar{v}^2\bar{v}^2} & D_{\bar{v}^2\bar{p}_\phi} \\ D_{\bar{p}_\phi\bar{\mu}} & D_{\bar{p}_\phi\bar{v}^2} & D_{\bar{p}_\phi\bar{p}_\phi} \end{pmatrix}$$

where

$$A_{pass} = \frac{\pi}{\omega_{c0} t_b} (\frac{t_b B_0 E_0 q^2}{v_{th} \omega m^2})^2 (JE)^2 \tag{3.149}$$

and

$$(JE)^2 = (J_0 \bar{E}_+)^2 + (J_2 \bar{E}_-)^2 \tag{3.150}$$

The diffusion coefficients are

$$D_{\bar{\mu}\bar{\mu}} = D_{\bar{\mu}\bar{v}^2} = D_{\bar{v}^2\bar{\mu}} = D_{\bar{v}^2\bar{v}^2} \tag{3.151}$$

where

$$D_{\bar{\mu}\bar{\mu}} = \frac{\bar{\mu}}{\hat{T}_{bpass}} \frac{1}{g\sqrt{v^2 - \bar{\mu}}} \tag{3.152}$$

and

$$D_{\bar{\mu}\bar{p}_\phi} = D_{\bar{v}^2\bar{p}_\phi} = D_{\bar{p}_\phi\bar{\mu}} = D_{\bar{p}_\phi\bar{v}^2} = \frac{f^2 N}{2\omega_{c0} t_b} D_{\bar{\mu}\bar{\mu}} \tag{3.153}$$

The diffusion coefficient in toroidal momentum space is

$$D_{\bar{p}_\phi,\bar{p}_\phi} = (\frac{f^2 N}{2\omega_{c0} t_b})^2 D_{\bar{\mu},\bar{\mu}} \tag{3.154}$$

All spatial quantities (g, fields) are evaluated at $x = x_{res}$ where

$$x_{res} = \sqrt{\frac{1}{A_c}(\bar{p} + \sigma\sqrt{\bar{v}^2 - \bar{\mu}})} \tag{3.155}$$

The diffusion coefficients of equation (3.151) relate to heating as they describe change in the minority ion perpendicular energy, while the diffusion coefficient in (3.154) relates to radial transport since any change in the minority ion toroidal momentum can lead to a change in radial position as defined by equation (2.31).

3.7.5 Analytical estimate of diffusion coefficients for trapped particles

The diffusion coefficients for trapped particles are derived in the case of heating on axis. If we neglect the Doppler shift effect, then resonant trapped particles have four localized resonances per poloidal period. The resonance locus is given by the intersection of the orbit with resonant layer. If the banana tips are close to the resonant layer then the two close resonances merge and can be treated as a single interaction as done in section (3.6.3). We also assume, as we did for passing particles, that the ion motion is stochastic so that resonances between the two tips are decorrelated. The phase integral in a poloidal period is given by

$$Real(\int_0^{T_b} \frac{e^{i\psi}}{t_b} dt) = Real(\frac{I_1 + I_2}{t_b}) = Real(\frac{2I_1}{t_b}) \tag{3.156}$$

where the phase integral is approximated by equation (3.140) when $y < -0.3079$

$$\int_0^{T_b} e^{i\psi_L} \frac{dt}{t_b} = e^{i\psi_t} \frac{2\sqrt{2\pi}}{|\omega_{cb0}\bar{\mu}g_t/4|^{1/3}} |y|^{-1/4} \tag{3.157}$$

where y is defined by equation (3.138). The quantity $y > 0$ measures the distance of the banana tip from the resonant layer and is defined to be negative when the tip intersects the resonant layer from the high-field side of the torus. If the banana tip is located on the low-field side of the torus, the resonant interaction can still occur, however, it is mild and can be neglected when $y > 0$. To avoid the singularity that arises when the tip of the banana intersects the resonance layer, we take the asymptotic limit of the phase integral when $0 > y > -0.3079$, namely for banana tips almost on resonance

$$\int_0^{2\pi} e^{-i\psi} \frac{dt}{t_b} = e^{-i\psi_t} 0.28 \frac{4\pi}{|\frac{\omega_{cb0}\bar{\mu}g}{4}|^{1/3}} \tag{3.158}$$

where we let $Ai(y) \approx 0.28$. The diffusion coefficient tensor for trapped particles in a large aspect ratio tokamak, at leading order in ϵ when $y < -0.3079$ is given by

$$\hat{\mathbf{D}}_{\mathbf{trapp}} = A_{trapp} \begin{pmatrix} D_{\bar{\mu}\bar{\mu}} & D_{\bar{\mu}\bar{v}^2} & D_{\bar{\mu}\bar{p}_\phi} \\ D_{\bar{v}^2\bar{\mu}} & D_{\bar{v}^2\bar{v}^2} & D_{\bar{v}^2\bar{p}_\phi} \\ D_{\bar{p}_\phi\bar{\mu}} & D_{\bar{p}_\phi\bar{v}^2} & D_{\bar{p}_\phi\bar{p}_\phi} \end{pmatrix}$$

where

$$A_{trapp} = \frac{4\pi}{\omega_{c0} t_b} \left(\frac{t_b B_0 E_0 q^2}{v_{th} \omega m^2}\right)^2 (JE)^2 \tag{3.159}$$

and

$$(JE)^2 = (J_0 \vec{E}_+)^2 + (J_2 \vec{E}_-)^2 \tag{3.160}$$

The diffusion coefficients are

$$D_{\bar{\mu}\bar{\mu}} = D_{\bar{\mu}\bar{v}^2} = D_{\bar{v}^2\bar{\mu}} = D_{\bar{v}^2\bar{v}^2} \tag{3.161}$$

where

$$D_{\bar{\mu}\bar{\mu}} = \frac{\bar{\mu}}{\hat{T}_{btrapp}} \frac{1}{\sqrt{g}\sqrt{|\bar{v}^2 - \bar{\mu}|}} \tag{3.162}$$

and

$$D_{\bar{\mu}\bar{p}_\phi} = D_{\bar{v}^2\bar{p}_\phi} = D_{\bar{p}_\phi\bar{\mu}} = D_{\bar{p}_\phi\bar{v}^2} = \frac{f^2 N}{2\omega_{c0} t_b} D_{\bar{\mu}\bar{\mu}} \tag{3.163}$$

The diffusion coefficient in toroidal momentum for trapped particles is

$$D_{\bar{p}_\phi,\bar{p}_\phi} = (\frac{f^2 N}{2\omega_{c0} t_b})^2 D_{\bar{\mu},\bar{\mu}} \tag{3.164}$$

The diffusion coefficient tensor for trapped particles in a large aspect ratio tokamak when $0 > y > -0.3079$ using (3.158) is given by

$$\hat{\mathbf{D}}_{\mathbf{trapp}} = A_{trapp} \begin{pmatrix} D_{\bar{\mu}\bar{\mu}} & D_{\bar{\mu}\bar{v}^2} & D_{\bar{\mu}\bar{p}_\phi} \\ D_{\bar{v}^2\bar{\mu}} & D_{\bar{v}^2\bar{v}^2} & D_{\bar{v}^2\bar{p}_\phi} \\ D_{\bar{p}_\phi\bar{\mu}} & D_{\bar{p}_\phi\bar{v}^2} & D_{\bar{p}_\phi\bar{p}_\phi} \end{pmatrix},$$

where

$$A_{trapp} = \frac{(0.28\pi)^2}{(\omega_{c0} t_b)^{2/3}} (\frac{t_b B_0 E_0 q^2}{v_{th} \omega m^2})^2 (JE)^2 \tag{3.165}$$

and

$$(JE)^2 = (J_0 \bar{E}_+)^2 + (J_2 \bar{E}_-)^2 \tag{3.166}$$

The diffusion coefficients are

$$D_{\bar{\mu}\bar{\mu}} = D_{\bar{\mu}\bar{v}^2} = D_{\bar{v}^2\bar{\mu}} = D_{\bar{v}^2\bar{v}^2} \tag{3.167}$$

where

$$D_{\bar{\mu}\bar{\mu}} = \frac{(\bar{\mu})^{1/3}}{\hat{T}_{btrapp}} \frac{1}{(g)^{2/3}} \tag{3.168}$$

and

$$D_{\bar{\mu}\bar{p}_\phi} = D_{\bar{v}^2\bar{p}_\phi} = D_{\bar{p}_\phi\bar{\mu}} = D_{\bar{p}_\phi\bar{v}^2} = \frac{f^2 N}{2\omega_{c0} t_b} D_{\bar{\mu}\bar{\mu}} \tag{3.169}$$

The diffusion coefficient in toroidal momentum for trapped particles whose tips are near the resonant layer is

$$D_{\bar{p}_\phi,\bar{p}_\phi} = (\frac{f^2 N}{2\omega_{c0} t_b})^2 D_{\bar{\mu},\bar{\mu}} \tag{3.170}$$

All spatial quantities (g, fields) are evaluated at $x = x_{tip}$ where

$$x_{tip} = \sqrt{\frac{1}{A_c} \bar{p}_\phi} \tag{3.171}$$

As pointed out in the passing particle section, the coefficients of (3.167) give heating, while the coefficient in equation (3.170) gives the neoclassical radial transport of the banana tips of the trapped ions.

3.8 Scaling of diffusion coefficients

3.8.1 Tokamak parameters

We will now evaluate diffusion coefficients for a standard tokamak with the following parameters

- safety factor q ≈ 2 ; major radius $R_0 = 1.5$m
- inverse aspect ratio $\frac{a}{R_0} = \frac{1}{3}$
- toroidal magnetic field amplitude B = 4 T
- toroidal current I = 10^6 Ampere
- the ion minority species has 100 Kev temperature
- the ion majority thermal speed is approximately $3.0 \times 10^5 m/sec$
- the electron density is $n_e = 2.0 \times 10^{13} m^{-3}$
- the minority density is $n_{min} = 0.05 n_e$
- a typical toroidal wavenumber for tokamak experiments is $N = 10$.

The field amplitude can be roughly estimated if the average wave power density $< P >$ is known. The following formula [3, 21] relates the field amplitude to the averaged power density $< P >$

$$< P > (W/m^3) = n_{min} \frac{\pi q^2}{m} |E_+|^2 \frac{1}{\sqrt{2\pi k_\parallel^2 v_\parallel^2}} \approx 10 |E_+|^2 \qquad (3.172)$$

where the electric field amplitude is given in V/m. Equation (3.172) is written for a Maxwellian plasma in the limit of resonance on axis and neglecting $k_\perp$ and E_- as pointed out by Hammett [21].

3.8.2 Passing particle diffusion coefficient evaluation

The characteristic bounce period is approximated as

$$\hat{T}_{bpass} = \frac{4q_s}{\sqrt{\bar{v}^2 - (1-\hat{\epsilon})\bar{\mu}}K(k_p)} \approx \frac{4\pi}{\sqrt{\bar{v}^2 - \bar{\mu}}} \tag{3.173}$$

where we let $K(k_p) \approx \pi/2$ for a very passing particle.
The magnitude of the coefficient A_{pass} is estimated to be

$$A_{pass} \approx \frac{E_+^2}{7 * 10^7} \tag{3.174}$$

where the electric field amplitude is measured in V/m. The overall diffusion coefficient for the normalized magnetic moment is

$$A_{pass}D_{\bar{\mu}\bar{\mu}} \approx \frac{1}{10^9}\frac{\bar{\mu}E_+^2}{g} \tag{3.175}$$

We recall that the heating coefficients are

$$D_{\bar{\mu}\bar{\mu}} = D_{\bar{\mu}\bar{v}^2} = D_{\bar{v}^2\bar{\mu}} = D_{\bar{v}^2\bar{v}^2} \tag{3.176}$$

The cross-coefficients are given by

$$D_{\bar{\mu}\bar{p}_\phi} = D_{\bar{v}^2\bar{p}_\phi} = D_{\bar{p}_\phi\bar{\mu}} = D_{\bar{p}_\phi\bar{v}^2} = \frac{f^2N}{2\omega_{c0}t_b}D_{\bar{\mu}\bar{\mu}} \approx 0.5 \times 10^{-2}D_{\bar{\mu}\bar{\mu}} \tag{3.177}$$

Equation (3.177) states that convective transport due to a change in toroidal momentum is a slow process compared to heating for passing particles. The diffusion coefficient for the toroidal momentum is given by

$$D_{\bar{p}_\phi \bar{p}_\phi} \approx \frac{2.5}{10^5} D_{\bar{\mu}\bar{\mu}} \tag{3.178}$$

Equation (3.178) indicates that spatial diffusion is slower than velocity space diffusion by two orders of magnitude. This conclusion was also reached by Chen [13] using a different approach.

3.8.3 Passing particle coefficients discussion

The overall diffusion coefficient dependence can be derived from equations (3.172) and (3.175)

$$A_{pass} D_{\bar{\mu}\bar{\mu}} \approx \frac{< P >}{10^{10}} \frac{\bar{\mu}}{g} \tag{3.179}$$

where $< P >$ has the dimensions of MW/m^3. The diffusion coefficient is linearly proportional to $\bar{\mu}$. Since the diffusion is mainly in perpendicular energy, the heating process becomes more efficient as the minority ion perpendicular energy increases with time.

The normalized magnetic moment is equal to unity for thermal particles and is usually one or two orders of magnitude larger for energetic particles. The coefficient is also linearly proportional to the wave power density. This parameter is given by the intensity of the RF source. A representative number for $< P >$ can be $10 MW/m^3$, which entails a reasonable electric field amplitude of 10 V/cm [21, 13] according to equation (3.172).

Finally, the coefficient is inversely proportional to g, which represents the projection of the magnetic field versor in the poloidal direction. It is evident that g approaches zero as we approach the magnetic axis. One might conclude that the diffusion coefficient tends to infinity as we get nearer to the magnetic axis. In reality, our approximate formula breaks down near the axis. This can be understood when we realize we are

not allowed to neglect drifts when a particle resonates near the magnetic axis. To obtain a more exact diffusion coefficient, one has to compute the resonance integrals including the full particle motion and the Doppler-shift.
We can approximate $g \approx \frac{x}{5}$ for standard tokamak parameters using equation (2.63). The overall diffusion coefficient can span three orders of magnitude depending on the phase-space region, wave power density, and equilibrium fields.

3.8.4 Trapped particle diffusion coefficients

The characteristic bounce period for trapped particles is given by

$$\hat{T}_{btrapp} = \frac{8q_s}{\sqrt{2\hat{\epsilon}\bar{\mu}}} K(1/k_t) \approx \frac{30}{\sqrt{\hat{\epsilon}}\sqrt{\bar{\mu}}} \tag{3.180}$$

For trapped particles whose tips touch the resonant layer on axis, the bounce period does not differ more than one order of magnitude from this value. The constant A_{trapp} is approximately given by

$$A_{trapp} \approx \frac{4}{7}\frac{E_+^2}{10^7} \tag{3.181}$$

The overall diffusion coefficient for trapped particles is

$$A_{trapp} D_{\bar{\mu}\bar{\mu}t} \approx \frac{E_+^2}{4 \times 10^8}\, \bar{\mu}^{3/2} \sqrt{\frac{\hat{\epsilon}}{g}}\, \frac{1}{\sqrt{|\bar{v}^2 - \bar{\mu}|}} \tag{3.182}$$

The ratio $\frac{\hat{\epsilon}}{g}$ is the safety factor, hence it is known to be of the order of unity. We also recall that the following diffusion coefficients are related to heating

$$D_{\bar{\mu}\bar{\mu}} = D_{\bar{\mu}\bar{v}^2} = D_{\bar{v}^2\bar{\mu}} = D_{\bar{v}^2\bar{v}^2} \tag{3.183}$$

As for the passing particles, the cross-coefficients are given by

$$D_{\bar{\mu}\bar{p}_\phi} = D_{\bar{v}^2\bar{p}_\phi} = D_{\bar{p}_\phi\bar{\mu}} = D_{\bar{p}_\phi\bar{v}^2} = \frac{f^2 N}{2\omega_{c0} t_b} D_{\bar{\mu}\bar{\mu}} \approx 0.5 \times 10^{-2} D_{\bar{\mu}\bar{\mu}} \tag{3.184}$$

The last coefficient is given by

$$D_{\bar{p}_\phi\bar{p}_\phi} \approx \frac{2.5}{10^5} D_{\bar{\mu}\bar{\mu}} \tag{3.185}$$

The same conclusions drawn for passing particle coefficients also apply to trapped particles.

3.8.5 Trapped particle coefficients discussion

The overall diffusion coefficient for trapped particles has the following dependence

$$A_{trapp} D_{\bar{\mu}\bar{\mu}t} \approx \frac{< P >}{4 \times 10^9} \bar{\mu}^{3/2} \frac{1}{\sqrt{|\bar{v}^2 - \bar{\mu}|}} \tag{3.186}$$

Equation (3.186) applies to particles that have banana tips close to the resonance layer. These particles are heated more efficiently than the passing ones.
This is because the diffusion coefficient in velocity space is proportional to $\bar{\mu}^{3/2}$. It is worth noting that the only factor dependent on the particle position is $\frac{1}{\sqrt{|\bar{v}^2-\bar{\mu}|}}$. This factor becomes larger as the particle banana tips get closer to the resonance layer. For trapped particles whose tips are exactly on the resonant layer, the singularity of (3.186) is resolved by using the Airy function. The magnitude of the diffusion coefficient can easily span three orders of magnitude depending on phase-space region, power density and equilibrium parameters. It is important to point out that these scalings are rough analytical approximations whose validity applies to a restricted phase space domain and when the Doppler-shift can be neglected.

3.9 Summary

In this chapter, we derived general quasilinear coefficients for the constants of motion. They show that the minority heating time scale is much faster than convective transport and diffusive transport time scales. Moreover, the heating process is more effective for trapped particles and increases more than linearly with higher minority temperature. This scaling is probably the main reason why fast wave minority heating is an effective method to heat the plasma. For future investigation, we note that a parallel electric field component of the wave was not included in our model. Its presence in a quasilinear formulation may lead to an interesting mechanism for enhanced transport. The importance of a parallel electric field component can be evaluated on the basis of a self-consistent model since the parallel velocity diffusion arising from a parallel electric field may lead to a considerable distortion of the distribution function [47].

Chapter 4

Collision operators for fast minority ions

4.1 Introduction

In this chapter, we treat the fast ion collision operator [3]. This operator is characterized by two fundamental time scales: the slowing-down time scale and the pitch-angle scattering time scale. In the first section, the fast ion collision operator is presented. In the second section, we compute the Coulomb collision coefficients to compare the collision times due to electron and ion background species. In the last section, collisions are examined through a Monte Carlo approach. This formulation is highly instructive because it separates the convective collision terms from the diffusive ones.

4.2 Collision diffusion coefficients for fast ions

In a RF-heated tokamak, an anisotropic minority species is colliding with Maxwellian electrons and ions. Minority ions heated by the fast wave can become much hotter than the majority ion species in a strong RF-heating regime. However, the average tail velocity is usually smaller than the electron thermal velocity because of the large difference in mass between electrons and ions. We can, therefore, assume the following inequality for the minority tail velocity

$$v_{thi} << v_{min} << v_e \tag{4.1}$$

An example can be given for Alcator parameters where $T_{deut} = T_e = 3keV$ and $T_{min} \approx 50keV$, computing the velocities yields

$$v_{thi} \approx 4.0\times10^5(m/sec) << v_{min} \approx 2.0\times10^6(m/sec) << v_e \approx 2.0\times10^7(m/sec) \tag{4.2}$$

Equation (4.1) is the fundamental assumption that leads to a relatively simple collision operator for fast ions. The other assumption is that the minority density is much smaller than the background species density, hence minority self collisions are not included in the collision operator. In pitch-angle coordinates (v, ξ), the collision operator is derived in Appendix K, equation (K.29) can be written as [3, 5]

$$(\frac{\partial f}{\partial t})_c = \frac{1}{\tau_s v^3}[v\frac{\partial}{\partial v}(v^3 + v_c^3)f + Z_{eff2}\frac{v_c^3}{2}\frac{\partial}{\partial \xi}(1-\xi^2)\frac{\partial f}{\partial \xi}] \tag{4.3}$$

where the critical velocity is given by

$$v_c = (\frac{3\sqrt{\pi}m_e Z_{eff1}}{4m_{min}})^{1/3}\, v_{the} = 0.09(\frac{m_H}{m_{min}}Z_{eff1})^{1/3}\, v_{the} \tag{4.4}$$

and the effective charge is $Z_{eff1} = \frac{n_i Z_i^2 m_m}{n_e m_i}$.
The slowing down time is given by

$$\tau_s = \frac{\epsilon_0 m_m^2 v_c^3}{e^2 e_m^2 Z_{eff1} n_e ln\Lambda} \tag{4.5}$$

The effective charge by the background ions is

$$Z_{eff2} = \frac{n_i Z_i^2}{n_e Z_{eff1}} \tag{4.6}$$

The electron drag is equal to the ion drag when the minority ion velocity is equal to the critical velocity. In a strong minority RF-heating regime, minority ions can exceed the critical velocity making the electron drag the main contribution.

4.2.1 Coulomb diffusion coefficients

An alternative and equivalent approach to the study of collisions is given by the collision Coulomb coefficients [48]. The slowing-down Coulomb diffusion coefficient [1] is given by

$$< \Delta v_{\|} >= -v \sum_{f=i,e} \frac{C_f l_f^2}{v} (1 + \frac{m_m}{m_f}) G(l_f v) \tag{4.7}$$

It is also called the dynamical friction coefficient and represents the rate at which minority ions are slowed down in the direction parallel to their motion. The symbols $\|$ and $\perp$ refer to the parallel and perpendicular direction of motion, respectively. The other diffusion coefficient is the energy-exchange rate of increase

$$< (\Delta v_{\|})^2 >= v^2 \sum_{f=i,e} \frac{C_f}{v^3} G(l_f v) \tag{4.8}$$

and the deflection rate is

$$< (\Delta v_{\perp})^2 >= v^2 \sum_{f=i,e} \frac{C_f}{v^3} [\Phi(l_f v) - G_(l_f v)] \tag{4.9}$$

where $l_f^2 = m_f / 2T_f$ and

[1] the terminology and the symbolism adopted in this chapter are consistent with Spitzer's and Stix's works [48, 3]

$$C_f = \frac{8\pi n_f Z_f^2 Z^2 e^4 ln\Lambda}{m_m^2} \tag{4.10}$$

The error function is defined as

$$\Phi(x) = \frac{2}{\sqrt{\pi}} \int_0^x dy e^{-y^2} \tag{4.11}$$

The Chandrasekhar function is

$$G(x) = \frac{\Phi(x) - x\Phi'(x)}{2x^2} \tag{4.12}$$

Stix [3] computed two simple approximations for the error and the Chandrasekhar function. These approximations give the right asymptotic behavior of the two functions, while at intermediate energies give a fractional error that is less than thirty percent.

These approximations are

$$G(x) \approx \frac{\epsilon x}{1 + 2\epsilon x^3} \tag{4.13}$$

and

$$\Phi(x) \approx \epsilon \frac{3x + 2x^3}{1 + 2\epsilon x^3} \tag{4.14}$$

where $\epsilon = \frac{2}{3\sqrt{\pi}}$.

We will use these approximations in computing the Coulomb coefficients numerically.

4.2.2 Ion contribution to Coulomb coefficients

Minority ions are much more energetic than majority ions, hence it is convenient to use the asymptotic forms of the Coulomb functions.

For $x_i = l_i v >> 1$, we have

$$G(x) \approx \frac{1}{2x^2} \; ; \; \Phi(x) \approx 1 \tag{4.15}$$

The energy-normalized diffusion coefficients due to ion-ion collision for a deuterium majority species are

$$\frac{< \Delta v_{\|} >}{v} = -\frac{C_i}{2}(1 + \frac{m_m}{m_f})\frac{l_i^3}{x_i^3} \tag{4.16}$$

$$\frac{< (\Delta v_{\|})^2 >}{v^2} = \frac{C_i}{2}\frac{l_i^3}{x_i^5} \tag{4.17}$$

$$\frac{< (\Delta v_{\perp})^2 >}{v^2} = \frac{C_i l_i^3}{x_i^3} \tag{4.18}$$

4.2.3 Electron contribution to the Coulomb coefficients

The minority ion velocity is usually less than the electron thermal velocity, however, for very energetic particles colliding with the cold edge of the plasma, $x_e = l_e v$ can become of the order of unity. For instance, this occurs when 1 MeV hydrogen ions collide with 0.1 KeV electrons.

We keep the full functional dependence for the minority ion-electron diffusion coefficients to obtain

$$\frac{< \Delta v_{\|} >}{v} = -\frac{C_e l_e^3}{x_e}\frac{m_m}{m_e}G(x_e) \tag{4.19}$$

$$\frac{<(\Delta v_{\parallel})^2>}{v^2} = \frac{C_e l_e^3}{x_e^3} G(x_e) \tag{4.20}$$

$$\frac{<(\Delta v_{\perp})^2>}{v^2} = \frac{C_e l_e^3}{x_e^3} [\Phi(x_e) - G(x_e)] \tag{4.21}$$

4.2.4 Comparison between the electron and ion Coulomb coefficients

We now compare the minority ion-electron and the ion-ion collision coefficients. The bulk electron and ion species can be taken to have the same density and approximately the same temperature

$$n_e \approx n_i \; ; \; T_e \approx T_i \tag{4.22}$$

The two constants C_e and C_i are approximately equal.
We also take a plasma density $n \approx 10^{21}\ m^{-3}$ and an electron temperature of 1 KeV, which represents standard Alcator C-Mod parameters. It is simpler to work with one normalized velocity variable, therefore, we make the substitution in the ion-ion coefficients

$$x_i = 60.43 * x_e \tag{4.23}$$

The three characteristic collision times given by (4.6), (4.7) and (4.8) for both background electrons and ions are computed numerically versus x_e and plotted in figures

(4.1), (4.2) and (4.3), respectively. In figure (4.1), the longitudinal slowing-down frequency for backgorund ions is larger than the electron counterpart for $x_e < 0.1$. For mildly energetic ions ($x_e >= 0.2$) the electron longitudinal slowing-down frequency dominates the ion contribution. In figure (4.2), the energy-exchange rate electron contribution is much larger than the ion contribution except for very small x_e. Finally, the deflection frequency in figure (4.3) is primarily due to background ions because of their large mass, but the electron contribution is of equal importance at high energies.

4.2.5 Collision diffusion coefficients for delta distribution function

An important class of simulation techniques is given by Monte Carlo methods. These methods are based on the use of a random function to generate random kicks in velocity space. The probability function of random kicks is not generally known, however moments of the probability function can be derived from the equations of motion and conservation. In this case, we start from the collision operator to derive the moments of random velocity kicks.

The collision operator is made up of diffusive and convective terms in velocity space. If our distribution function is initially a delta function in energy and pitch-angle, collisions will make the delta function spread in velocity and move toward lower energies. The distribution function is

$$f = \delta(v - v_0)\delta(\xi - \xi_0) \tag{4.24}$$

The convective coefficients are

$$< \Delta v >= -\frac{v + v_c^3/v^2}{\tau_s}\delta t \tag{4.25}$$

and

$$< \Delta\xi >= -\frac{Z_{eff2}}{\tau_s}\frac{v_c^3}{v^3}\xi\delta t \tag{4.26}$$

The diffusive spreads in velocity space for fast ions are

$$< \Delta v\Delta v >= 0 \tag{4.27}$$

and

$$< \Delta\xi\Delta\xi >= \frac{Z_{eff2}}{\tau_s}\frac{v_c^3}{v^3}(1-\xi^2)\delta t \tag{4.28}$$

These coefficients are derived in Appendix L.

The convective term (4.24) in energy is dominating over the other terms for highly energetic minority ions. The spread in energy is zero to the leading order in T_e/T_{min}. Pitch-angle scattering is both diffusive and convective with time scales of the same orders. Pitch-angle scattering time scales are longer than the collision drag time scale for minority ion velocity much larger than the critical velocity $v >> v_c$.

4.3 Summary

Fast ion collisions were reviewed using three different approaches: the fast ion collision operator, the Coulomb diffusion coefficients and the Monte Carlo discrete operator. We have also examined the various collision times and compared the collision contributions due to background ions and electrons.

Chapter 5

Ion Fluxes in a Tokamak due to RF heating

5.1 Introduction

The purpose of this chapter is to study the RF-driven fluxes of barely confined trapped ions. The particle and energy fluxes are computed for a simple resonant distribution function. The multi-dimensional flux integrals are approximated and solved numerically in the limit of trapped resonant ions whose tips are on the resonant layer. The fluxes are plotted as functions of the total RF power and the RF-power density profile.

5.2 Banana tip motion for Trapped Particles

It has been observed experimentally that resonant trapped particles banana tips are very close to the resonance layer [21]. This effect can be explained in terms of diffusion in velocity space due to wave-particle resonance. In the case of ICRF heating, the increase in perpendicular energy is much greater than the increase in parallel energy

$$|\delta v_{\parallel}|_{RF} << |\delta v_{\perp}|_{RF} \tag{5.1}$$

The ion parallel velocity is a function of space for a single particle orbit. If we neglect the drifts, the parallel velocity can be written as

$$v_{\|} = \pm(\frac{2}{m}(E - \mu B_0 + \epsilon\mu B_0))^{1/2}(1 - k^2 sin^2\frac{\theta}{2})^{1/2} \tag{5.2}$$

where k^2 is the trapping parameter given by

$$k^2 = \frac{2\epsilon\mu B_0}{E - \mu B_0 + \epsilon\mu B_0} \tag{5.3}$$

Trapped particles have trapping parameters greater than unity: $k^2 > 1$. The trapping parameter also yields the poloidal angle of the banana tips

$$\theta_{tip} = 2sin^{-1}(\frac{1}{k}) \tag{5.4}$$

It is evident from equation (5.4) that when k^2 increases, θ_{tip} decreases and vice versa. When the poloidal angle of the banana tip decreases, then by definition, the trapped particle becomes more trapped. Our goal is to show that this is exactly what happens when a trapped particle gains RF energy. The next step is to find a relationship for the increase in energy with respect to the increase in magnetic moment. This relationship can be readily derived by assuming that the total increase in energy is equivalent to the total increase in perpendicular energy

$$\delta\mu = \frac{\delta E}{B_{res}} \tag{5.5}$$

where B_{res} is the magnitude of the magnetic field at the resonance point. The variation of k^2 yields

$$k^2 + \delta k^2 = \frac{2\epsilon(\mu + \delta\mu)B_0}{D + \delta\mu(B_{res} - B_0 + \epsilon B_0)} \tag{5.6}$$

where $D = E - \mu B_0 + \epsilon\mu B_0 > 0$.

After some algebra, we have

$$(1 + \delta\mu(B_{res} - B_0 + \epsilon B_0)/D)\frac{\delta k^2}{k^2} = \frac{\delta\mu}{\mu}(1 - \mu(B_{res} - B_0 + \epsilon B_0)/D) \tag{5.7}$$

If $\delta\mu > 0$, then $\delta k^2 > 0$ for

$$(1 - \mu(B_{res} - B_0 + \epsilon B_0)/D) > 0 \tag{5.8}$$

Manipulating inequality (5.8) yields

$$E - \mu B_{res} > 0 \tag{5.9}$$

Equation (5.9) is satisfied for all the trapped particles that intersect the resonance layer. When the trapped minority ion gains perpendicular energy, its banana tips move toward the resonance layer. If the minority ion orbit does not intersect the resonant layer, it does not interact with the wave and, therefore, its banana tips do not move. This simplified model does not account for collisions, Doppler-shift resonance, and diffusion in parallel velocity. However, for highly energetic ions, collisions are rare and the ion moves with its tips toward the resonant layer. Once the particle tips have reached the resonance layer, they can move along it because of the parallel momentum exchanged with the wave, while the resonant ion transfers its energy to the electron and ion bulks along its path. The radial movement of the tips and the pitch-angle scattering occur on a slower time scale than the angular movement of the banana tips

given by equation (5.7). In a strong RF-heating regime where pitch-angle scattering is not fast enough to make the resonant distribution function isotropic, most of the resonant ions become trapped with their banana tips in the resonance layer region. For this reason, the resonant distribution function is essentially comprised of trapped ions.

5.3 Radial Motion of Trapped Particles

Trapped particles that are barely confined are subject to radial motion due to changes in momentum and energy through wave interaction and collisions. We derive a relationship between the radial displacement of a particle and the amount of momentum and energy that is exchanged between the minority ions and the wave. The starting point of the derivation is the orbit equation (2.46) at the torus midplane

$$ax^4 + c_1x^2 + d_1x + e = 0 \tag{5.10}$$

where $x = \frac{r}{a_r}$ and a_r is the minor radius of the torus. The coefficients of the polynomial are given in equations (2.44), (2.45), (2.47), and (2.48). The following relationship holds for the orbit coefficients of a barely confined particle ($x = 1$)

$$a + c_1 + d_1 + e = 0 \tag{5.11}$$

Equation (5.11) also expresses a relationship among the constants of motion as functions of the coefficients c_1, d_1, and e. We can arbitrarily choose any two constants of motion, since the third constant has to satisfy equation (5.11) through the polynomial coefficients. Small changes in the constants of motion cause small changes in the coefficients of the orbit equation.

To derive an equation for the changes, we perturb the constants of motion by small

variations given by $\delta\bar{\mu}$, $\delta\bar{v}^2$, and $\delta\bar{p}$. Since the constants of motion are also functions of the polynomial coefficients of equation (5.10), the variation of the coefficients c_1, d_1, and e correspond to the variation of the constants of motion. The small changes in the constants of motion lead to a small change $\delta x << x$, of the radial intersection of the ion orbit with the outer side of the midplane. To derive a relationship between δx and $(\delta\bar{\mu}, \delta\bar{v}^2, \delta\bar{p})$, we perturbed the orbit equation (5.10) as follows

$$a(x+\delta x)^4 + (c1+\delta c_1)(x+\delta x)^2 + (d_1+\delta d_1)(x+\delta x) + e + \delta e = 0 \tag{5.12}$$

Equation (5.12) is solved in terms of δx by keeping the perturbative linear terms to yield

$$\delta x = -\frac{\delta c_1 + \delta d_1 + \delta e}{4A_c(A_c-\bar{p}) - \frac{2a_r}{R_0}(1+\frac{a_r}{R_0})\bar{v}^2 + \frac{a_r\bar{\mu}}{R_0}} \tag{5.13}$$

where we used equations (2.44), (2.45), (2.47), and (2.48) to write the denominator of equation (5.13) as a function of the constants of motion.

The radial displacement δx can also be written in terms of the location of the banana tips (x_0, θ_0) by using equations (2.57) and (2.58). By doing so, we obtain

$$\delta x = \frac{1}{A_c^2}\frac{\delta\bar{v}^2(1+a_r/R_0)^2 - \delta\bar{\mu}(1+a_r/R_0) + 2A_c(1-x_0^2)\delta\bar{p}}{D(x_0,\theta_0)} \tag{5.14}$$

where the denominator is given by

$$D(x_0,\theta_0) = 4(1-x_0^2) + (-1+\frac{a_r}{R_0}(x_0 cos\theta_0 - 2))\frac{(1-x_0^2)^2}{(1+\frac{a_r}{R_0})(1-x_0 cos\theta_0)} \tag{5.15}$$

The denominator is always positive for the trapped particles that intersect the resonant layer. The direction of the radial displacement is outward for a positive numer-

ator and inward for a negative numerator. The changes in the phase-space variables caused by cyclotron resonance satisfy the following relations

$$\delta\bar{v}^2 = \frac{\delta\bar{\mu}}{h_{res}} + 2|\bar{v}_{\|}|_{res}\delta\bar{v}_{\|} \tag{5.16}$$

$$\delta\bar{p} = -h_{res}\delta\bar{v}_{\|} \tag{5.17}$$

where the subscript *res* refers to the resonance location. By using equations (5.16) and (5.17), the change in energy is replaced by the change in parallel velocity to yield a new expression for the radial displacement

$$\delta x = \frac{1}{A_c^2}\frac{\delta\bar{\mu}(\frac{(1+a_r/R_0)^2}{h_{res}} - (1+a_r/R_0)) + \frac{A_c\delta\bar{v}_{\|}}{h_{res}}(2(1+\frac{a_r}{R_0})^2|x^2 - x_0^2|_{res} - 2(1-x_0^2)h_{res}^2)}{D(x_0,\theta_0)} \tag{5.18}$$

To analyze equation (5.18), we begin by neglecting the diffusion in parallel velocity, letting $\delta\bar{v}_{\|} = 0$, as suggested by equation (5.1). The radial displacement is directed outward for $\delta\bar{\mu} > 0$ and vice versa. This behavior is explained by the fact that the orbits of trapped particles become wider as they gain perpendicular energy.

We also find that the magnitude of the displacement increases when we move the resonance layer toward the high field side of the tokamak. This dependence can be understood by examining the orbit equation (5.18): for increasing h_{res} and $\delta\bar{\mu} > 0$, δx decreases. The constants of motion are related to each other through the condition of bare confinement given by equation (5.10), which restricts the phase-space domain to two constants of motion. The radial displacement δx is a linear combination of $\delta\bar{\mu}$ and $\delta\bar{v}^2$, therefore there are an infinite number of linear combinations of the changes $\delta\bar{v}^2$ and $\delta\bar{\mu}$ that make the radial displacement equal to zero. The ratio of the changes is equal to a particular constant when $\delta x = 0$

$$\frac{\delta\bar{\mu}}{\delta\bar{v}^2} = const_{(\delta x=0)} \tag{5.19}$$

On the other hand, when parallel velocity diffusion is negligible, the ratio of the two changes is fixed as a function of the resonance layer position through h_{res}, namely

$$\frac{\delta\bar{\mu}}{\delta\bar{v}^2} = h_{res} \tag{5.20}$$

We conclude that the radial displacement is different from zero except when $h_{res} = const_{(\delta x=0)}$. It is also evident that the larger $|h_{res} - const_{(\delta x=0)}|$, the larger the radial displacement δx.

Strictly speaking, the widening of the banana from perpendicular heating is not a neoclassical transport process. As a matter of fact, neoclassical transport theory [49] treats the total change of angular momentum of plasma species caused by a parallel collisional friction force. However, the radial displacement of wide banana orbits leads to particle and energy loss and must be included in a more general definition of transport. The essential feature of the radial displacement is its dependence on $\delta\bar{\mu}$. Such dependence was not included in previous work on RF-driven transport [13, 50].

To study the properties of this transport mechanism, we have neglected the change in parallel velocity because of equation (5.1). The radial velocity of trapped minority ions due to a change in magnetic moment is given by

$$< V_r > = < \frac{\delta x}{\delta t} > = \frac{a_r}{A_c^2} \frac{< \delta\bar{\mu} > (\frac{(1+a_r/R_0)^2}{h_{res}} - (1 + a_r/R_0))}{T_{btrapp} D(x_0, \theta_0)} \tag{5.21}$$

where we used the average change in radial coordinate in one poloidal period and let $\delta t = T_{btrapp}$. Also $< \delta\bar{\mu} >$ is the average change in magnetic moment that the particle experiences in one poloidal period. This velocity can be compared to the

drift velocity of banana tips when the wave spectrum is asymmetric. The radial drift of the banana tips [13, 21] is given by

$$\delta r = \frac{\delta v_{\|}}{\omega_{c\theta}} \tag{5.22}$$

where the poloidal cyclotron frequency is $\omega_{c\theta} = qB_\theta/m$ and is defined as positive when the toroidal current has the same direction as the toroidal field. We can readily obtain the change in toroidal momentum from the guiding center equations (3.101) and (3.102). The result at leading order in ϵ is

$$\delta p_\phi = \frac{N}{\omega}\delta E \tag{5.23}$$

where N is the toroidal wavenumber of the fast wave. Combining equations (5.22) and (5.23) yields the radial displacement of the trapped particle banana tips as a function of the change in energy

$$\delta r = -\frac{N\delta E}{mR\omega\omega_{c\theta}} \tag{5.24}$$

The average drift velocity is obtained by taking the average displacement and dividing it by the bounce period, where the average gain in energy corresponds to the energy averaged over an ensemble of particles that interact randomly with the wave. By doing so, we obtain

$$< V_{tip} >= -\frac{N < \delta E >}{mRT_{btrapp}\omega\omega_{c\theta}} \tag{5.25}$$

Chen and Hammett [13, 21] also obtained this expression. Since we neglected diffusion in parallel velocity, we can compute the change in normalized magnetic moment for a given change in energy

$$\delta\bar{\mu} = \frac{\delta E}{T_i} \tag{5.26}$$

where T_i is the bulk ion temperature. When we substitute equation (5.26) in equation (5.21), we obtain the average radial velocity of the banana orbit widening as a function of the change in energy

$$< V_r > \approx \frac{0.5 a_r}{A_c^2} \frac{< \delta E >}{T_i D(x_0, \theta_0) T_{btrapp}} \tag{5.27}$$

where $a/R_0 \approx 1/3$. To compare the magnitude of the radial velocities given by equations (5.25) and (5.27), their ratio is

$$|\frac{< V_{tip} >}{< V_r >}| \approx |\frac{10 N A_c^2 q_s D(x_0, \theta_0)}{(\omega_{c0} t_b)^2}| \tag{5.28}$$

For instance let's take $D \approx 3$ and $N \approx 10$, then this ratio is smaller than unity for typical tokamak parameters [22]. In the case of small-width banana orbits, $D << 1$ contributes to make the ratio in equation (5.28) even smaller. Chen [13] concluded that RF-driven convection of fast minority ions due to an asymmetric wave spectrum can certainly be comparable or larger than neoclassical transport. From the small ratio of the radial velocities in equation (5.28), we deduce that the banana-widening effect can lead to a substantial loss of minority ions. In particular, the loss of energy can be even more critical because the trapped ions subject to this drift are highly energetic.

In figure (5.1), the denominator $D(x_0, \theta_0)$ is plotted as a function of the location of the banana tip for an inverse aspect ratio $a/R_0 = 1/3$. By examining equation (5.1), we see that D is fairly independent of the poloidal angle of the banana tip. The denominator D is slightly larger for banana tips located toward the high-field side of the tokamak. D reaches its maximum for trapped particles whose tips are located near

the plasma axis. The denominator is of the order of a few units in this region, hence these trapped particles experience very little radial displacement for a fixed value of change in perpendicular energy. As the banana tips drift out radially, the banana width of barely confined ions becomes increasingly smaller as D approaches zero. The radial velocity of thin banana particles is much larger than the thick bananas (potato orbit particles). However, when computing the velocity we must account for the spatial dependence of the magnitude of the resonant changes in velocity space. These changes are a function of the electric field radial profile.

Before we derive an analytical expression for the changes in velocity space, we return to equation (5.18) to estimate the contribution of $\delta\bar{v}_{\|}$ to radial displacement. The direction of the change in parallel velocity must be given to find the direction of the radial displacement. Signs of the changes in parallel velocity and radial position are a function of the toroidal wavenumber sign, and the relative direction of the toroidal magnetic field and toroidal current. When the ion perpendicular energy increases, the signs of the change in parallel velocity and radial position are given by the following table for $\delta\bar{\mu} > 0$

$N > 0$	$\delta\bar{v}_{\|} < 0$	$\sigma_{BJ}\delta x < 0$
$N < 0$	$\delta\bar{v}_{\|} > 0$	$\sigma_{BJ}\delta x > 0$

These relationships are based on equations (5.23) and (5.24) where N is the toroidal wavenumber and σ_{BJ} is equal to ± 1, respectively, when the current has the same direction of the toroidal field and vice versa. If we launch an asymmetric-spectrum wave whose parallel wavevector is parallel to the magnetic field, by convention we have $N > 0$. We assume that the poloidal flux is positive when the current and the toroidal field are pointing in the same direction. We can readily derive a relationship between the change in parallel velocity and perpendicular velocity by using equations (3.83) and (3.84) at leading order in ϵ

$$|\delta v_{\parallel}| \approx |\frac{N}{2R_0\omega_{c0}}\delta v_{\perp}^2| \tag{5.29}$$

The $\delta\bar{v}_{\parallel}$ contribution to the radial displacement δx in equation (5.18) can compensate for the outward drift due to the increase in perpendicular energy if the spectrum of our wave is asymmetric and negative ($N < 0$) and the current and the magnetic field are antiparallel. However, the magnitude of radial displacement due to a change in magnetic moment is usually larger than the one due to the change in parallel velocity, as can be seen by examining the contributions ratio from equations (5.18) and (5.29)

$$|\frac{\delta x_{v_{\parallel}}}{\delta x_{\mu}}| \approx 2A_c(1-x_0^2)N\frac{\rho_{Lth}}{R_0} \tag{5.30}$$

The inverse of the ratio of the Larmor radius to the major radius for a 1 KeV thermal particle is approximately 10^3 and N is of the order of ten. A typical number for A_c is 30 for one MA of toroidal current. If the total current is increased to the order of tens of MA, then the parallel momentum inward drift can balance the outward displacement due to $\delta\bar{\mu}$. This balance between RF-driven convection and banana-widening displacement leads to an interesting mechanism for profile control.

5.4 Evaluation of fluxes for a model minority distribution function

5.4.1 Introduction

We have examined the qualitative aspects of radial motion for resonant barely confined particles in section (5.2). In this section, we will estimate the fluxes generated by RF-heating using a simplified analytical model.

Let's consider a situation where strong RF-heating act to generate an anisotropic mi-

nority distribution function. On average, the amount of energy that every minority ion absorbs through resonant interaction depends upon the spatial distribution of the wave field in the tokamak and its phase space variables. Furthermore, energetic ions can span the entire cross-section of the tokamak and have barely confined orbits that touch the plasma edge. The evaluation of the total flux due to radial displacement given by equation (5.21) requires information on the resonant minority distribution in the entire tokamak. Unfortunately, only a few approximate analytic and computational distribution functions on the resonant minority distribution are found in the literature [3, 21, 51, 52, 47, 50, 32]. It is also likely that if the exact distribution were known analytically, it would be unwieldy to use for analytical estimates of the fluxes. For these reasons, we have adopted a simple distribution model that, despite its simplicity, retains most of the physics of RF heating. The distribution used here is a hybrid between Hammett's and Chang's formulations [21, 53].

5.4.2 Model distribution function

A model distribution function for resonant minority trapped ions in pitch-angle variables on the resonance layer may be given by

$$f = N_{res} n(x) \frac{2}{\pi^2} \left(\frac{M}{2T_{eff}}\right)^{3/2} \frac{1}{\delta\psi}\, e^{-\frac{Mv^2}{2T_{eff}}}\, e^{-\frac{\psi_r^2}{(\delta\psi)^2}} \tag{5.31}$$

where we assume heating on axis where $x = r/a$ is the radial coordinate along the resonant layer, $n(x)$ is a radial profile and N_{res} is the total number of resonant minority ions. T_{eff} is the effective temperature of the minority ion species. We assume a strong-RF heating regime where the effective temperature is much higher than the majority ion temperature. The pitch-angle variable $\psi_r = v_\parallel / v$ is evaluated at the resonant layer. When the banana tips touch the resonance layer, then $\psi_r = 0$. The pitch-angle spread $\delta\psi$ in equation (5.31) is much smaller than unity, since pitch angle scattering occurs at a slower rate than heating

$$\delta\psi << 1 \tag{5.32}$$

Equation (5.32) indicates that most resonant trapped ions have their banana tips near the resonant layer.

To verify that the distribution function in equation (5.31) is properly normalized, we integrate over the entire velocity space yielding

$$\int d^3v\ f = \int_0^\infty 2\pi v^2 dv \int_{-1}^{+1} d\psi_r f \approx N_{res} n(x) \tag{5.33}$$

The result of equation (5.33) would be exact if the extremes of integration in the pitch-angle variable integration were plus and minus infinity. However, the approximation in equation (5.33) is nonetheless accurate, as shown by the following integral

$$\int_{-1}^{1} e^{-\psi_r^2/\delta_\psi^2} d\psi \approx \sqrt{\pi}\delta\psi \tag{5.34}$$

Finally, the resonant minority distribution function is integrated over the strip volume that contains the resonant trapped particles and velocity space to yield the total number of resonant trapped minority ions in the tokamak as

$$N_{res} \approx \int_{layer} dV \int d^3v f \tag{5.35}$$

This normalization is computed as

$$N_{res} = 2\pi R_0 a \int_0^1 dx \int_0^{\delta y} dy \int_0^\infty 2\pi v^2 dv \int_{-1}^{+1} d\psi f \tag{5.36}$$

where the horizontal strip width $\delta y \approx R_0 \delta\psi$ is proportional to the pitch angle width

in the linear approximation.

5.4.3 Discussion of the model distribution function

We justify the analytic model of equation (5.31) by examining the Fokker-Planck equation structure for a RF-heated minority and comparing the various terms. A generalized Fokker-Planck equation can be expressed by

$$\frac{\partial f}{\partial t} = \frac{\partial f}{\partial t}_{RF} + \frac{\partial f}{\partial t}_{coll.drag} + \frac{\partial f}{\partial t}_{pitch-angle} + \frac{\partial f}{\partial t}_{radialtransport} \tag{5.37}$$

In strongly RF-heated tokamaks, the resonant wave interaction operator of equation (5.37) has the shortest time scale among all other operators. The resonant particle exchanges energy with the wave on a bounce time scale. Collision times are usually longer. As seen in Chapter 4, the collision operator for energetic ions is essentialy comprised of two terms: pitch-angle scattering and drag. For minority velocities larger than the critical velocity, electron drag dominates over pitch-angle scattering. This scaling conflicts with neoclassical theory [49], where pitch-angle scattering is the dominant collisional effect. Finally, the transport time scale is the longest time scale. Hammett and Chang found analytic solutions for a model Fokker-Planck equation without the radial transport operator. In particular, Hammett [21] advanced the following model Fokker-Planck equation [1]

$$\frac{\partial f}{\partial t} = \frac{2T_{tail}P_{RF}}{3n_m}\delta(\frac{\psi}{\delta\psi})\frac{\partial^2 f}{\partial E^2} + \frac{2T_{tail}}{\tau_s}\frac{\partial f}{\partial E} + \frac{\nu_{ii}}{2}\frac{\partial^2 f}{\partial \psi^2} \tag{5.38}$$

whose steady-state solution is

$$f = e^{-|\psi|/\delta\psi}e^{-E/T_{tail}} \tag{5.39}$$

[1] In his thesis, Hammett omitted to label the temperature as T_{tail} in his simplified equation.

where the tail temperature and the pitch-angle spread are

$$T_{tail} = \frac{P_{RF}\tau_s}{3n_m} \; ; \; (\delta\psi)_{Hammett} = \sqrt{\nu_{ii}\tau_s}/2 \tag{5.40}$$

Hammett's distribution function is similar to equation (5.31). In equation (5.31) we adopt a Gaussian function for the pitch-angle dependence and normalize it in phase space. Another method to recover the Maxwellian-energy dependence of equation (5.38) is to examine how the velocity dependence arises and balance the fastest diffusion operators: wave heating and electron drag. Next, we average the two simplified operators over the pitch angle variable to obtain the following balance equation

$$\frac{2TP_{RF}}{3n_m}\frac{\partial^2 f}{\partial E^2} + \frac{2T}{\tau_s}\frac{\partial f}{\partial E} = 0 \tag{5.41}$$

whose solution is a Maxwellian distribution function with temperature T_{eff}

$$f = f_0 e^{-\frac{E}{T_{eff}}} \tag{5.42}$$

where the effective temperature is

$$T_{eff} = \frac{P_{RF}\tau_s}{3n_m} \tag{5.43}$$

Equations (5.41) and (5.43) state that the energy the minority species absorb is collisionally damped on the majority species. Equations (5.41) and (5.43) are approximate relationships because they are derived for resonant distribution functions defined on a single flux surface. Large banana-width ions can collisionally transfer their energy in any region of the torus instead of on a single flux surface of a tokamak. In fact,

the collisional slowing-down time for a hydrogen minority species [5] is a function of space through the density and temperature profiles of the majority species

$$\tau_s \approx \frac{1.3 * 10^{18} T_e^{3/2}(x)}{n_e(x)} sec \tag{5.44}$$

where the electron temperature is in KeV and the electron density is in m^{-3}.

The pitch-angle distribution is governed by the RF-diffusion operator. As we have seen in Chapter 3 equation (3.105), the RF operator depends on the parallel velocity or pitch-angle at resonance ψ_r. More precisely, the phase integral has a singular dependence on the pitch-angle of the type $1/\psi_r$ which can be eliminated in several ways. The simplest approach is based on computing the phase integral of two closely correlated resonances. This yields the well-known Airy function [45], as derived in equation (3.114). Another way of treating the singularity is to include H_2 to our wave-particle treatment [54]. The linear treatment of wave-particle interaction usually breaks down when the amount of energy exchanged in a resonant interaction increases. For instance, we computed the change in the phase space variables by integrating the changes in the constants of motion along the unperturbed orbit, however, when the interaction is very strong, the resonance integral must be computed by updating the phase space variables to its new values along the resonant trajectory. Fortunately, Becoulet [39] showed that the linear treatment is valid even for strong wave-particle interaction.

Finally, collisions [55] can be an important detuning factor in a resonance process. The pitch-angle of a resonant particle can change by pitch-angle scattering as does the phase between the wave and the particle, resulting in a shifted resonance. In general, collisions cause minority trapped particles to spread around the resonance layer as shown by equation (5.31), whereas RF heating tends to push them toward the resonance layer.

The pitch-angle distribution of the resonant ion density on the layer is a function of

the collision times. We multiply Hammett's spread by two as an estimate of the pitch-angle spread in the distribution function given by equation (5.31) to compensate for the fact that the Gaussian function falls faster than e^{-x}

$$\delta_\psi \approx \sqrt{\nu_{ii}\tau_s} \tag{5.45}$$

The pitch-angle spread of equation (5.45) is smaller than unity since the electron drag time scale is much shorter than the pitch angle scattering time scale for energetic ions. In this section we discussed equation (5.31) and provided physical arguments to bolster the validity of the model distribution function. In the next section, we will use equation (5.31) to compute the minority fluxes due to orbit widening. Some analytical approximations must be made for density, temperature and field profiles to obtain a closed analytic expression for the RF-induced loss of energy. We address this in the next section.

5.4.4 Approximations for density, temperature and RF power profiles

Approximate analytical formulae for the density profile $n(x)$, temperature profile $T_e(x)$, heating power density P_{RF}, kinetic energy $v_0^2(x)$, energy spread $\delta v(x)$, effective temperature $T_{eff}(x)$ and radial velocity $V_r(x)$ are given as function of $x = r/a$, a radial coordinate along the resonant layer.

Model functions for density, temperature and heating power profiles

We adopt the following model function for the density, power and temperature profiles as done in previous research [56, 57]

$$n_m = n_{m0} n(x) = n_{m0} \frac{(1-x^2)^{\gamma_n}}{(\gamma_n + 1)^{-1}} \tag{5.46}$$

$$T_e(x) = T_{e0}\frac{(1-x^2)^{\gamma_T}}{(\gamma_T+1)^{-1}} \tag{5.47}$$

$$P_{RF}(x) = P_{RF0}\frac{(1-x^2)^{\gamma_P}}{(\gamma_P+1)^{-1}} \tag{5.48}$$

where γ_n, γ_T and γ_P are positive parameters that yield the peakedness of the profiles, while $\frac{n_{m0}}{(\gamma_n+1)^{-1}}, \frac{T_{e0}}{(\gamma_T+1)^{-1}}$ and $\frac{P_{RF0}}{(\gamma_P+1)^{-1}}$ are minority density, majority temperature and RF power density at the plasma axis, respectively.

We also assume that the minority density and the majority density have the same radial profiles because of the quasineutrality condition. Furthermore, an analytic expression for the electric field profile $|E_+(x)|$ is also needed to compute the radial velocity. The electric field profile can be obtained by using a linear relationship between the RF power density and the squared amplitude of the electric field

$$P_{RF} \propto D_{\mu\mu} \propto |E_+|^2 \tag{5.49}$$

The electric field profile is

$$|E_+| = |E_{+0}|\frac{(1-x^2)^{\gamma_P/2}}{(\gamma_P+1)^{-1/2}} \tag{5.50}$$

where $\gamma_P/2$ is the profile parameter and $\frac{|E_{+0}|}{(\gamma_P+1)^{-1/2}}$ is the wave amplitude at the plasma axis.

An approximation for the kinetic energy in the flux integrals

Velocity v_0 is the velocity that a barely confined trapped particle has when its tips are on the resonance layer. It is also a function of the tip radial position x_0 as in

equation (2.55). The fluxes are computed to the limit of resonant barely confined particles whose tips are on resonance, hence we can let $v^2 = v_0^2$ in equation (5.31). Moreover, since the distribution function of equation (5.31) is defined on the resonance layer, the radial coordinate x and the radial location of the banana tips are approximately equal. These approximations are given by

$$x \approx x_0 \; ; \; v^2 \approx v_0^2 = \frac{9}{4} A_c^2 \, v_{th}^2 (x_0^2 - 1)^2 \tag{5.51}$$

The approximations in equation (5.51) break down for trapped ions whose banana tips are located near the edge of the plasma, because the spread in velocity is no longer negligible compared to the total velocity. However, the peaked power density profile makes the error small near the edge of the plasma.

An approximation for the energy spread in the flux integrals

The energy spread δv is challenging to compute. We can find an estimate for it by initially assuming that most trapped ions have their tips on the resonance layer. They eventually undergo a small pitch-angle scattering that moves the tips off resonance by a distance $(\delta x, \delta\theta)$ from its original location (x_0, θ_0). We also have a rough estimate of the magnitude of the pitch-angle spread from equation (5.45). It includes most particles when it is approximately equal to two standard deviations

$$|\delta\psi_{res}| = |\frac{\delta v_{\|res}}{v}| = 2\sqrt{\nu_{ii}\tau_s} \tag{5.52}$$

Pitch-angle scattering at constant energy changes the toroidal momentum of the resonant particle. The change in toroidal momentum leads to a change in the radial position of the trapped particle banana tips. This change can be estimated by taking the variation of the toroidal momentum in terms of its banana tip location yielding

$$\delta\bar{p} = 2A_c x_0 \delta x_0 \tag{5.53}$$

The relationship between the absolute value of the change of the pitch angle upon scattering and the absolute value of the change of the toroidal momentum is given by

$$|\delta\psi_{res}| = \frac{\delta\bar{p}}{\bar{v}} = \frac{4}{3}\frac{x_0}{1-x_0^2}|\delta x_0| = 2\sqrt{\nu_{ii}\tau_s} \tag{5.54}$$

Equation (5.54) shows the radial position change of the banana tips when the toroidal momentum changes occur due to pitch angle scattering using equations (5.52) and (5.53). A barely confined resonant ion can also move along the resonant layer by keeping the poloidal angle constant and changing its energy according to equation (2.55). For small radial displacements along the resonant layer, the equivalent change in energy can be computed by perturbing equation (2.55)

$$|\delta\bar{v}^2| = 9A_c^2 x_0(1-x_0^2)|\delta x_0| \tag{5.55}$$

Using the relation $|\delta\bar{v}^2| = 2\bar{v}|\delta\bar{v}|$ and equation (5.55), we obtain an expression for absolute change in velocity as a function of the radial displacement along the resonant layer

$$|\delta\bar{v}| = 3A_c x_0|\delta x_0| \tag{5.56}$$

By substituting equation (5.55) for $|\delta x_0|$ in equation (5.53) we obtain the absolute value of the velocity spread $|\delta\bar{v}|$ as a function of the magnitude of the pitch-angle spread

$$|\delta v| = \frac{9}{2} A_c v_{th} (1 - x_0^2) \sqrt{\nu_{ii} \tau_s} \tag{5.57}$$

where we unnormalized the velocity spread by multiplying by v_{th}. Equation (5.57) is not an explicit function of x because the collision times must be expressed as functions of x. The collisionally dependent factors in equation (5.31) will be explicitly written as a function of x in the next subsections.

Radial dependence of the effective temperature

The effective temperature T_{eff} can be computed using density, temperature and the power density profile given by equations (5.46), (5.47), and (5.48)

$$T_{eff} = \frac{P_{RF0} \tau_{s0}}{3 n_{m0}} \frac{(\gamma_P + 1)(\gamma_T + 1)^{3/2}}{(\gamma_n + 1)^2} (1 - x_0^2)^{(\gamma_P + 3\gamma_T/2 - 2\gamma_n)} \tag{5.58}$$

where

$$\tau_{s0} = \alpha_n \frac{1.3\ 10^{18} T_{e0}^{3/2}}{n_{e0}} \tag{5.59}$$

and the parameter $\alpha_n = n_{m0}/n_{e0} << 1$ is the ratio between the minority species density and the majority species density. Collision time τ_s should be averaged over the orbital ion motion, but since trapped particles spend most of their time near the banana tip location, the averaged collision time can be evaluated at the banana tip radius with good approximation. The normalizing factor of the Maxwellian in equation (5.31) is

$$\left(\frac{M}{2T_{eff}}\right)^{3/2} = \left(\frac{3 M n_{m0}}{2 P_{RF0} \tau_{s0}} \frac{(\gamma_n + 1)^2}{(\gamma_P + 1)(\gamma_T + 1)^{3/2}}\right)^{3/2} (1 - x_0^2)^{-\frac{3}{2}(\gamma_P + 3\gamma_T/2 - 2\gamma_n)} \tag{5.60}$$

Radial dependence of the pitch-angle spread

The pitch-angle spread is given by [21]

$$\sqrt{\nu_{ii}\tau_s} = \left(\frac{Z_{eff}}{2A < Z_i^2/A_i > (1 + E^{3/2}/E_c^{3/2})}\right)^{1/2} \tag{5.61}$$

where E is minority particle kinetic energy, A is the atomic number, the effective charge is $Z_{eff} =< Z_i^2 >$ and the critical energy is

$$E_c = 14.8\ A\ T_e(KeV) < Z_i^2/A_i >^{2/3} \tag{5.62}$$

As pointed out in Chapter 4, in a strong RF-heating regime we have $E >> E_c$. The resonant particle energy E is given by equation (2.55) for barely confined orbits

$$E = \frac{1}{2} M v_{th}^2 \frac{9}{4} A_c^2 (1 - x_0^2)^2 \tag{5.63}$$

We also approximate $\frac{T_{e0}}{\gamma_T + 1} \approx \frac{1}{2} M v_{th}^2$ to obtain the pitch angle spread as a function of the banana tip radius

$$\sqrt{\nu_{ii}\tau_s} \approx \frac{1}{\sqrt{2}} \left(\frac{60}{9} \frac{1}{A_c^2}\right)^{3/4} (1 - x_0^2)^{\frac{3}{4}(\gamma_T - 2)} \tag{5.64}$$

Equation (5.64) indicates that the orbital average of collision times is roughly equivalent to an estimate of collision times at the banana tips. The spread in energy can now be computed as an explicit function of x_0 using equations (5.57) and (5.64)

$$|\delta v| \approx \frac{9A_c}{2\sqrt{2}}(\frac{60}{9}\frac{1}{A_c^2})^{3/4}\ (1-x_0^2)^{(\frac{3}{4}\gamma_T-1/2)}v_{th} \tag{5.65}$$

Radial dependence of the Maxwellian factor in the model distribution function

The energy-dependent exponent of the resonant distribution function can be written as a function of the radial position of the banana tips when they are on the resonant layer. Using equations (5.46)-(5.48) and (5.51) we obtain

$$\frac{1}{2}\frac{mv^2}{T_{eff}} \approx \frac{27A_c^2}{8}\frac{mv_{th}^2 n_{e0}}{P_{RF0}\tau_{s0}}\alpha_n \frac{(\gamma_n+1)^2}{(\gamma_T+1)^{3/2}(\gamma_P+1)}(1-x_0^2)^{2+2\gamma_n-\gamma_P-\frac{3}{2}\gamma_T} \tag{5.66}$$

5.4.5 Calculation of power lost due to RF-induced flux

We can now compute the normalization factor for the resonant distribution function using the density and temperature profiles given by equations (5.46) and (5.47). We point out that the density and temperature profiles enter the normalization constant through the collision times, which in their turn give the pitch-angle spread. The result is

$$f(x,\bar{v}) = \frac{N_{res}}{2\pi a R_0^2}\ g(\gamma_n,\gamma_T)\ (1-x^2)^{\gamma_n}\frac{M}{2\pi T_{eff}}^{3/2} e^{-Mv^2/2T_{eff}}\frac{2}{\sqrt{\pi}}\frac{exp(-\frac{\psi^2}{\delta\psi^2})}{\delta\psi} \tag{5.67}$$

where

$$g(\gamma_n,\gamma_T) = \frac{1}{\frac{1}{\sqrt{2}}(\frac{60}{9}\frac{1}{A_c^2})^{3/4}\int_0^1 dx(1-x^2)^{\gamma_n+\frac{3}{4}(\gamma_T-2)}} \tag{5.68}$$

We start with the model distribution function for minority particles as given by equation (5.31). The distribution function is bi-maxwellian in energy and pitch-angle. The spread in pitch-angle space is given by equation (5.46) as a function of collision times. We compute the energy lost through RF-driven flux when minority particles cross the resonant layer and they are lost at the edge of the plasma. The energy lost can be computed by estimating the number of particles that cross the plasma boundary in a poloidal period. We compute the ratio of the maximum energy lost to the total energy content of the minority species . The result is

$$\frac{Maximumenergy\ lost}{total\ energy\ content} \approx \frac{\int dV \int_{v_b^2-\delta v_{MAX}^2}^{v_b^2} \int_{-\delta\psi}^{\delta\psi} d\psi\, dv\, 2\pi v^2\, f\, mv^2/2}{\int dV \int_0^{v_b^2} \int_{-\delta\psi}^{\delta\psi} d\psi\, dv\, 2\pi v^2\, f\, mv^2/2} \tag{5.69}$$

where dV is the volume that comprises the resonant ions, $v_b^2 = 9A_c^2 v_{th}^2/4$ and δv_{MAX} is the positive kick in energy gained by a resonant ion in one semi-poloidal period. The range of the velocity space integral is over all particles that are deconfined due to RF; v_b^2 is the energy of an ion which in the absence of the wave is confined, but which in the presence of it gains an energy δv_{MAX} that will deconfine it. The maximum kick in energy is computed by integrating the equation of motion in the vicinity of the plasma layer where most absorption takes place. The result is

$$\delta v_{MAX}^2 \approx \frac{2qv}{m^2}\sqrt{mB_0\mu/2}E_{+0}I \tag{5.70}$$

where the phase integral I is

$$I \approx \frac{0.56\pi R_0}{(\mu B_0/m)^{2/3}(1/\omega_{c0}R_0)^{1/3}} \tag{5.71}$$

To compute the fraction of energy lost we also used equations (5.31), (5.35), (5.36),

(5.44), (5.45), (5.53-5.57). We also assumed that the effective temperature is much less than the maximum confined energy. The integrals over dx in equation (5.69) are to be solved numerically for different values of the normalized power density.

5.4.6 Discussion of particle and energy fluxes

Before we compute the power loss integrals in equation (5.69), we obtain an estimate of the magnitude of RF-driven tranport for barely confined particles and compare this estimate to other sources of particle and energy loss such as neoclassical and classical RF-driven transport. Previous work by Chen [13] shows that RF-driven convection flux due to an asymmetry in the ICRF wave spectrum (with a typical asymmetry $k_{\|}\rho_L << 1$) is larger than the RF-driven symmetric flux by a factor of

$$|\Gamma^{asymmetric}/\Gamma^{symmetric}| = \frac{1}{k_{\|}\rho_L}\frac{a}{\rho_\theta} \tag{5.72}$$

where ρ_θ is the Larmor radius in a poloidal magnetic field. We also compare the RF-driven asymmetric flux to neoclassical transport using the results from equation (3.26). The result of this comparison is given by

$$\frac{\Gamma^{asymmetric}}{\Gamma^{neoclassical}} \approx k_{\|}R\frac{a^2}{R_2}\frac{1}{q_s}\frac{1}{\tau_s\nu_{ii}} \tag{5.73}$$

In a strongly RF-heated tokamak where the average minority ion energy is higher than the critical energy E_c, pitch-angle scattering is negligible with respect to electron drag. If $k_{\|}R > 10$, the RF-driven convective flux is larger than the neoclassical one. We have already compared the RF driven flux due to finite orbit effects to the asymmetric flux in section (5.2), the result being that barely confined particle flux is usually larger than asymmetric flux for standard tokamak parameters [22]. In addition, it is always present in a RF-heated tokamak, while the asymmetric flux is generated only in the presence of an asymmetric spectrum.

We can readily estimate the ratio between barely confined particle flux and the neoclassical transport by using equations (5.28) and (5.75)

$$|\frac{\Gamma^{finiteorbit}}{\Gamma^{neoclassical}}| \approx \frac{a^2}{R^2}\frac{1}{q_s^2}\frac{1}{\tau_s \nu_{ii}}\frac{(\omega_{c0}t_b)^2}{A_c^2 D_{x_0,\theta_0}} \tag{5.74}$$

This ratio is larger than unity for standard tokamak parameters [22]. The importance of RF-driven flux due to banana widening is underscored by the fact that the lost resonant ions are highly energetic and, hence cause a significant loss in heating efficiency.

We now compute the ratio energy loss to total RF power as function of the total energy content of the minority species. This ratio is much less unity. If the heating time is known, then we can obtain an estimate for the ratio between the power lost and the power delivered to the minority species. Generally speaking, the heating time should be of the order of the drag time τ_s. In equation (5.48), P_{RF0} yields the RF power density at the plasma axis, while γ_P gives the profile shape. We solve the power loss integrals of equation (5.69) numerically and plot the power loss ratio as a function of the total power loss. We adopt the following parameters in our computation: $a/R_0 = 1/3$, toroidal current $I \approx 1MA$, electron thermal energy 1 KeV and minority density $10^{18}m^{-3}$. We also take the RF power profile parameter $\gamma_P = 5$ and for standard tokamak parameters [22], we assume $\gamma_{n,T} = O(1)$ [57] because this ordering is also observed experimentally. For computational purposes, we use the following profile parameters

$$\gamma_n = 1 \quad \gamma_T = 2 \tag{5.75}$$

In figure (5.2), the ratio energy loss to the total minority energy is plotted for different values of the total RF power for three different values of the toroidal current. The range of RF power density is chosen so that $E_0/T_{eff0} >> 1$. We plot the loss

fraction for a tokamak with a toroidal current of 1.3, 1.5 and 2 MA. From figure (5.2), it is clear that the fraction of the energy lost increase with increasing RF power for a given toroidal current, except at very low powers ($P_{RF} < 1\ MW$) where the fraction of the energy loss is always negligible and approximately constant. If we examine the loss dependence at low currents we see even at 2 MW the fraction of energy lost is relevant if one considers that the poloidal period is the timescale for this process. The worst scenario occurs when the RF power exceeds $3MW$, and the increase in energy loss starts becoming substantial as the RF power increases. At higher currents ($I > 1.3MA$) the energy loss is significantly reduced. An explanation for this behavior is provided by the examination of the confinement parameter. The confinement parameter $\frac{E_0}{T_{eff0}}$ is the ratio between the energy of the most energetic particle that a tokamak can confine and the minority-heated tail energy. A typical value of this parameter can be obtained by considering a tokamak, where the central electron density is $n_e = 10^{20}m^{-3}$, the central electron temperature $T_e = 3KeV$, and the drag collision time is $\tau_s = 0.07sec.$ Furthermore, we assume that 4 MW of RF power is distributed in a volume of 1 m^3 with a minority fraction of one percent. This leads to an estimate for the effective ion temperature of approximately 600 KeV using equation (5.66). A toroidal current of 0.7 MA yields a confinement parameter equal to unity: $\frac{E_0}{T_{eff0}} = 1$. A ratio of unity for the confinement parameter is a disaster for confinement because it means that most energetic particles are not well confined. It is intuitive that the higher the confinement parameter, the less RF-driven power loss.

Since the confinement parameter is proportional to the square of the toroidal current, we can keep the flux to a minimum by enhancing the current when RF power is increased. We also see that even a small increase in the toroidal current has a tremendous impact on the fraction of power lost through banana widening, this stems from the fact that fewer and fewer particles touch the plasma edge as we increase the toroidal current. This result suggests that an increase in RF-heating power may require additional toroidal current in tokamaks to reduce the particle and energy loss due to RF-driven flux.

5.4.7 Summary

We derived the radial displacement of barely confined particles caused by small changes of its constants of motion. This displacement occurs with changes in perpendicular energy and parallel momentum of the resonating ion. The displacement is computed for phase-space diffusion due to ICRF wave-particle interaction. The RF-driven flux due to banana-width effects is comparable to or larger than the standard neoclassical flux and asymmetrically-driven flux, and becomes smaller when the resonance layer is moved toward the low-field side of the torus. The combined effect of perpendicular energy heating and parallel momentum leads to an improved confinement for a suitable asymmetric wave spectrum.

Finally,the ratio of power loss to the total RF power was computed for standard tokamak parameters. We point out that our estimate of the power loss is an upper limit because of our choice of the distribution function. As expected, the power loss increases with increasing RF power. The confinement parameter is important to determine the power loss dependence on RF power. A reduction of the confinement parameter can be achieved by increasing the toroidal current for a given RF power.

5.5 Future research projects

Transport in the presence of ICRF heating is far from being completely understood. We need to find an accurate solution for resonant species distribution functions and their radial profiles. This can be achieved by generalized diffusion codes based on sophisticated full phase-space quasilinear models. There is also a need to understand the impact of mode conversion on transport of resonant species. This problem requires computational work using ray-tracing or even full-wave codes in toroidal geometry. Another related research topic is the inclusion of Doppler-shift in the resonance condition, which can lead to spatial asymmetries in the distribution function for unidirectional waves and RF-induced transport. Our model based on banana widening in the edge region of the tokamak could be extended to the entire tokamak

plasma to study the challenging topics of RF current profile control and removal of ashes from the tokamak. Last but not least, the role played by finite orbit resonant particles on MHD instabilities needs to be understood since it may lead to different growth rates than those given by current models.

Appendix A

Particle and guiding-center variables

Here we list the transformations from particle variables to guiding-center variables up to a linear term in ϵ[9] . In order to avoid confusion between the particle and the guiding-center variables, only the guiding-center variables carry the subscript 'gc'. The guiding-center variables are: $(\mathbf{X_{gc}}, v_{\|gc}, \phi_{gc}, \mu)$. The particle variables are: $(\mathbf{x}, v_{\|}, \phi, v_{\perp})$. The direct transformations are:

$$\mathbf{X_{gc}} = \mathbf{x} - \frac{\epsilon v_{\perp}\mathbf{a}}{\omega_c} + O(\epsilon^2) \tag{A.1}$$

$$v_{\|gc} = v_{\|} - \frac{\epsilon}{2\omega_c}[v_{\perp}^2(Z_2 - \frac{1}{2}Z_0 + S_0) + 2v_{\|}v_{\perp}F_0] + O(\epsilon^2) \tag{A.2}$$

$$\phi_{gc} = \phi + \frac{\epsilon}{2\omega_c^2}[2v_{\perp}(-\omega_c F_2 + \mathbf{c}\cdot\nabla\omega_c) - \omega_c v_{\|}S_1 + 2\omega_c\frac{v_{\|}^2}{v_{\perp}}F_1] + O(\epsilon^2) \tag{A.3}$$

$$\frac{1}{q}\mu = \frac{v_{\perp}^2}{2\omega_c} + \frac{\epsilon}{2\omega_c^3}[v_{\perp}^3\mathbf{a}\cdot\nabla\omega_c + \omega_c v_{\perp}^2 v_{\|}(S_0 - Z_0) + 2\omega_c v_{\perp}v_{\|}^2F_0] + O(\epsilon^2) \tag{A.4}$$

All fields on the right-hand side are evaluated at the physical particle position $\mathbf{x}$. Here $(\mathbf{a}, \mathbf{b}, \mathbf{c})$ is a right-handed rotating triad of unit vectors where $\mathbf{b} = \frac{\mathbf{B}}{B}$. Also

$$Z_0 = \mathbf{b}\cdot\nabla\times\mathbf{b}\ ;\ Z_2 = \mathbf{b}\cdot\nabla\mathbf{c}\cdot\mathbf{a} \tag{A.5}$$

$$F_0 = \mathbf{b} \cdot \nabla \mathbf{b} \cdot \mathbf{a} \; ; \; F_1 = \mathbf{b} \cdot \nabla \mathbf{b} \cdot \mathbf{c} \tag{A.6}$$

$$F_2 = \mathbf{a} \cdot \nabla \mathbf{c} \cdot \mathbf{a} \; ; \; S_0 = \frac{1}{2}(\mathbf{a} \cdot \nabla \mathbf{b} \cdot \mathbf{c} + \mathbf{c} \cdot \nabla \mathbf{b} \cdot \mathbf{a}) \tag{A.7}$$

$$S_1 = \frac{1}{2}(\mathbf{a} \cdot \nabla \mathbf{b} \cdot \mathbf{a} - \mathbf{c} \cdot \nabla \mathbf{b} \cdot \mathbf{c}) \tag{A.8}$$

Higher order and inverse transformations can be found in the original paper by Littlejohn [9].

Appendix B

Poisson brackets and starred fields

The equations of motion are obtained in the framework of Hamiltonian dynamics [9]. Given a dynamical variable Y, the resulting equation of motion is

$$\dot{Y} = [[Y, H]] \tag{B.1}$$

where the double brackets are Poisson brackets for G.C. variables. The Poisson brackets are defined as

$$[[f, g]] = A1 + B1 + C1 \tag{B.2}$$

where f and g are any two phase-space quantities and

$$A1 = \frac{1}{qB^*} \nabla f \cdot (\mathbf{b} \times \nabla g) \tag{B.3}$$

$$B1 = \frac{\mathbf{B}^*}{mB^*} \cdot (\nabla f \frac{\partial g}{\partial v_{\|}} - \frac{\partial f}{\partial v_{\|}} \nabla g) \tag{B.4}$$

$$C1 = \frac{q}{m} (\frac{\partial f}{\partial \phi} \frac{\partial g}{\partial \mu} - \frac{\partial f}{\partial \mu} \frac{\partial g}{\partial \phi}) \tag{B.5}$$

The starred fields are defined as

$$\mathbf{B}^* = \mathbf{B} + \epsilon v_\parallel \nabla \times \mathbf{b} + \frac{\epsilon^2 \mu}{2m}[\mathbf{b}((\nabla \cdot \mathbf{b})^2 - \nabla \mathbf{b} : \nabla \mathbf{b}) \tag{B.6}$$
$$-2(\nabla \cdot \mathbf{b})\mathbf{b} \cdot \nabla \mathbf{b} + 2\mathbf{b} \cdot \nabla \mathbf{b} \cdot \nabla \mathbf{b} - \nabla \times (b_0 \mathbf{b})]$$

and

$$B^* = \mathbf{b} \cdot \mathbf{B}^* = B + \epsilon v_\parallel b_0 \tag{B.7}$$
$$+\frac{\epsilon^2 \mu}{2m}[\nabla^2 \mathbf{b} \cdot \mathbf{b} + (\nabla \cdot \mathbf{b})^2 + (\mathbf{b} \cdot \nabla \mathbf{b})^2] \tag{B.8}$$

where $\mathbf{b}$ is the unit versor of the equilibrium magnetic fields and

$$b_0 = \mathbf{b} \cdot (\nabla \times \mathbf{b}) \tag{B.9}$$

where $\epsilon = \frac{m}{q}$.

Equations (2.4),(2.5),(2.6) and (2.7) can be now derived by making use of the Poisson brackets in equations (B.3),(B.4) and (B.5) and the Hamiltonian in equation (2.3). The dynamical equation for the guiding center position vector is

$$\dot{\mathbf{X}}_{\mathbf{gc}} = [[\mathbf{X}_{\mathbf{gc}}, H_0]] = \tag{B.10}$$
$$= \frac{1}{qB^*} \nabla \mathbf{X}_{\mathbf{gc}} \cdot (\mathbf{b} \times \nabla H_0) + \tag{B.11}$$
$$+ \frac{\mathbf{B}^*}{mB^*} \cdot (\nabla \mathbf{X}_{\mathbf{gc}} \frac{\partial H_0}{\partial v_\parallel} - \frac{\partial \mathbf{X}_{\mathbf{gc}}}{\partial v_\parallel} \nabla H_0) + \tag{B.12}$$
$$+ \frac{q}{m}(\frac{\partial \mathbf{X}_{\mathbf{gc}}}{\partial \phi} \frac{\partial H_0}{\partial \mu} - \frac{\partial \mathbf{X}_{\mathbf{gc}}}{\partial \mu} \frac{\partial H_0}{\partial \phi}) = \tag{B.13}$$
$$= \frac{1}{B^*}(v_\parallel \mathbf{B}^* + \epsilon \mathbf{b} \times \frac{\mu}{m} \nabla B) \tag{B.14}$$

where we used the following identities:

$$\nabla \mathbf{X_{gc}} = \mathbf{I} \; ; \; \nabla H_0 = \mu \nabla B \; ; \; \frac{\partial \mathbf{X_{gc}}}{\partial \phi} = \frac{\partial H_0}{\partial \phi} = 0 \tag{B.15}$$

The dynamical equation for the parallel velocity is

$$\dot{v_{\|}} = [[v_{\|}, H_0]] = \tag{B.16}$$

$$= \frac{1}{qB^*} \nabla v_{\|} \cdot (\mathbf{b} \times \nabla H_0) + \tag{B.17}$$

$$+ \frac{\mathbf{B}^*}{mB^*} \cdot (\nabla v_{\|} \frac{\partial H_0}{\partial v_{\|}} - \frac{\partial v_{\|}}{\partial v_{\|}} \nabla H_0) + \tag{B.18}$$

$$+ \frac{q}{m} (\frac{\partial v_{\|}}{\partial \phi} \frac{\partial H_0}{\partial \mu} - \frac{\partial v_{\|}}{\partial \mu} \frac{\partial H_0}{\partial \phi}) = \tag{B.19}$$

$$= \frac{\mathbf{B}^*}{mB^*} \cdot (-\mu \nabla B) \tag{B.20}$$

where we used the following identities:

$$\nabla v_{\|} = \frac{\partial v_{\|}}{\partial \mu} = \frac{\partial v_{\|}}{\partial \phi} = 0 \tag{B.21}$$

The dynamical equation for the magnetic moment is

$$\dot{\mu} = [[\mu, H_0]] = \tag{B.22}$$

$$= \frac{1}{qB^*} \nabla \mu \cdot (\mathbf{b} \times \nabla H_0) + \tag{B.23}$$

$$+ \frac{\mathbf{B}^*}{mB^*} \cdot (\nabla \mu \frac{\partial H_0}{\partial v_{\|}} - \frac{\partial \mu}{\partial v_{\|}} \nabla H_0) + \tag{B.24}$$

$$+ \frac{q}{m} (\frac{\partial \mu}{\partial \phi} \frac{\partial H_0}{\partial \mu} - \frac{\partial \mu}{\partial \mu} \frac{\partial H_0}{\partial \phi}) = 0 \tag{B.25}$$

where we used the following identities:

$$\nabla\mu = \frac{\partial\mu}{\partial v_{\|}} = \frac{\partial\mu}{\partial\phi} = \frac{\partial H_0}{\partial\phi} = 0 \tag{B.26}$$

The dynamical equation for the gyrophase is

$$\dot{\phi} = [[\phi, H_0]] = \tag{B.27}$$

$$= \frac{1}{qB^*}\nabla\phi \cdot (\mathbf{b} \times \nabla H_0) + \tag{B.28}$$

$$+ \frac{\mathbf{B}^*}{mB^*} \cdot (\nabla\phi \frac{\partial H_0}{\partial v_{\|}} - \frac{\partial\phi}{\partial v_{\|}}\nabla H_0) + \tag{B.29}$$

$$+ \frac{q}{m}(\frac{\partial\phi}{\partial\phi}\frac{\partial H_0}{\partial\mu} - \frac{\partial\phi}{\partial\mu}\frac{\partial H_0}{\partial\phi}) = \frac{q}{m}B \tag{B.30}$$

where we used the following identities:

$$\nabla\phi = \frac{\partial\phi}{\partial v_{\|}} = \frac{\partial\phi}{\partial\mu} = 0 \; ; \; \frac{\partial H_0}{\partial\mu} = B \tag{B.31}$$

Appendix C

Vector identities for the specified equilibrium

We list some vectorial identities for the magnetic field versor in toroidal coordinates that are used in the guiding-center equations of motion.
The curl of the versor is

$$\nabla \times \mathbf{b} = \frac{1}{rR}(\frac{\partial}{\partial \theta}(Rb_\zeta))\mathbf{e_r} - \frac{1}{R}\frac{\partial}{\partial r}(Rb_\zeta)\mathbf{e}_\theta + \frac{1}{r}\frac{\partial}{\partial r}(rb_\theta)\mathbf{e}_\zeta \tag{C.1}$$

A simple calculation yields

$$\nabla \times \mathbf{b} = -\frac{1}{hR_0}sin\theta f\mathbf{e_r} - \frac{1}{h}\frac{\partial}{\partial r}(hf)\mathbf{e}_\theta + (\frac{\partial g}{\partial r} + \frac{g}{r})\mathbf{e}_\zeta \tag{C.2}$$

The divergence of the versor is

$$\nabla \cdot \mathbf{b} = -\frac{gsin\theta}{R} \tag{C.3}$$

Also

$$(\mathbf{b} \cdot \nabla)\mathbf{b} = -\mathbf{b} \times (\nabla \times \mathbf{b}) = (-\frac{f^2}{h}\frac{\partial h}{\partial r} - \frac{g^2}{r})\mathbf{e_r} + \frac{f^2}{hR_0}sin\theta\mathbf{e}_\theta - \frac{fg}{hR_0}sin\theta\mathbf{e}_\zeta \tag{C.4}$$

$$b_0 = \mathbf{b} \cdot (\nabla \times \mathbf{b}) = f\frac{\partial g}{\partial r} + \frac{fg}{r} - \frac{fg}{h}\frac{\partial h}{\partial r} - g\frac{\partial f}{\partial r} \tag{C.5}$$

$$\nabla \times (b_0 \mathbf{b}) = \frac{1}{rR}[\frac{\partial}{\partial \theta}(Rb_0 f)]\mathbf{e_r} - \frac{1}{R}\frac{\partial}{\partial r}(Rb_0 f)\mathbf{e}_\theta + \frac{1}{r}\frac{\partial}{\partial r}(rgb_0)\mathbf{e}_\zeta \tag{C.6}$$

The components of the $\nabla \mathbf{b}$ tensor are

$$(\nabla \mathbf{b})_{r\theta} = \frac{\partial g}{\partial r} \tag{C.7}$$

$$(\nabla \mathbf{b})_{r\zeta} = \frac{\partial f}{\partial r} \tag{C.8}$$

$$(\nabla \mathbf{b})_{\theta r} = -\frac{g}{r} \tag{C.9}$$

$$(\nabla \mathbf{b})_{\zeta r} = -\frac{f}{R}\frac{\partial R}{\partial r} \tag{C.10}$$

$$(\nabla \mathbf{b})_{\zeta \theta} = -\frac{f}{rR}\frac{\partial R}{\partial \theta} \tag{C.11}$$

$$(\nabla \mathbf{b})_{\zeta \zeta} = \frac{g}{rR}\frac{\partial R}{\partial \theta} \tag{C.12}$$

More vectorial identities are

$$\mathbf{b} \cdot \nabla \mathbf{b} \cdot \nabla \mathbf{b} = [-\frac{f^2 g}{rR} sin\theta + \frac{f^2 g}{R^2} sin\theta cos\theta]\mathbf{e_r} + [-\frac{f^2}{R}\frac{\partial g}{\partial r} cos\theta \tag{C.13}$$

$$-\frac{g^2}{r}\frac{\partial g}{\partial r} - \frac{f^2 g}{R^2} sin^2\theta]\mathbf{e}_\theta + [-\frac{f^2}{R}\frac{\partial f}{\partial r} cos\theta - \frac{g^2}{r}\frac{\partial f}{\partial r} + \frac{fg^2}{R^2} sin^2\theta]\mathbf{e}_\zeta \tag{C.14}$$

$$\nabla^2 \mathbf{b} \cdot \mathbf{b} = \frac{g}{R}\frac{\partial}{\partial r}[R(\frac{\partial g}{\partial r} + \frac{g}{r})] + \frac{f}{r}\frac{\partial}{\partial r}[\frac{r}{h}\frac{\partial}{\partial r}(hf)] - \frac{f}{r}\frac{\partial}{\partial \theta}(\frac{f}{R} sin\theta) + \tag{C.15}$$

$$- \frac{g^2}{rR} cos\theta - \frac{g^2}{R^2} sin^2\theta \tag{C.16}$$

$$\nabla \mathbf{b} : \nabla \mathbf{b} = -\frac{g}{r}\frac{\partial g}{\partial r} - \frac{f}{h}\frac{\partial f}{\partial r}\frac{\partial h}{\partial r} + \frac{g^2}{r^2 h^2}(\frac{\partial h}{\partial \theta})^2 \tag{C.17}$$

$$\mathbf{b} \times \nabla B = gB_0[-\frac{\partial}{\partial r}(\frac{1}{hf})e_\zeta] + fB_0[\frac{\partial}{\partial r}(\frac{1}{hf})e_\theta - \frac{1}{r}\frac{\partial}{\partial \theta}(\frac{1}{hf})e_\mathbf{r}] \tag{C.18}$$

The full expression for B^* is

$$B^* = \frac{B_0}{hf} + \epsilon v_\parallel [fg' + \frac{fg}{r} - \frac{fg}{R} cos\theta - gf'] + \tag{C.19}$$

$$+\frac{\epsilon^2 M}{2}[g(g'' - \frac{g}{r^2}) + ff'' - \frac{f^2}{R^2} cos^2\theta + \frac{g^4}{r^2}$$

$$+\frac{f^4 cos^2\theta}{R^2} + 2\frac{f^2 g^2}{rR} cos\theta]$$

The derivatives of the versor are

$$f' = -4\frac{r}{a^2}(\frac{A_{\varsigma 0}}{aB_0})^2 f^3 \tag{C.20}$$

$$f'' = -\frac{4}{a^2}(\frac{A_{\varsigma 0}}{aB_0})^2 (f + 3rf')f^2 \tag{C.21}$$

$$g' = -\frac{ff'}{g} \tag{C.22}$$

$$g'' = -\frac{f'^2 + ff''}{g} + \frac{ff'}{g^2} g' \tag{C.23}$$

where we let

$$f = (1 + 4x^2(A_{\varsigma 0}/aB_0)^2)^{-1/2} \tag{C.24}$$

Appendix D

Guiding-center equations for time integration

We list the guiding-center equations relative to poloidal and toroidal guiding-center position for a given equilibrium in terms of a magnetic field versor $\mathbf{b}$. The equation of motion for the poloidal coordinate is obtained by dotting equation (2.4) for the guiding-center position vector with the unit versor in the poloidal direction yielding

$$r\frac{d\theta}{dt} = \frac{1}{B^*}(v_{\|}\mathbf{B}^* + \epsilon\mathbf{b} \times \frac{\mu}{m}\nabla B) \cdot \mathbf{e}_\theta \tag{D.1}$$

The next step is to divide equation (D.1) by r to obtain

$$\frac{d\theta}{dt} = \frac{v_{\|}}{rB^*}\mathbf{B}^* \cdot \mathbf{e}_\theta + \frac{\epsilon\mu}{mrB^*}\mathbf{b} \times \nabla B \cdot \mathbf{e}_\theta \tag{D.2}$$

where the right-hand terms in equation (D.2) are computed by using the relationships in Appendices B and C to yield

$$\frac{v_{\|}}{rB^*}\mathbf{B}^* \cdot \mathbf{e}_\theta = \frac{v_{\|}}{rB^*}[\frac{g}{hf}B_0 + \epsilon v_{\|}(-\frac{f}{R}cos\theta - f') + \tag{D.3}$$
$$+\frac{\epsilon^2\mu}{2m}(g(\frac{gg'}{r} + \frac{ff'}{R}cos\theta) - 2\frac{f^2g'}{R}cos\theta -$$

$$-2\frac{g^2g'}{r} + \frac{b_0 f}{R}cos\theta + fb_0' + b_0 f')]$$

$$\frac{\epsilon\mu}{mrB^*}\mathbf{b}\times\nabla B\cdot\mathbf{e}_\theta = \frac{\epsilon\mu}{mrB^*}fB_0[-\frac{cos\theta}{fhR} - \frac{f'}{hf^2}] \tag{D.4}$$

where

$$b_0 = fg' + \frac{fg}{r} - \frac{fg}{R}cos\theta - gf' \tag{D.5}$$

$$b_0' = \frac{f'g + fg'}{r} - \frac{fg}{r^2} - gf'' - \frac{fg' + f'g}{R}cos\theta - \frac{fg}{R^2}cos^2\theta + fg'' \tag{D.6}$$

The toroidal angle motion equation is computed by dotting equation (2.4) with the unit versor in the toroidal direction yielding

$$R\frac{d\zeta}{dt} = \frac{1}{B^*}(v_\parallel\mathbf{B}^* + \epsilon\mathbf{b}\times\frac{\mu}{m}\nabla B)\cdot\mathbf{e}_\zeta \tag{D.7}$$

The next step is to divide equation (D.7) by R to obtain

$$\frac{d\zeta}{dt} = \frac{1}{B^*R}[v_\parallel\mathbf{B}^*\cdot\mathbf{e}_\zeta + \epsilon\frac{\mu}{m}\mathbf{b}\times\nabla B\cdot\mathbf{e}_\zeta] \tag{D.8}$$

where the right-hand side terms are computed by using the vectorial relationships in Appendices B and C yielding

$$\mathbf{B}^*\cdot\mathbf{e}_\zeta = \frac{B_0}{h} + \epsilon v_\parallel(g' + \frac{g}{r}) + \frac{\epsilon^2\mu}{2m}[\frac{fgg'}{r} - \frac{f^2f'}{R}cos\theta - 2\frac{g^2}{r}f' - \frac{gb_0}{r} - g'b_0 - gb_0'] \tag{D.9}$$

$$\mathbf{b}\times\nabla B\cdot\mathbf{e}_\zeta = gB_0[\frac{cos\theta}{fhR} + \frac{f'}{hf^2}] \tag{D.10}$$

Appendix E

Normalized quantities for normalized guiding-center equations

This appendix contains a list of all normalized quantities used in the guiding-center equations of Chapter 2. The normalized magnetic field is

$$\frac{B^*}{B_0} = B^{**} = \frac{1}{hf} + \frac{1}{\omega_{c0} t_b} \frac{\bar{v}_{\|th}}{a/R_0} \hat{b_0} + (\frac{1}{2\omega_{c0} t_b} \frac{R_0}{a})^2 \bar{\mu} c_0 \tag{E.1}$$

where the normalized quantity $\hat{b_0}$ is

$$\hat{b_0} = fg^* + \frac{fg}{x} - \frac{fg}{h} \frac{a}{R_0} cos\theta - gf^* \tag{E.2}$$

and

$$c_0 = g(g^{**} - \frac{g}{x^2}) - \frac{f^2}{h^2}(\frac{a}{R_0} cos\theta)^2 + \frac{g^4}{x^2} + \frac{f^4 cos^2\theta}{h^2}(\frac{a}{R_0})^2 + 2\frac{f^2 g^2}{xh} \frac{a}{R_0} cos\theta \tag{E.3}$$

The derivatives of the components of the versor **b** are

$$f^* = -4x(\frac{A_{\zeta 0}}{aB_0})^2 f^3 \tag{E.4}$$

$$f^{**} = -4(\frac{A_{\zeta 0}}{aB_0})^2(f + 3xf^*)f^2 \tag{E.5}$$

$$g^* = -\frac{ff^*}{g} \tag{E.6}$$

$$g^{**} = -\frac{f^{*2} + ff^{**}}{g} + \frac{ff^*}{g^2}g^* \tag{E.7}$$

$$\hat{b_0^*} = \frac{f^*g + fg^*}{x} - \frac{fg}{x^2} - gf^{**} - \frac{fg^* + f^*g}{h}\frac{a}{R_0}cos\theta - \frac{fg}{h^2}\frac{a^2}{R_0^2}cos^2\theta + fg^{**} \tag{E.8}$$

Appendix F

Derivation of condition on existence of maximal radial position

We need to find $d^2x/d(cos\theta)^2$ to make sure that our particle in phase space has a maximum radial excursion at $x = 1$ and $cos\theta = 1$.
The algebraic equation is

$$ax^4 + (c2 + c3 * cos^2(\theta)) * x^2 + cos(\theta)d_1 * x + e = 0 \tag{F.1}$$

Carrying out the implicit derivatives yields

$$\frac{dx}{d(cos(\theta))} = -\frac{2c3cos\theta * x^2 + d_1 * x}{4ax^3 + 2 * (c2 + c3cos^2(\theta)) * x + cos(\theta)d_1} \tag{F.2}$$

We multiply the first derivative by $-cos\theta$. This yields an expression for the second derivative. To have a maximum, we let $d^2x/d(cos\theta)^2 < 0$. This inequality can be written as

$$\frac{2c3cos^2\theta * x^2 + cos(\theta)d_1 * x}{4ax^3 + 2 * (c2 + c3cos^2(\theta)) * x + cos(\theta)d_1} < 0 \tag{F.3}$$

We take the point $x = 1$ and $cos\theta = 1$.

The inequality becomes

$$\frac{2c3 + d_1}{4a + 2c_1 + d_1} < 0 \tag{F.4}$$

Since the numerator is always a negative quantity, we can write the inequality in terms of the constants of motion as

$$\frac{-\frac{8}{9}\bar{v}^2 + \frac{\bar{\mu}}{3}}{4 * Ac^2 - 4 * A_c\bar{p} - \frac{8}{9}\bar{v}^2 + \frac{\bar{\mu}}{3}} < 0 \tag{F.5}$$

This result completes our derivation.

Appendix G

Wave Hamiltonian derivation

To start, we express the wave vector $\mathbf{k}$ in terms of the local triad

$$\mathbf{k} = k_{\|}\mathbf{b} + k_{\perp}(\mathbf{e_1} cos\alpha + \mathbf{e_2} sin\alpha) \tag{G.1}$$

where α is the angle between $k_{\perp}$ and $\mathbf{e_1}$. We assume that $(\mathbf{e_1}, \mathbf{e_2}, \mathbf{b})$ form a local orthonormal basis.

Let's also define a rotating orthonormal frame $(\mathbf{a}, \mathbf{b}, \mathbf{c})$ such that

$$\mathbf{a} = \mathbf{e_1} cos\phi_{gc} - \mathbf{e_2} sin\phi_{gc} \tag{G.2}$$

$$\mathbf{c} = -\mathbf{e_1} sin\phi_{gc} - \mathbf{e_2} cos\phi_{gc} \tag{G.3}$$

The gyroradius vector is $\rho = \frac{v_{\perp}}{\omega_c}\mathbf{c}$. We also make use of the following formula

$$e^{igcos\phi} = \sum_n J_n(g) e^{in(\phi+\pi/2)} \tag{G.4}$$

The exponential in the eikonal for the field can be written as

$$e^{i(\mathbf{k}\cdot\mathbf{x}-\omega t)} \simeq \sum_n J_n(k_{\perp}\rho) e^{i\psi_n} \tag{G.5}$$

where

$$\psi_n = \mathbf{k}\cdot\mathbf{X_{gc}} - \omega t + n(\phi + \alpha + \pi/2) \tag{G.6}$$

We want to consider the case of fast-wave heating. A fairly good approximation is to assume the parallel electric field to be negligible [39]. We also want to work with an electric field rather than a vector potential. The linear Hamiltonian is given by

$$H_1 = -q\mathbf{v} \cdot \mathbf{A_1} \tag{G.7}$$

neglecting the parallel electric field for the fast-Alfven wave and using Faraday's law yields

$$H_1 = -q\mathbf{v}_\perp \cdot \mathbf{A}_{1\perp} = \frac{iq\mathbf{v}_\perp \cdot \mathbf{E}_{1\perp}}{\omega} \tag{G.8}$$

The linear Hamiltonian can be written as

$$H_1 = \sum_{\mathbf{k}} \sum_n \frac{iq}{\omega} \mathbf{v}_\perp \cdot \mathbf{E}_{\perp \mathbf{k}} J_n(k_\perp \rho) e^{i\psi_n(\mathbf{k})} \tag{G.9}$$

where we used the eikonal dependence for the electric field given by equation (G.5) We can manipulate H_1 further by substituting $\mathbf{v}_\perp = v_\perp \mathbf{c}$ in H_1 to obtain

$$H_1 = \sum_k \sum_n \frac{iq}{2\omega} \sqrt{2B(X_{gc})\mu/m} [J_{n-1} e^{-i\alpha} E_+ + J_{n+1} e^{i\alpha} E_-] e^{i\psi_n(\mathbf{k})} \tag{G.10}$$

where the electric field components are

$$E_\pm(X_{gc}) = \mathbf{E}_\perp \cdot (\mathbf{e_1} \pm i\mathbf{e_2}) \tag{G.11}$$

In this thesis we deal with fundamental harmonic wave-particle resonance ($n = 1$) due to a monochromatic fast-Alfven wave, therefore the wave Hamiltonian in (G.10) simplifies to

$$H_1 = \frac{iq}{2\omega} \sqrt{2B(X_{gc})\mu/m} [J_0 e^{-i\alpha} E_+ + J_2 e^{i\alpha} E_-] e^{i\psi_1(\mathbf{k})} \tag{G.12}$$

The Hamiltonian given by equation (G.12) is employed in calculating the wave-particle resonant changes of the guiding-center variables.

Appendix H

Derivation of quasilinear equation

We substitute equations (3.38), (3.40) and (3.41) in the Vlasov equation given by equation (3.37) to yield

$$\frac{\partial(f_0+f_1)}{\partial t}+\dot{\mathbf{J}}_1\cdot\frac{\partial(f_0+f_1)}{\partial \mathbf{J}}+(\Omega+\dot{\Theta}_1)\cdot\frac{\partial(f_0+f_1)}{\partial \Theta}=0 \tag{H.1}$$

We now average the full Vlasov equation over the orbital frequencies to obtain

$$<\frac{\partial(f_0+f_1)}{\partial t}+\dot{\mathbf{J}}_1\cdot\frac{\partial(f_0+f_1)}{\partial \mathbf{J}}+(\Omega+\dot{\Theta}_1)\cdot\frac{\partial f_1}{\partial \Theta}>_{\omega,\phi_{gc},\theta}=0 \tag{H.2}$$

where we used the following relationship based on equation (3.38)

$$\frac{\partial f_0}{\partial \Theta}=0 \tag{H.3}$$

We substitute the eikonal expressions into the linear terms. By doing so only the zero and quadratic terms in λ survive the operation of averaging because of equation (3.51). The result is the following quasilinear equation

$$\frac{\partial f_0}{\partial t_{QL}} + \frac{1}{4} < \dot{\mathbf{J}}_\mathbf{1}^* \cdot \frac{\partial f_1}{\partial \mathbf{J}} + \dot{\mathbf{\Theta}}_\mathbf{1}^* \cdot \frac{\partial f_1}{\partial \mathbf{\Theta}} + c.c. >_{\omega,\phi_{gc},\theta} = 0 \tag{H.4}$$

where the time variable is the quasilinear time since we averaged over the fast times. The angles are given by

$$\mathbf{\Theta} = (\theta, \zeta, \phi_{gc}) \tag{H.5}$$

Equations (H.4) and (H.5) yield the quasilinear equation (3.50). We now derive the slowly varying term of the perturbed distribution function given by equation (3.61). We start by writing the linearized Vlasov equation given by equation (3.60)

$$\frac{\partial f_1}{\partial t} + \omega_c \frac{\partial f}{\partial \phi_{gc}} + \omega_\theta \frac{\partial f}{\partial \theta} + \omega_\zeta \frac{\partial f}{\partial \zeta} = -\dot{\mathbf{J}}_\mathbf{1} \cdot \frac{\partial f_0}{\partial \mathbf{J}} \tag{H.6}$$

where ω_θ and ω_ζ are respectively the poloidal and toroidal frequencies. We substitute the eikonal expressions for the fields and the distribution function given by equations (3.42) and (3.43) into the linearized Vlasov equation and take the derivative over the phase given by equation (3.44) to obtain the following differential equation

$$\frac{d\theta}{dt_L}\frac{df_1^|}{d\theta} - i(\omega - \omega_c - N\omega_\zeta - M\omega_\theta) f_1^| = -\dot{\mathbf{J}}_\mathbf{1}^| \cdot \frac{\partial f_0}{\partial \mathbf{J}} \tag{H.7}$$

where t_L is the total time derivative along the unperturbed orbit. We assumed that the slowly varying term of the linearized distribution function is a function of the poloidal angle, but it is independent of the toroidal angle because the toroidal system is axisymmetric and also independent of the gyrophase. We can also recognize the resonance condition in the second term of the left-hand side of equation (H.7). We proceed to integrate the linearized differential equation multiplying it by the integrat-

ing factor given by

$$\frac{dt_L}{d\theta} exp(-i \int_{t'}^{t_L} (\omega - \omega_c - N\omega_\zeta - M\omega_\theta) dt'_L) \tag{H.8}$$

The differential equation can be now written in the following form

$$\frac{d}{d\theta}(f_1^| exp(-i \int_{t'}^{t_L} (\omega - \omega_c - N\omega_\zeta - M\omega_\theta) dt'_L)) = -\dot{\mathbf{J}}_\mathbf{1}^| \cdot \frac{\partial f_0}{\partial \mathbf{J}} \frac{dt_L}{d\theta} exp(-i \int_{t'}^{t_L} (\omega - \omega_c - N\omega_\zeta - M\omega_\theta) dt'_L) \tag{H.9}$$

which can be integrated to give

$$f_1^| exp(-i \int_{t'}^{t_L} (\omega - \omega_c - N\omega_\zeta - M\omega_\theta) dt'_L) = -\dot{\mathbf{J}}_\mathbf{1}^| \cdot \frac{\partial f_0}{\partial \mathbf{J}} \int_{-\infty}^{t'} dt''_L exp(-i \int_{t'}^{t''_L} (\omega - \omega_c - N\omega_\zeta - M\omega_\theta) dt'_L) \tag{H.10}$$

We make the assumption of a system with no memory, therefore we can translate the limits of integration in the time integrations without affecting the value of the integral. By doing so we obtain the solution for the linearized distribution function

$$f_1^| = -exp(i \int_0^{t''_L} (\omega - \omega_c - N\omega_\zeta - M\omega_\theta) dt'_L) \dot{\mathbf{J}}_\mathbf{1}^| \cdot \frac{\partial f_0}{\partial \mathbf{J}} \int_0^{\infty} dt''_L exp(-i \int_0^{t''_L} (\omega - \omega_c - N\omega_\zeta - M\omega_\theta) dt'_L) \tag{H.11}$$

which can be written in the more compact form given by equation (3.61)

$$f_1^| = -e^{i\psi_L} \dot{\mathbf{J}}_\mathbf{1}^| \cdot \frac{\partial f_0}{\partial \mathbf{J}} \int_0^{\infty} e^{-i\psi_L} dt'_L \tag{H.12}$$

where the phase along the unperturbed orbit is given by

$$\psi_L(0,t_L) = \int_0^{t_L} (\omega - \omega_c - N\omega_\zeta - M\omega_\theta) dt_L^{'} \tag{H.13}$$

We now derive equation (3.74). The convective term is

$$- < f_1 \frac{\partial}{\partial \mathbf{J}} \cdot \mathbf{J_1} >_{\omega,\phi,\theta} = -\frac{1}{2} - < f_1^{|*} \frac{\partial}{\partial \mathbf{J}} \cdot \mathbf{J_1^{|}} >_{\omega,\phi,\theta} \tag{H.14}$$

We substitute equation (3.70) into the right-hand side of equation (H.14) and use equation (3.56) to obtain

$$- < f_1 \frac{\partial}{\partial \mathbf{J}} \cdot \mathbf{J_1} >_{\omega,\phi,\theta} = \frac{1}{4} < e^{i\psi_L} \mathbf{J_1^{|*}} \cdot \frac{\partial f_0}{\partial \mathbf{J}} (\int_0^{T_b} e^{-i\psi_L} dt_L) \frac{\partial}{\partial \mathbf{J}} \cdot \mathbf{J_1^{|*}} >_{\omega,\phi,\theta} \tag{H.15}$$

The orbit-averaging operator acts only on the fast varying phase $e^{i\psi_L}$ to yield

$$- < f_1 \frac{\partial}{\partial \mathbf{J}} \cdot \mathbf{J_1} >_{\omega,\phi,\theta} = \frac{1}{4} \frac{|\int_0^{T_b} e^{i\psi_L} dt_L|^2}{T_b} \mathbf{J_1^{|*}} \cdot \frac{\partial f_0}{\partial \mathbf{J}} \frac{\partial}{\partial \mathbf{J}} \cdot \mathbf{J_1^{|*}} \tag{H.16}$$

Rearranging the right-hand side of equation (H.16) we obtain equation (3.74)

$$- < f_1 \frac{\partial}{\partial \mathbf{J}} \cdot \mathbf{J_1} >_{\omega,\phi,\theta} = \frac{1}{4} \frac{|\int_0^{T_b} e^{i\psi} dt_L|^2}{T_b} (\frac{\partial}{\partial \mathbf{J}} \cdot \mathbf{J_1^{|*}}) \mathbf{J_1^{|*}} \cdot \frac{\partial f_0}{\partial \mathbf{J}} \tag{H.17}$$

This completes our derivation of equation (3.74).

Appendix I

Derivation of the linear equations of motion

We derive the linear equations (3.85)-(3.88). The linear equation of motion for the guiding-center vector is found from equations (B.2)-(B.5). Substituting $f = \mathbf{X_{gc}}$ and $g = H_1$

$$\dot{\mathbf{X}}^{\mathbf{1}}_{\mathbf{gc}} = [[\mathbf{X_{gc}}, H_1]] = \frac{1}{qB^*}\nabla \mathbf{X_{gc}} \cdot (\mathbf{b} \times \nabla H_1) = \frac{1}{qB^*}(\mathbf{b} \times \nabla H_1) \tag{I.1}$$

where the Poisson brackets given by equations (B.4) and (B.5) are zero because $\mathbf{X_{gc}}$ is independent of the other guiding center variables and $\partial H_1/\partial v_{||} = 0$ where H_1 is given by equation (3.84). The spatial derivative acts on the phase to yield equation (3.85)

$$\dot{\mathbf{X}}^{\mathbf{1}}_{\mathbf{gc}} = \frac{1}{qB^*}(\mathbf{b} \times \hat{H}_1 \nabla e^{i\psi_1}) = \frac{i}{qB^*}(\mathbf{b} \times \nabla \psi_1 H_1) \tag{I.2}$$

The linear equation of motion for the magnetic moment is derived from equations (B.2)-(B.5) substituting $f = \mu$ and $g = H_1$ to obtain equation (3.86)

$$\dot{\mu}^1 = [[\mu, H_1]] = -\frac{q}{m}\frac{\partial H_1}{\partial \phi} = -i\frac{q}{m}H_1 \tag{I.3}$$

where the Poisson brackets given by equations (B.3) and (B.4) are zero because μ does not depend on the other guiding-center variables and the derivative of the linear Hamiltonian over the gyrophase yields unity because of equation (3.83).
The derivation of the linear equation for the gyrophase is obtained from equations (B.2)-(B.5) substituting $f = \phi$ and $g = H_1$ to yield

$$\dot{\phi}^1_{gc} = \frac{q}{m}\frac{\partial \phi}{\partial \phi}\frac{\partial H_1}{\partial \mu} = \frac{q}{m}\frac{\partial H_1}{\partial \mu} \tag{I.4}$$

where the Poisson brackets given by equations (B.3) and (B.4) are zero because ϕ does not depend on the other guiding-center variables. The linear equation of motion for $v_\parallel$ is derived from equations (B.2)-(B.5) substituting $f = v_\parallel$ and $g = H_1$ to yield

$$\dot{v_\parallel}^1 = -\frac{\mathbf{B}^*}{mB^*} \cdot \nabla H_1 = -\frac{i\mathbf{B}^*}{mB^*} \cdot \nabla \psi_1 H_1 \tag{I.5}$$

where the other Poisson brackets are zero because $v_\parallel$ is independent of the other guiding-center variables.

Appendix J

Derivation of the guiding-center variable changes caused by wave-particle resonance

We derive the changes in the guiding-center variables caused by wave-particle resonant interaction. The linear wave Hamiltonian is given by equations (3.82)-(3.84), where we assumed the wave to be monochromatic. The Bessel functions J_0 and J_2 are obtained by letting $n = 1$ in equation (G.9). The electric field is expressed in terms of its left and right circularly polarized components $\mathbf{E}_\pm$ defined in equation (G.11). We begin by integrating the guiding-center vector position equation of motion (3.85) along its unperturbed orbit to obtain

$$(\delta \mathbf{X_{gc}})_{res} = \int_{res} d\mathbf{X_{gc}} = \int_{res} dt_L \frac{i}{qB^*} \mathbf{b} \times \nabla \psi_1 H_1 \tag{J.1}$$

We use the result in equations (3.95) and (3.96) and the linear Hamiltonian in (3.82) to obtain

$$(\delta \mathbf{X_{gc}})_{res} = \frac{i}{qB^*}[(\frac{gN}{R} - \frac{fM}{r})\mathbf{e_r} - fk_\perp \mathbf{e}_\theta + gk_\perp \mathbf{e}_\zeta]\hat{H}_1 \int_{res} e^{i\psi} dt_L \tag{J.2}$$

We substitute equation (3.84) into equation (J.2), use the leading order approximation $B^* \approx B$ from equations (C.19), (2.10) and (3.97), the resonant change in the guiding-center position vector becomes

$$(\delta \mathbf{X_{gc}})_{res} \approx [\frac{1}{2\omega}(2\mu/mB)^{1/2}[(-\frac{gN}{R}+\frac{fM}{r})\mathbf{e_r}+fk_\perp \mathbf{e}_\theta - gk_\perp \mathbf{e}_\zeta](J_0 e^{-i\alpha}E_+ + J_2 e^{i\alpha}E_-)]_{res} I \tag{J.3}$$

By dotting equation (J.3) with $\mathbf{e_r}$,$\mathbf{e}_\theta$ and $\mathbf{e}_\zeta$ respectively, we obtain equations (3.98)-(3.100).

The resonant change in the magnetic moment is obtained by integrating equation (3.86) along the particle's unperturbed orbit to yield

$$(\delta\mu)_{res} = \int_{res} d\mu = -\frac{iq}{m}\int_{res} dt_L H_1 \tag{J.4}$$

Using (3.95) the right-hand side of (J.4) becomes

$$(\delta\mu)_{res} \approx -(\frac{iq}{m}\hat{H}_1)_{res}\int_{res} e^{i\psi_L} dt_L \tag{J.5}$$

Using (3.84) and (3.97) the right-hand side of (J.5) becomes

$$(\delta\mu)_{res} \approx [(\frac{q}{m})^2 \frac{1}{\omega}(mB\mu/2)^{1/2}(J_0 e^{-i\alpha}E_+ + J_2 e^{i\alpha}E_-)]_{res} I \tag{J.6}$$

The resonant change in parallel velocity is computed by integrating (3.88) along the particle's unperturbed orbit

$$(\delta v_\parallel)_{res} = \int_{res} dv_\parallel = -\int_{res} dt_L \frac{i\mathbf{B}^*}{mB^*}\cdot\nabla\psi_1 H_1 \tag{J.7}$$

Using (3.95) and (3.97) the right-hand side of (J.7) becomes

$$(\delta v_{\parallel})_{res} \approx -(\frac{i\mathbf{B}^*}{mB^*} \cdot \nabla\psi_1 \hat{H}_1)_{res} I \tag{J.8}$$

From equation (B.6) the magnetic starred field to order ϵ is given by

$$\mathbf{B}^* \approx \mathbf{B} + \frac{m}{q} v_{\parallel} \nabla \times \mathbf{b} \tag{J.9}$$

The magnetic field vector can be written as $\mathbf{B} = B\mathbf{b}$, hence equation (J.9) becomes at leading order in ϵ

$$\mathbf{B}^* \approx B\mathbf{b} - \frac{m}{q} v_{\parallel} \frac{sin\theta}{h_{R_0}} f\mathbf{e_r} \tag{J.10}$$

where only the radial component of $\nabla \times \mathbf{b}$ from equation (C.2) has been kept since the poloidal and toroidal component are dominated by $\mathbf{B}$. We divide equation (J.10) by B, where we approximated $B^* \approx B$ from (B.7) to obtain equation (3.103)

$$\frac{\mathbf{B}^*}{B} \approx \mathbf{b} - \frac{v_{\parallel}}{\omega_c} \frac{f sin\theta}{R} \mathbf{e_r} \tag{J.11}$$

Dotting equation (3.89) with (J.11) yields

$$\frac{\mathbf{B}^*}{B^*} \cdot \nabla\psi_1 \approx \mathbf{b} - \frac{v_{\parallel}}{\omega_c} \frac{f sin\theta}{R} \mathbf{e_r} \cdot \nabla\psi_1 \approx \frac{fN}{R} + \frac{gM}{r} + \frac{k_{\perp} v_{\parallel}}{\omega_c R} f sin\theta \tag{J.12}$$

where we used the relation $\mathbf{b} = f\mathbf{e}_\zeta + g\mathbf{e}_\theta$. We now substitute (J.12) into (J.8) to obtain equation (3.102)

$$(\delta v_{\parallel})_{res} \approx [(\frac{fN}{R} + \frac{gM}{r} + \frac{k_{\perp}v_{\parallel}}{\omega_c R} f sin\theta)\frac{q}{2m\omega}(2\mu B/m)^{1/2}(J_0 e^{-i\alpha}E_+ + J_2 e^{i\alpha}E_-)]_{res} I \tag{J.13}$$

The change in the gyrophase is obtained by integrating equation (3.87) along the unperturbed particle's orbit

$$(\delta\phi)_{res} = \int_{res} d\phi = \frac{q}{m}\int_{res} dt_L \frac{\partial H_1}{\partial \mu} = \frac{q}{m}\frac{\partial}{\partial \mu}(\hat{H}_{1res} I) \tag{J.14}$$

The partial derivative acts only on I because $\hat{H}_1$ is evaluated at resonance. Using (3.84) the right-hand side of (J.14) becomes

$$(\delta\phi)_{res} = (\frac{iq^2}{2m\omega}(2B\mu/m)^{1/2}(J_0 e^{-i\alpha}E_+ + J_2 e^{i\alpha}E_-))_{res}\frac{\partial I}{\partial \mu} \tag{J.15}$$

The phase integral I is a function of the constants of motion and therefore depends on μ. There is no general analytic formula for $\partial I/\partial\mu$, since it depends on the constants of the motion, the resonance location and the topology of the particle's orbit.

Appendix K

Derivation of a fast minority ion collision operator

The starting equation is the Landau form of the Fokker-Planck collision operator [12]. The collision operator is

$$(\frac{\partial f_i}{\partial t})_c = \frac{e_i^2 e_j^2}{2\epsilon_0} ln\Lambda \frac{1}{m_i} \frac{\partial}{\partial \mathbf{v_i}} \cdot \int d^3 v_j \omega \cdot (\frac{1}{m_i} \frac{\partial}{\partial \mathbf{v_i}} - \frac{1}{m_j} \frac{\partial}{\partial \mathbf{v_j}}) f_i f_j \tag{K.1}$$

where the index i refers to the minority species, while the index j refers to the background species and

$$\omega = \frac{\partial^2 g}{\partial \mathbf{v_i} \partial \mathbf{v_i}} = \frac{1}{g^3}(g^2 \mathbf{I} - \mathbf{gg}) \tag{K.2}$$

The relative velocity is given by

$$g = |\mathbf{g}| = |\mathbf{v_i} - \mathbf{v_j}| \tag{K.3}$$

The collision operator can be integrated by parts to yield

$$(\frac{\partial f_i}{\partial t})_c = \frac{e_i^2 e_j^2}{2\epsilon_0} ln\Lambda \frac{1}{m_i^2} \frac{\partial}{\partial \mathbf{v_i}} \cdot [\frac{\partial f_i}{\partial \mathbf{v_i}} \cdot \int d^3 v_j \omega f_j - \frac{m_i}{m_j} f_i \frac{\partial}{\partial \mathbf{v_i}} \cdot \int d^3 v_j \omega f_j] \tag{K.4}$$

where we made use of

$$\frac{\partial}{\partial \mathbf{v_i}} \cdot \omega = -\frac{\partial}{\partial \mathbf{v_j}} \cdot \omega \tag{K.5}$$

Using the first expression for ω, the collision operator can be written as

$$(\frac{\partial f_i}{\partial t})_c = \frac{e_i^2 e_j^2}{2\epsilon_0} ln\Lambda \frac{1}{m_i^2} n_{0j} v_{thj} \frac{\partial}{\partial \mathbf{v_i}} \cdot [\frac{\partial f_i}{\partial \mathbf{v_i}} \cdot \frac{\partial^2 F(x_{ij})}{\partial \mathbf{v_i} \partial \mathbf{v_i}} - \frac{m_i}{m_j} f_i \frac{\partial}{\partial \mathbf{v_i}} \cdot \frac{\partial^2 F(x_{ij})}{\partial \mathbf{v_i} \partial \mathbf{v_i}}] \tag{K.6}$$

where we define the function F as

$$F(x_{ij}) = \frac{1}{n_{0j} v_{thj}} \int d^3 v_j f_j g_{ij} \tag{K.7}$$

where $x_{ij} = v_i / v_{thj}$.

Taking the derivatives in equation (K.6), the collision operator becomes

$$(\frac{\partial f_i}{\partial t})_c = \frac{e_i^2 e_j^2}{2\epsilon_0} ln\Lambda \frac{1}{m_i^2} n_{0j} v_{thj} \frac{\partial}{\partial \mathbf{v_i}} \cdot [F_1 + F_2] \tag{K.8}$$

where

$$F_1 = \frac{\partial f_i}{\partial \mathbf{v_i}} \cdot (\frac{\partial^2 x_{ij}}{\partial \mathbf{v_i} \partial \mathbf{v_i}} F' + \frac{\partial x_{ij}}{\partial \mathbf{v_i}} \frac{\partial x_{ij}}{\partial \mathbf{v_i}} F'') \tag{K.9}$$

and

$$F_2 = -\frac{m_i}{m_j} f_i \left(\frac{\partial}{\partial \mathbf{v_i}} \cdot \frac{\partial^2 x_{ij}}{\partial \mathbf{v_i} \partial \mathbf{v_i}} F'' + \frac{\partial}{\partial \mathbf{v_i}} \cdot \frac{\partial x_{ij}}{\partial \mathbf{v_i}} \frac{\partial x_{ij}}{\partial \mathbf{v_i}} F'' + \frac{x_{ij}}{\partial \mathbf{v_i}} \cdot \frac{\partial^2 x_{ij}}{\partial \mathbf{v_i} \partial \mathbf{v_i}} F'' + \frac{\partial x_{ij}}{\partial \mathbf{v_i}} \cdot \frac{\partial x_{ij}}{\partial \mathbf{v_i}} \frac{\partial x_{ij}}{\partial \mathbf{v_i}} F'''\right) \tag{K.10}$$

The collision operator terms F_1 and F_2 can be simplified by using the following relations

$$\frac{\partial x_{ij}}{\partial \mathbf{v_i}} = \frac{1}{v_{thj}} \frac{\mathbf{v_i}}{v_i} \; ; \; \frac{\partial}{\partial \mathbf{v_i}} \cdot \frac{\partial x_{ij}}{\partial \mathbf{v_i}} = \frac{2}{v_{thj} v_i} \tag{K.11}$$

$$\frac{\partial^2 x_{ij}}{\partial \mathbf{v_i} \partial \mathbf{v_i}} = \frac{1}{v_{thj} v_i^3} (v_i^2 \mathbf{I} - \mathbf{v_i} \mathbf{v_i}) \tag{K.12}$$

$$\frac{\partial}{\partial \mathbf{v_i}} \cdot \frac{\partial^2 x_{ij}}{\partial \mathbf{v_i} \partial \mathbf{v_i}} = -\frac{2}{v_{thj}} \frac{\mathbf{v_i}}{v_i^3} \; ; \; \frac{\partial x_{ij}}{\partial \mathbf{v_i}} \cdot \frac{\partial x_{ij}}{\partial \mathbf{v_i}} \frac{\partial x_{ij}}{\partial \mathbf{v_i}} = 0 \tag{K.13}$$

The result of the simplification is

$$\left(\frac{\partial f_i}{\partial t}\right)_c = \Gamma_{ij} \frac{\partial}{\partial \mathbf{v_i}} \cdot \left[\frac{\partial f_i}{\partial \mathbf{v_i}} \cdot F_3 + 2 \frac{m_i}{m_j} f_i \frac{\mathbf{v_i}}{v_i^3} F_4\right] \tag{K.14}$$

where

$$F_3 = \frac{\partial^2 v_i}{\partial \mathbf{v_i} \partial \mathbf{v_i}} F' + \frac{\mathbf{v_i} \mathbf{v_i}}{v_i^3} x_{ij} F'' \tag{K.15}$$

$$F_4 = F' - x_{ij} F'' - \frac{x_{ij}^2}{2} F''' \tag{K.16}$$

and

$$\Gamma_{ij} = \frac{e_i^2 e_j^2}{2\epsilon_0} ln\Lambda \frac{n_{0j}}{m_i^2} \tag{K.17}$$

When the background species are Maxwellian, the integral for F can be derived to give

$$F(x) = (x + \frac{1}{2x})\Phi(x) + \frac{1}{2}\Phi'(x) \tag{K.18}$$

where the error function and its derivative are

$$\Phi(x) = \frac{2}{\sqrt{\pi}} \int_0^x e^{-t^2} dt \; ; \; ; \Phi' = \frac{2}{\sqrt{\pi}} e^{-x^2} \tag{K.19}$$

There are two asymptotic forms for F.
For $x << 1$ we have

$$F(x) \approx \frac{2}{\sqrt{\pi}}(1 + \frac{x^2}{3} - \frac{x^4}{30} + ...) \tag{K.20}$$

For $x >> 1$ we have

$$F(x) = x + \frac{1}{2x} - \frac{e^{-x^2}}{2\sqrt{\pi}x^4}(1 - \frac{3}{x^2} + ...) \tag{K.21}$$

We neglect collisions between fast minority ions because the minority species density is smaller than the majority species density. Minority ions are much more energetic than majority ions, therefore $x_{m,i} >> 1$ is a good approximation.
Keeping the leading order terms, the ion-ion collision terms become

$$F_3 \approx \frac{\partial^2 v_i}{\partial \mathbf{v_i} \partial \mathbf{v_i}} \; ; \; F_4 \approx 1 \tag{K.22}$$

The ion-ion collision operator becomes

$$(\frac{\partial f_i}{\partial t})_{c,ion} = \Gamma_{m,ion} \frac{\partial}{\partial \mathbf{v}} \cdot [\frac{\partial f}{\partial \mathbf{v}} \cdot \frac{\partial^2 v}{\partial \mathbf{v} \partial \mathbf{v}} + 2 \frac{m_{min}}{m_{ion}} f \frac{\mathbf{v}}{v^3}] \tag{K.23}$$

It is convenient to use spherical coordinates (v, θ, ϕ) and make the assumption of axisymmetric distribution function along the field.

The collision operator simplifies to

$$(\frac{\partial f_i}{\partial t})_{c,ion} = \frac{\Gamma_{min,ion}}{v^3} (2 \frac{m_{min}}{m_{ion}} v \frac{\partial f}{\partial v} + \frac{\partial}{\partial \xi} (1 - \xi^2) \frac{\partial f}{\partial \xi}) \tag{K.24}$$

where $\xi = v_{\|}/v$ is the pitch-angle. For minority ion-electron collisions, we assume that $x_{m,e} << 1$.

The collision terms at leading order are

$$F_3 \approx \mathbf{I} \frac{2}{3} \frac{x_{m,e}}{v} \; ; \; F_4 \approx \frac{2}{3} x_{m,e}^3 \tag{K.25}$$

Using the asymptotic form for the collision terms, the minority ion-electron collision operator can be written as

$$(\frac{\partial f_i}{\partial t})_{c,e} = \frac{4}{3\sqrt{\pi}} \Gamma_{m,e} \frac{x}{v} \frac{\partial}{\partial \mathbf{v}} \cdot [\frac{\partial f}{\partial \mathbf{v}} + 2 \frac{m_m}{m_e} \frac{x^2}{v^2} \mathbf{v} f] \tag{K.26}$$

The next step is to neglect the first term. This is equivalent to the following inequality

$$2 \frac{m_m}{m_e} x^2 >> 1 \tag{K.27}$$

The ion-electron collision operator simplifies to

$$(\frac{\partial f_i}{\partial t})_{c,e} = \frac{8}{3\sqrt{\pi}}\Gamma_{m,e}\frac{x_{m,e}^3}{v^3}\frac{m_m}{m_e}(v\frac{\partial f}{\partial v} + 3f) \tag{K.28}$$

Combining the ion and the electron contribution, the full collision operator becomes

$$(\frac{\partial f_i}{\partial t})_c = \frac{1}{v^3}[\frac{8}{3\sqrt{\pi}}\Gamma_{m,e}x_{m,e}^3\frac{m_m}{m_e}(v\frac{\partial f}{\partial v} + 3f) + \Gamma_{min,ion}(2\frac{m_{min}}{m_{ion}}v\frac{\partial f}{\partial v} + \frac{\partial}{\partial \xi}(1-\xi^2)\frac{\partial f}{\partial \xi})] \tag{K.29}$$

This is the standard form of the collision operator for fast minority ions [3].

Appendix L

Derivation of collision diffusion coefficients for delta distribution function

We derive the diffusion coefficients for a minority delta distribution function in pitch-angle velocity space (v, ξ) following Goldston [58]. The starting equation is the collision operator given by (4.2). The distribution function is a delta function in the velocity variables

$$f = \delta(v - v_0)\delta(\xi - \xi_0) \tag{L.1}$$

We begin by calculating the moments in velocity space of the distribution function change, which are defined as

$$< \frac{\partial v}{\partial t} >= \frac{\int (\partial f/\partial t)_c v^3 dv d\xi}{\int f v^2 dv d\xi} \tag{L.2}$$

$$< \frac{\partial v^2}{\partial t} >= \frac{\int (\partial f/\partial t)_c v^4 dv d\xi}{\int f v^2 dv d\xi} \tag{L.3}$$

$$< \frac{\partial \xi}{\partial t} >= \frac{\int \xi (\partial f/\partial t)_c v^2 dv d\xi}{\int f v^2 dv d\xi} \tag{L.4}$$

$$< \frac{\partial \xi^2}{\partial t} >= \frac{\int \xi^2 (\partial f/\partial t)_c v^2 dv d\xi}{\int f v^2 dv d\xi} \tag{L.5}$$

The quadratic moment in velocity is easily evaluated by substituting the delta distribution function in the integral

$$\int f v^2 dv d\xi = v_0^2 \tag{L.6}$$

To carry out the other integrals, we make use of the following relation

$$\int_{-\infty}^{\infty} f(t) \delta^{'}(t-a) dt = -f^{'}(a) \tag{L.7}$$

The results are

$$\int (\partial f/\partial t)_c v^3 dv d\xi = -\frac{v_0^3 + v_c^3}{\tau_s} \tag{L.8}$$

$$\int (\partial f/\partial t)_c v^4 dv d\xi = -\frac{2 v_0 (v_0^3 + v_c^3)}{\tau_s} \tag{L.9}$$

$$\int \xi (\partial f/\partial t)_c v^2 dv d\xi = -\frac{Z_{eff2}}{\tau_s} \frac{v_c^3}{v_0} \xi_0 \tag{L.10}$$

$$\int \xi^2 (\partial f/\partial t)_c v^2 dv d\xi = -\frac{Z_{eff2}}{\tau_s}\frac{v_c^3}{v_0}(3\xi_0^2 - 1) \tag{L.11}$$

The averaged derivatives can be written as functions of velocity and pitch-angle variables as

$$< \frac{\partial v}{\partial t} >= -\frac{v + v_c^3/v^2}{\tau_s} \tag{L.12}$$

$$< \frac{\partial v^2}{\partial t} >= -2\frac{v^2 + v_c^3/v}{\tau_s} \tag{L.13}$$

$$< \frac{\partial \xi}{\partial t} >= -\frac{Z_{eff2}}{\tau_s}\frac{v_c^3}{v^3}\xi \tag{L.14}$$

$$< \frac{\partial \xi^2}{\partial t} >= -\frac{Z_{eff2}}{\tau_s}\frac{v_c^3}{v^3}(3\xi^2 - 1) \tag{L.15}$$

The averaged displacement in velocity space is given by

$$v_{fin} = v_{in} + \delta t \ < \frac{\partial v}{\partial t} >= v_{in} - \delta t \ \frac{v_{in} + v_c^3/v_{in}^2}{\tau_s} \tag{L.16}$$

$$\xi_{fin} = \xi_{in} + \delta t \ < \frac{\partial \xi}{\partial t} >= \xi_{in} - \delta t \ \frac{Z_{eff2}}{\tau_s}\frac{v_c^3}{v_{in}^3}\xi_{in} \tag{L.17}$$

where the subscripts in and fin stand for the initial velocities and final velocities at every step of integration.

The spread in velocity space is

$$< \Delta v \Delta v >=< (v_2^2 - v_1^2 >=< v_2^2 + v_1^2 - 2v_1 v_2 >= \tag{L.18}$$

$$=< v_2^2 + v_1^2 - 2v_1(v_1 + \delta v) >= \delta t \, (< \frac{\partial v^2}{\partial t} > -2v < \frac{\partial v}{\partial t} >)$$

$$< \Delta \xi \Delta \xi >= \delta t \, (< \frac{\partial \xi^2}{\partial t} > -2\xi < \frac{\partial \xi}{\partial t} >) \tag{L.19}$$

The convective diffusion coefficients are

$$< \Delta v >= -\frac{v + v_c^3/v^2}{\tau_s} \delta t \tag{L.20}$$

and

$$< \Delta \xi >= -\frac{Z_{eff2}}{\tau_s} \frac{v_c^3}{v^3} \xi \delta t \tag{L.21}$$

The diffusive spreads for fast ions are

$$< \Delta v \Delta v >= 0 \tag{L.22}$$

$$< \Delta \xi \Delta \xi >= \frac{Z_{eff2}}{\tau_s} \frac{v_c^3}{v_{in}^3} (1 - \xi_{in}^2) \delta t \tag{L.23}$$

The diffusion coefficients (I.20), (I.21), (I.22), and (I.23) can be used in a Monte Carlo simulation to compute the velocity diffusion of fast minority ions.

Appendix M

Derivation of a RF-driven flux from the kinetic equation

We begin by writing the full kinetic equation

$$\frac{\partial f}{\partial t} + v_{\|}\frac{\partial f}{\partial l} + v_{dx}\frac{\partial f}{\partial x} = C(f) + Q(f) + T(f) \tag{M.1}$$

where l is a spatial coordinate along the field lines, C, Q are the collision and quasi-linear operator respectively and we introduced a radial operator

$$T = -\frac{\delta x}{\delta t}\frac{\partial f}{\partial x} \tag{M.2}$$

where δx is any radial displacement due to wave-particle interaction. We are interested in finding the flux in a steady-state case, therefore we let $\frac{\partial f}{\partial t} = 0$. We order the kinetic equation operators according to their time scales. To do so, we introduce a small parameter $\lambda_t << 1$. The ordering yields

$$v_{\|}\frac{\partial}{\partial l} \propto \lambda_t^0 \; ; \; (v_{dx}\frac{\partial}{\partial x}, C, Q) \propto \lambda_t^1 \; ; \; T \propto \lambda_t^2 \tag{M.3}$$

The next step is to expand the distribution function in terms of λ_t

$$f = \lambda_t^0 f_0 + \lambda_t^1 f_1 + ... \tag{M.4}$$

Inserting the expanded distribution function in the steady-state kinetic equation yields a zero order equation

$$\frac{\partial f_0}{\partial l} = 0 \tag{M.5}$$

which says that the zero order distribution function is constant along the field lines. At first order in λ_t the kinetic equation yields

$$v_{\|}\frac{\partial f_1}{\partial l} + v_{dx}\frac{\partial f_0}{\partial x} = C(f_0) + Q(f_0) \tag{M.6}$$

We bounce average the linear equation in λ_t to obtain

$$< C(f_0) + Q(f_0) >= 0 \tag{M.7}$$

where we made use of the fact that $< ... >$ is an annihilator for the streaming term and $< v_{dx} >= 0$. Solving the bounce-averaged linear kinetic equation yields f_0. At second order in λ_t we find

$$v_{\|}\frac{\partial f_2}{\partial l} + v_{dx}\frac{\partial f_1}{\partial x} = C(f_1) + Q(f_1) + T(f_0) \tag{M.8}$$

We proceed to bounce average the second order kinetic equation to obtain

$$< v_{dx}\frac{\partial f_1}{\partial x} >=< (C(f_1) + Q(f_1)) > + < T(f_0) > \tag{M.9}$$

We now introduce the bounce-averaged radial flux in terms of the linear distribution function

$$\Gamma_x =< \int f_1 v_{dx} d^3v >= \int < f_1 v_{dx} > d^3v \tag{M.10}$$

We can pull the radial derivative out of the bounce-averaging operator in the second-order kinetic equation and make use of the property $\partial v_{dx}/\partial x = 0$ to obtain

$$\frac{\partial}{\partial x} < v_{dx} f_1 >=< (C(f_1) + Q(f_1) > + < T(f_0) > \tag{M.11}$$

The spatial derivative of the flux can therefore be written as

$$\frac{\partial}{\partial x}\Gamma_x = \int < (C(f_1) + Q(f_1) > d^3v + \int < T(f_0) > d^3v \tag{M.12}$$

We now integrate the flux derivative from $x = x^*$ to $+\infty$, assuming that $f(x = +\infty) = 0$. The flux is

$$\Gamma_x(x^*) = \int \int_{+\infty}^{x^*} < (C(f_1)+Q(f_1) > d^3v dx + \int \int_{+\infty}^{x^*} < T(f_0) > d^3v dx = \Gamma_{1x}(x^*)+\Gamma_{2x}(x^*) \tag{M.13}$$

The total flux is the sum of two separate fluxes, the flux $\Gamma_{1x}(x^*)$ stems from collisions and wave-particle velocity scattering, the other flux $\Gamma_{2x}(x^*)$ is due to spatial displacement caused by wave-particle interaction. The first flux requires knowledge of the linear distribution function obtained by solving the second order kinetic equation. The second flux can be estimated since it is a function of f_0, a much easier function to compute. We write the second flux fully as

$$\Gamma_{2x}(x^*) = \int \int_{+\infty}^{x^*} < T(f_0) > d^3v dx = - \int d^3v \int_{+\infty}^{x^*} \frac{< \delta x > \partial f_0}{\delta t} \frac{\partial f_0}{\partial x} dx \qquad \text{(M.14)}$$

where we made use of the fact that the bounce-averaging operator acts only the radial displacement. The spatial integral is trivially solved if we specialize to the case where $< \delta x >$ is only dependent on the localized resonance interaction position. The driven flux can therefore be written as

$$\Gamma_{2x}(x^*) = - \int d^3v \frac{< \delta x >}{\delta t} f_0 \qquad \text{(M.15)}$$

This is the expression for the flux used in this thesis to study the radial transport of minority ions due to banana-broadening.

Appendix N

Figures

List of parameters used in numerical calculations [22]

- toroidal magnetic field intensity B_0= 5 T
- electron thermal temperature $T_e \approx 3Kev$
- inverse aspect ratio $a/R_0 = \frac{1}{3}$
- majority ion density $n_i = 10^{21}m^{-3}$
- toroidal plasma current $I = 1MA$

List of Figures

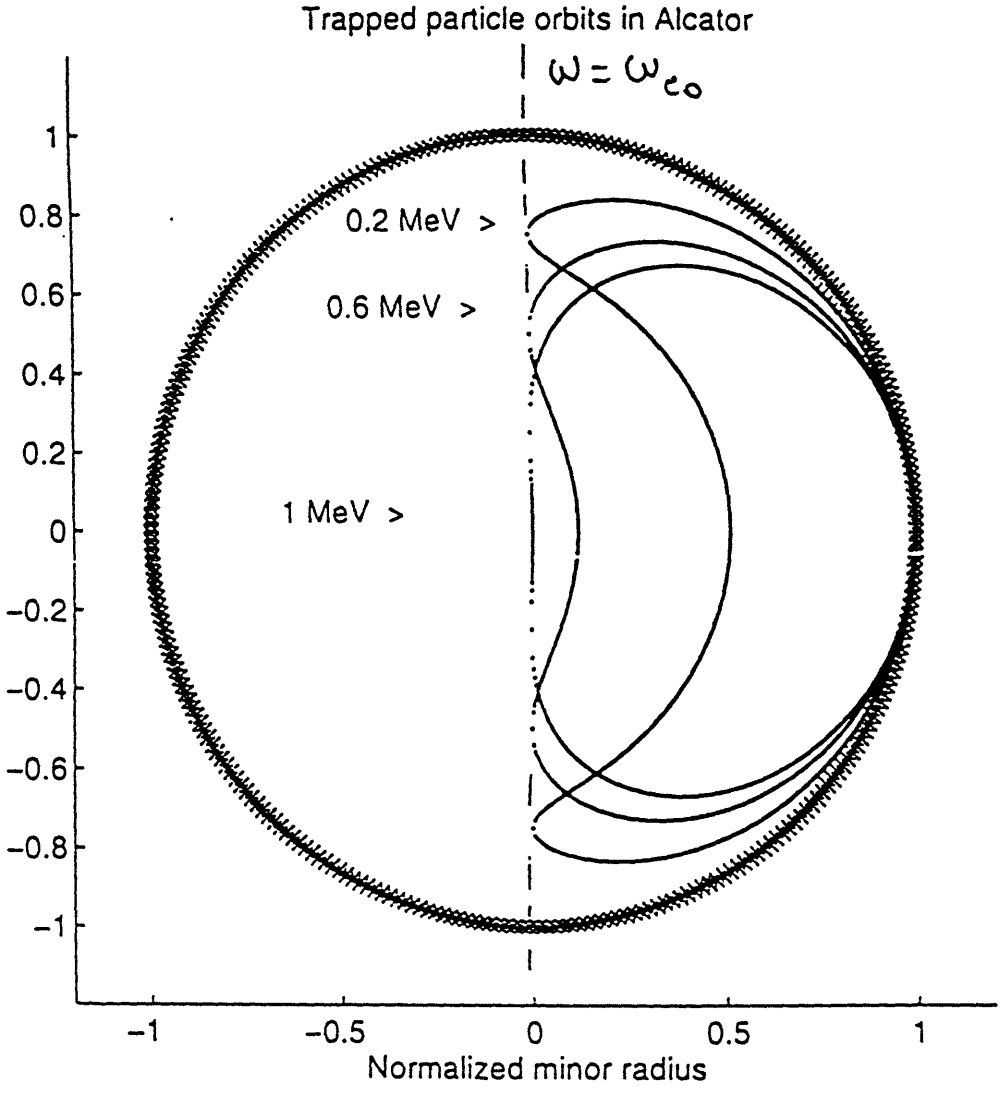

Figure (2.1): Barely confined particles orbit cross-sections for three different energies in a circular flux-surface tokamak. The orbits are computed for standard Alcator C-Mod parameters [22].

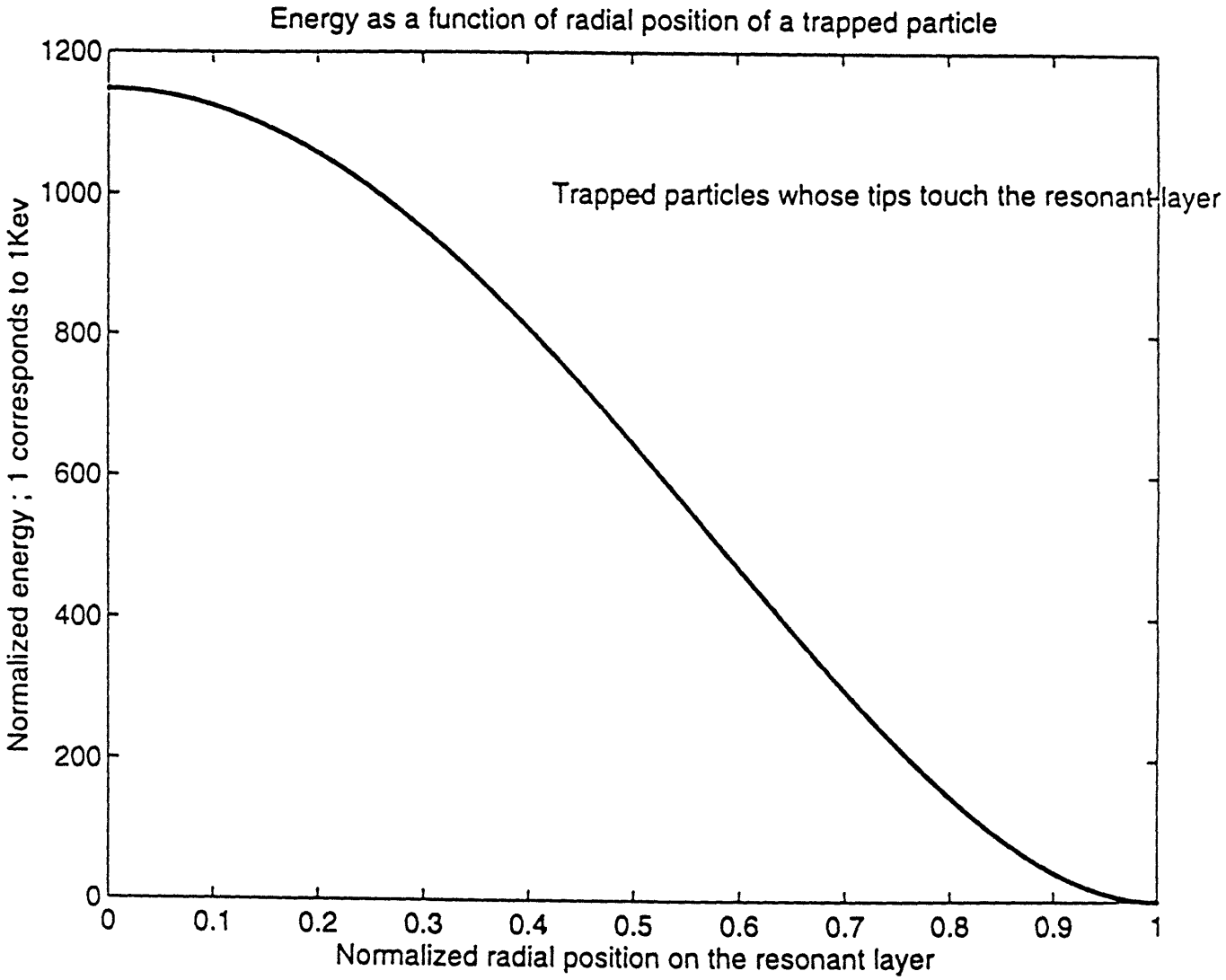

Figure (2.2): Barely confined trapped energy versus radial position of its banana tips for standard Alcator C-Mod parameters [22]. The energy is normalized to one KeV.

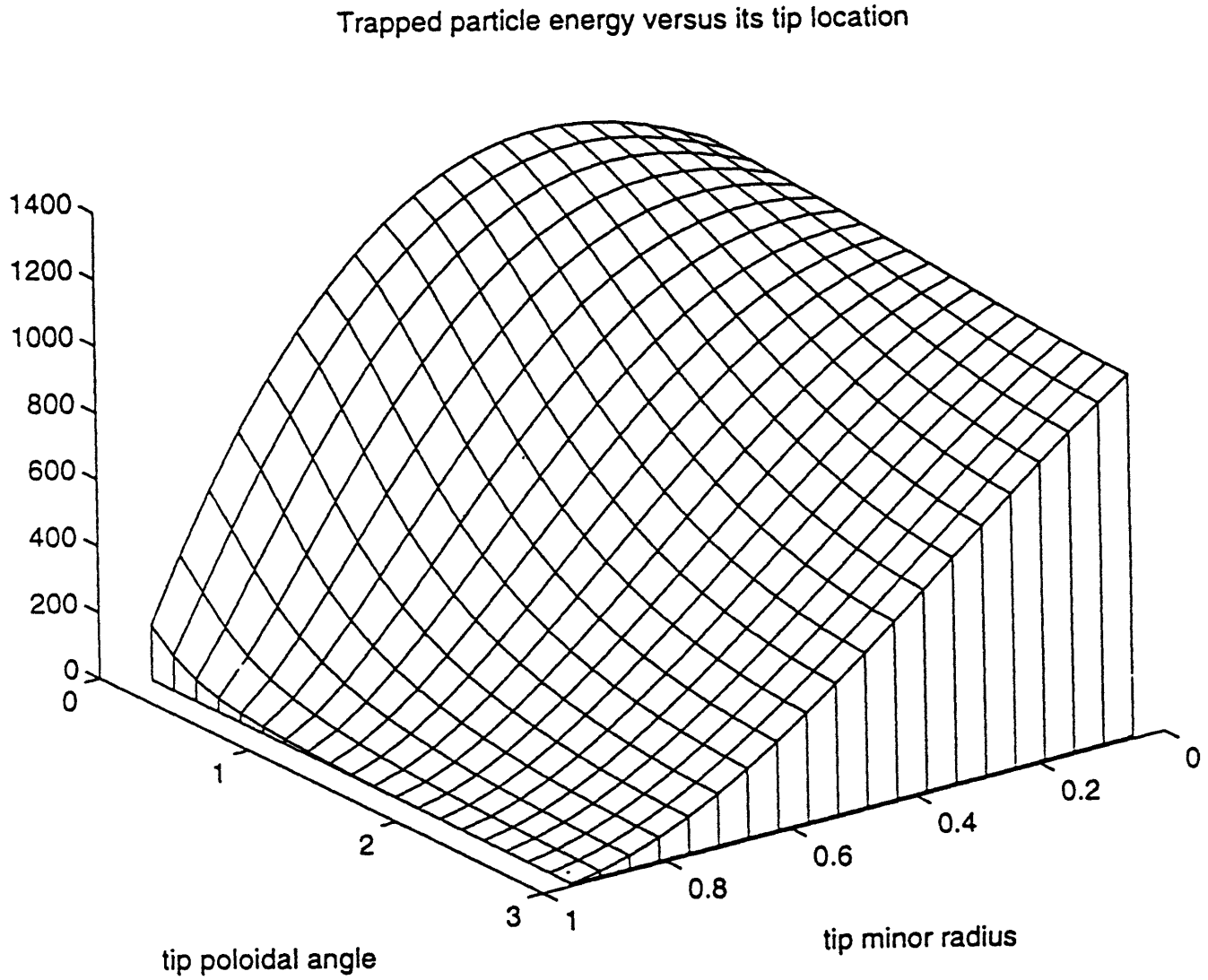

Figure (2.3): Barely confined trapped energy versus radial and poloidal-angle banana tip position for standard Alcator C-Mod parameters [22]. The energy is normalized to one KeV.

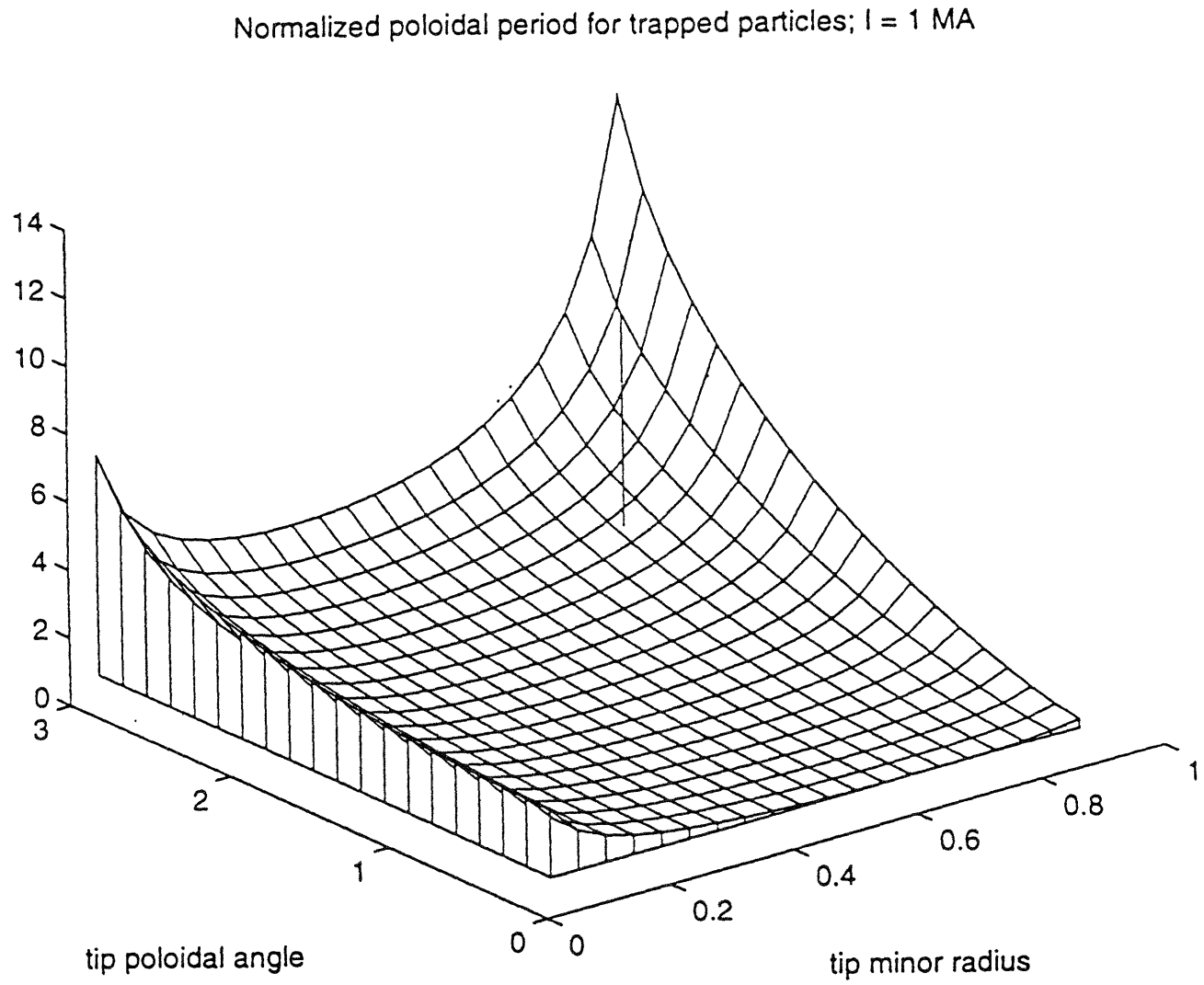

Figure (2.4): Trapped particle poloidal period normalized to $t_b = R_0/v_{th}$ versus radial and poloidal-angle banana tip position for standard Alcator C-Mod parameters [22].

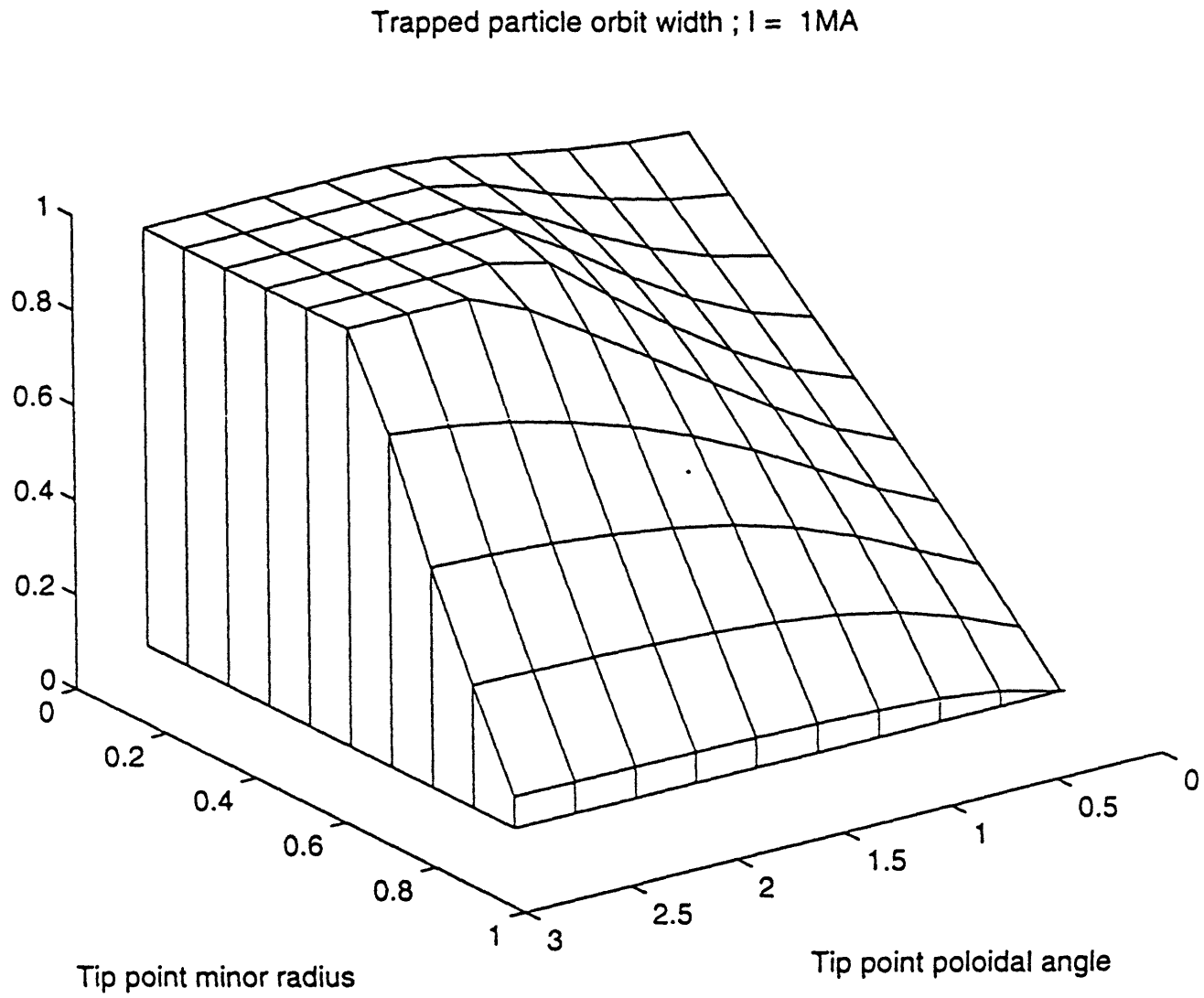

Figure (2.5): Barely confined trapped particle orbit width versus radial and poloidal-angle banana tip position for standard Alcator C-Mod parameters [22]. The width is normalized to the minor radius a.

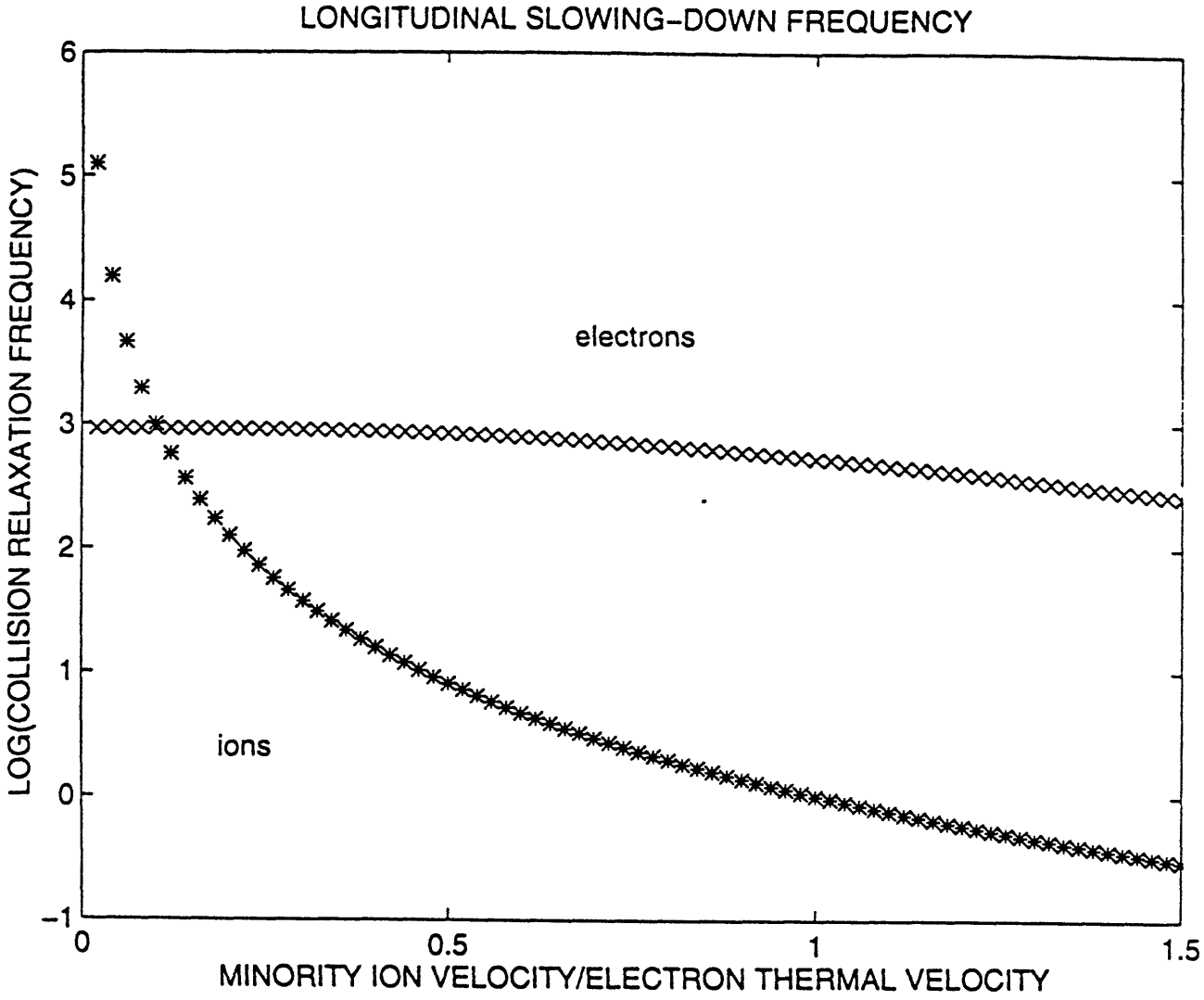

Figure (4.1): Longitudinal slowing-down ion-ion and ion-electron coefficients $< \Delta v_{\|} > /v(sec^{-1})$ as a function of the ratio ion tail velocity / electron thermal velocity for standard Alcator C-Mod parameters [22].

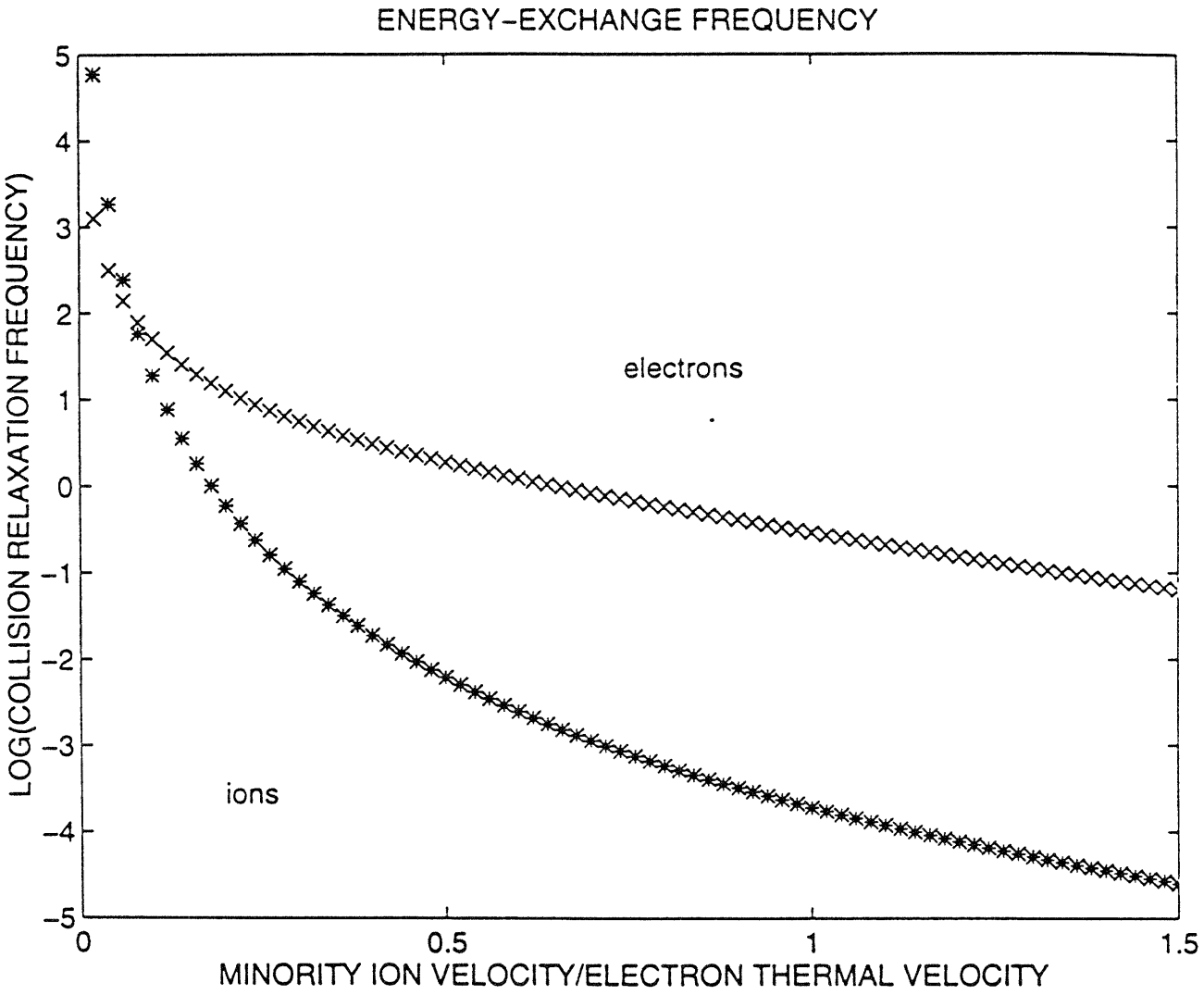

Figure (4.2): Energy-exchange ion-ion and ion-electron coefficients $< (\Delta v_{\|})^2 > /v^2(sec^{-1})$ as a function of the ratio ion tail velocity / electron thermal velocity for standard Alcator C-Mod parameters [22].

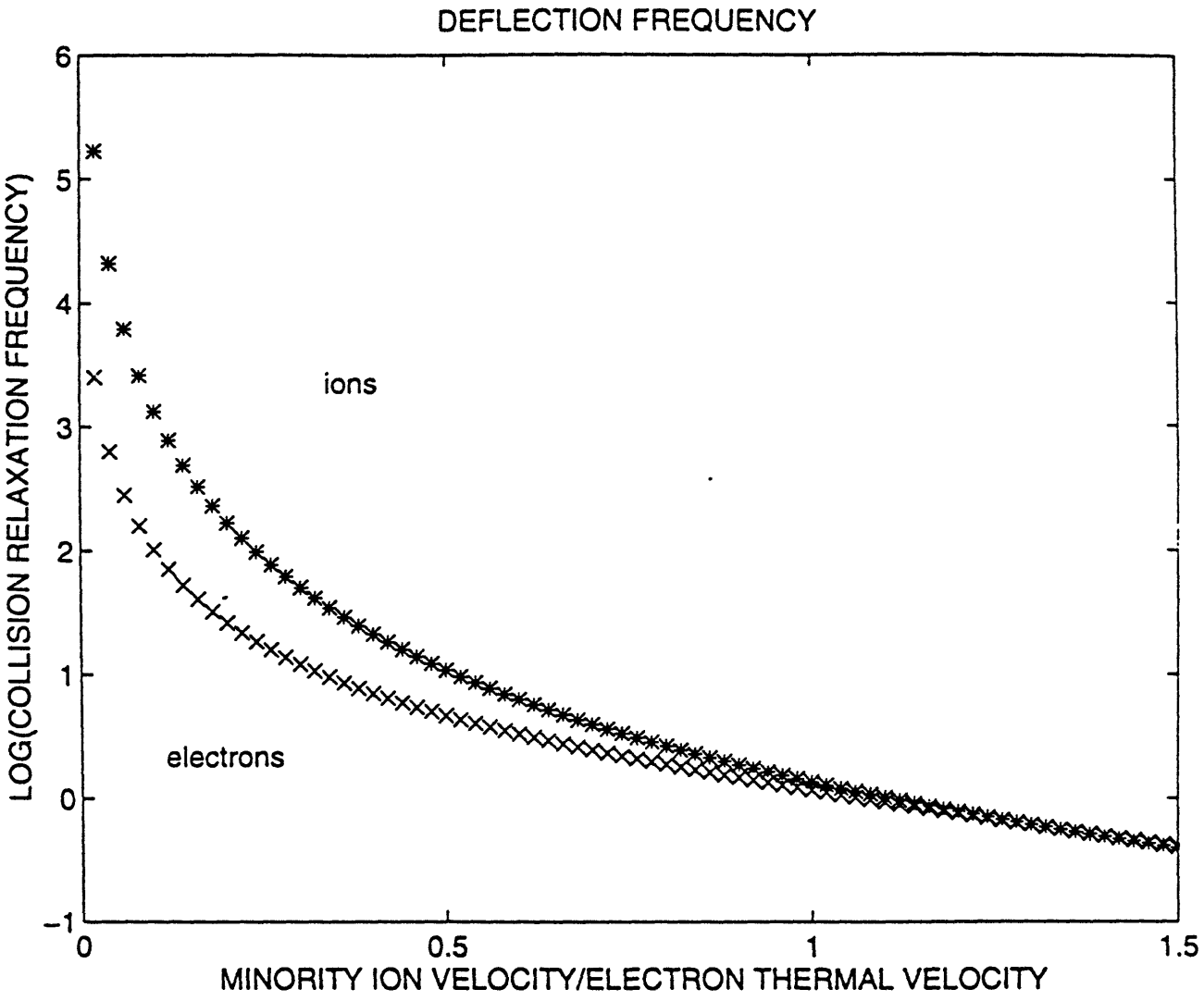

Figure (4.3): Ion-ion and ion-electron deflection rates $< \Delta v_{\perp}^2 > /v^2(sec^{-1})$ as a function of the ratio ion tail velocity / electron thermal velocity for standard Alcator C-Mod parameters [22].

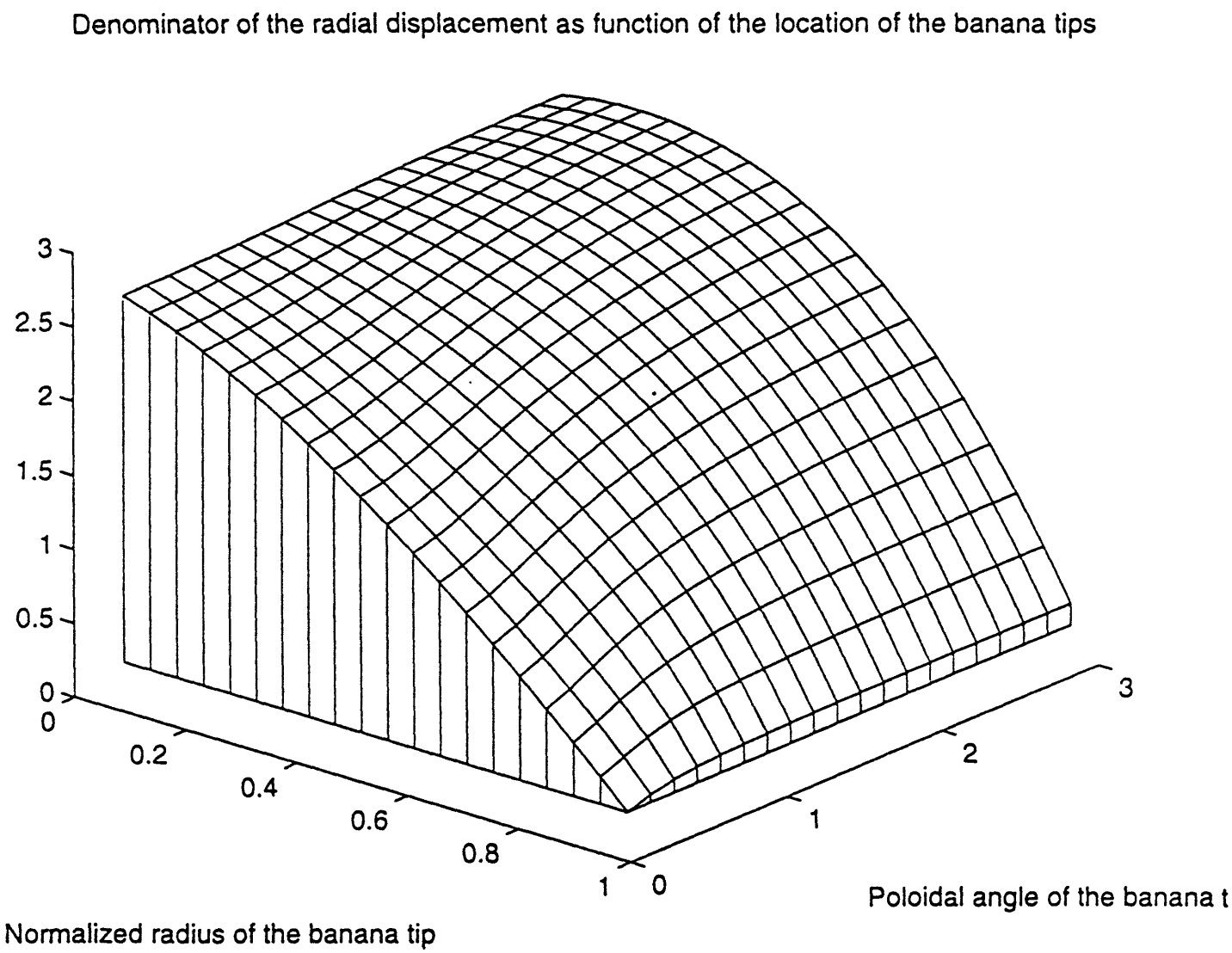

Figure (5.1): Denominator $D(x_0, \theta_0)$ of equation (5.18) as a function of the banana tip coordinates (x_0, θ_0) for $a/R_0 = 1/3$.

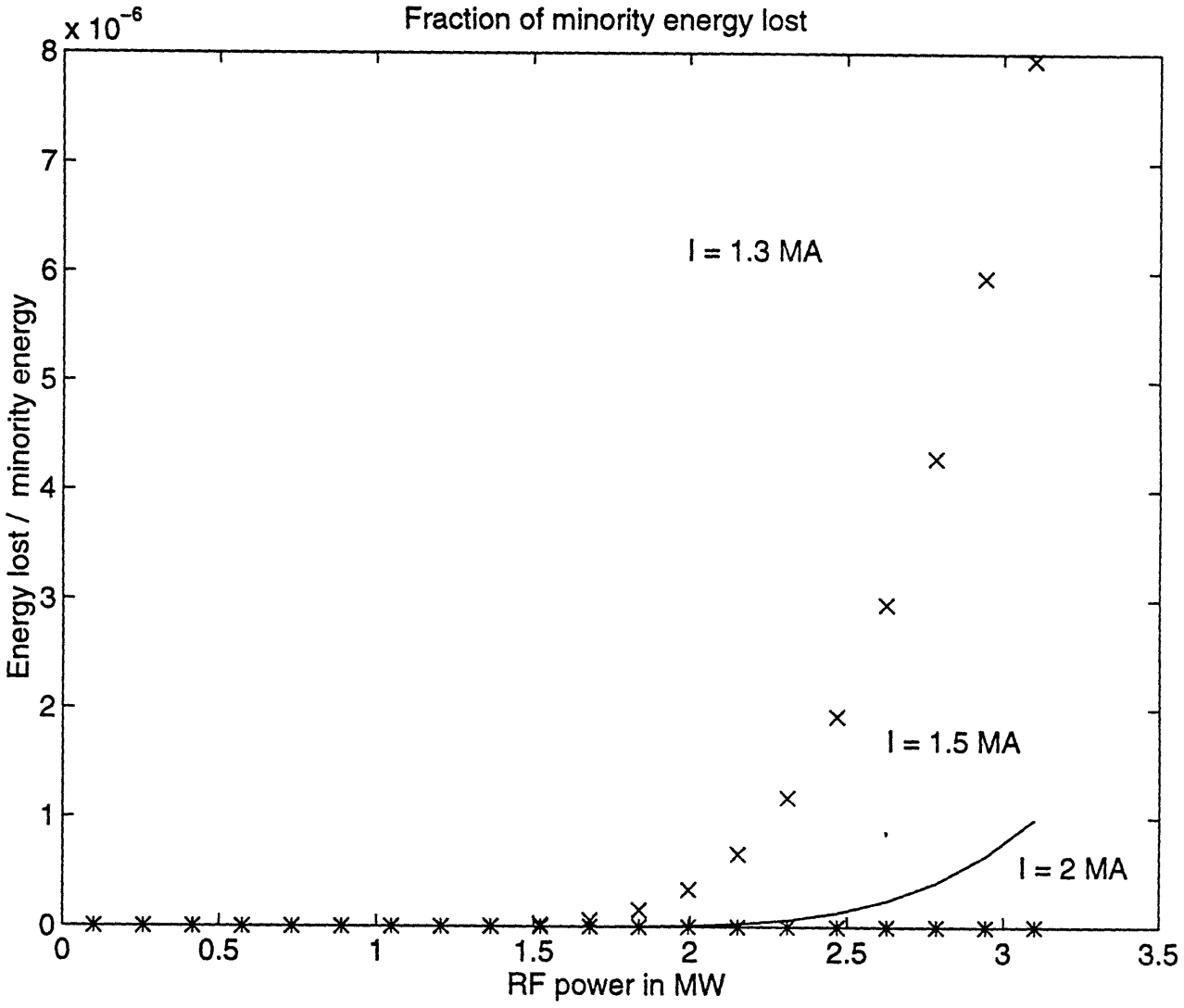

Figure (5.2): Ratio minority energy loss to the total energy of the minority species as a function of the total RF power for standard Alcator C-Mod parameters [22] and for three different values of the toroidal current.The full line refers to a toroidal current of 1.5 MA, the '*' line refers to a toroidal current of 2 MA and the 'x' line refers to a toroidal current of 1.3MA

Bibliography

[1] D.F.Start V.P.Bhatnagar, J.Jacquinot and B.J.P. Tubbing. High concentration minority ion cyclotron resonance heating in JET. *Nuclear Fusion*, 33:83+, 1993.

[2] G.Taylor *et alia.* Ion cyclotron range of frequencies heating on the tokamak fusion test reactor. *Physics of Plasmas*, 5:2437, 1993.

[3] Thomas S. Stix. Fast-wave heating of a two-component plasma. *Nuclear Fusion*, 15:737+, 1975.

[4] S.J. Buchsbaum. Resonance in a plasma with two ion species. *Physics of Fluids*, 3:418+, 1960.

[5] T.H.Stix. *Waves in Plasmas.* American Institute of Physics,NY, 1992.

[6] A.Bers and A.K.Ram. Lower-hybrid and fast alfven wave current drive: status of theory. Technical Report 3, Plasma Fusion Center,MIT, 1992.

[7] T.G.Northrop. *The Adiabatic Motion of Charged Particles.* Interscience, 1963.

[8] Morozov A. I. and L.S.Solovev. *Reviews of Plasma Physics*, volume 2. Consultants Bureau, 1963.

[9] Robert G. Littlejohn. Hamiltonian formulation of guiding center motion. *Physics of Fluids*, 24:1730+, 1981.

[10] Robert G. Littlejohn. Variational principles of guiding center motion. *Journal of Plasma Physics*, 29:111+, 1983.

[11] H.Goldstein. *Classical Mechanics.* Addison-Wesley,MA, 1959.

[12] Balescu R. *Transport Processes in Plasmas.* North-Holland, 1988.

[13] L.Chen, J.Vaclavik and G.W.Hammett. Ion radial transport induced by ICRF waves in tokamaks. *Nuclear Fusion*, 28:389+, 1988.

[14] Rome J. and Y-K.M.Peng. The topology of tokamak orbits. *Nuclear Fusion*, 19:1193+, 1979.

[15] R.B.White. *Theory of Tokamak Plasmas.* North-Holland, 1989.

[16] J.P. Freidberg. Ideal magneto hydrodynamic theory of magnetic fusion systems. *Review of Modern Physics*, 54:801+, 1982.

[17] J.P.Freidberg. *Ideal MagnetoHydroDynamics.* Plenum Press,NY, 1987.

[18] S.V.Putvinskii. *Alpha Particles in Tokamaks.* Reviews of Plasma Physics. Consultants Bureau, 1993.

[19] G.A.Cottrell and D.F.H. Start. A large-orbit model of fast ion slowing down during ICH : Comparison with JET data. *Nuclear Fusion*, 31:61+, 1991.

[20] R. Kaita *et alia.* Fast-ion orbit effects during ion cyclotron range of frequency experiments on the Princeton large torus. *Nuclear Fusion*, 23:1089+, 1983.

[21] Gregory W. Hammett. *Fast Ion Studies of Ion Cyclotron Heating in the PLT tokamak.* PhD thesis, Princeton University, 1986.

[22] I.H.Hutchinson *et alia.* First results from Alcator-CMOD. *Physics of Plasmas*, 1:1511, 1994.

[23] T.E.Stringer. Radial profile of Alpha-particle heating in a tokamak. *Plasma Physics*, 16:651+, 1973.

[24] F.Porcelli *et alia.* Solution of the drift-kinetic equation for global plasma modes and finite particle orbit widths. *Physics of Plasmas*, 1:470, 1994.

[25] V.L. Yakimenko. *Sov.Phys.JETP*, 17:1032, 1963.

[26] C.F. Kennel and F. Engelmann. Velocity space diffusion from weak plasma turbulence in a magnetic field. *Physics of Fluids*, 9:2377, 1966.

[27] Ira B. Bernstein and David C. Baxter. Relativistic theory of electron cyclotron resonance heating. *Physics of Fluids*, 27:2899+, 1984.

[28] Michael E. Mauel. Electron-cyclotron heating in a pulsed Mirror experiment. *Physics of Fluids*, 27:2899, 1984.

[29] G.D. Kerbel and M.G. McCoy. Kinetic theory and simulation of multi-species plasmas in tokamaks excited with electromagnetic waves in the ion-cyclotron range of frequencies. *Physics of Fluids*, 28:3629+, 1985.

[30] P.J. Catto and J.R.Myra. A quasilinear description for fast-wave minority heating permitting off-magnetic axis heating in a tokamak. *Physics of Fluids*, 4:187+, 1992.

[31] D.Anderson, M.Lisak and L.O. Pekkari. Electron-cyclotron heating in a pulsed mirror experiment. *Physics of Fluids*, 28:3590+, 1985.

[32] C.S.Chang,G.W.Hammett and R.J.Goldston. Neoclassical transport of energetic minority tail ions generated by ion-cyclotron resonance heating in tokamak geometry. *Physics of Fluids B*, 2:2383+, 1990.

[33] K.W. Whang and G.J. Morales. ICRF heating and its effect on single-particle confinement in tokamaks. *Nuclear Fusion*, 23:481+, 1983.

[34] T.Riyopoulos, T.Tajima, T.Hatori and D. Pfirsch. Diffusion induced by cyclotron resonance heating. *Nuclear Fusion*, 26:627+, 1986.

[35] W.G.F.Core. Wave induced ion transport in ICRH tokamak plasmas. *Nuclear Fusion*, 29:1101+, 1989.

[36] M.A. Kovanen. Monte Carlo study of high power (D)T ICRF heating in JET. *Nuclear Fusion*, 32:945, 1992.

[37] M.A. Kovanen, W.G.F. Core and T. Hellsten. Finite orbit effects in ICRF heated tokamak plasmas. *Nuclear Fusion*, 32:787, 1992.

[38] L.-G.Eriksson and P.Helander. Monte Carlo operators for orbit-averaged Fokker-Planck equations. *Physics of Plasmas*, 1:308, 1994.

[39] A.Becoulet, D.Fraboulet, G.Giruzzi,D.Moreau, and B.Saoutic. Hamiltonian analysis of fast wave current drive in tokamak plasmas. *Physics of Plasmas*, 1:2908, 1994.

[40] A.Becoulet, D.Gambier and A.Samain. Hamiltonian theory of the ion cylotron minority heating dynamics in tokamak plasmas. *Physics of Fluids*, 3:137, 1991.

[41] P.Helander and M.Lisak. The stochastic nature of ion-cyclotron-resonance wave-particle interaction in tokamaks. *Physics of Plasmas*, 4:1927, 1992.

[42] R.S.Sund and J.E.Scharer. Full wave field solutions and power conservation for the ion cyclotron range of frequencies (ICRF) in non uniform plasmas. *Physics of Fluids*, 3:1326, 1991.

[43] D.G.Swanson. Radio frequency heating in the ion-cyclotron range of frequencies. *Physics of Fluids*, 28:2645, 1985.

[44] R.C.Davidson. *Methods in Nonlinear Plasma Theory.* Academic Press,NY, 1972.

[45] F.Jaeger, A.J.Lichtenberg and M.A.Lieberman. Theory of electron cyclotron resonance heating part one.short time and adiabatic effects. *Plasma Physics*, 14:1073, 1972.

[46] S.C.Chiu and V.S.Chan. Neoclassical transport in the presence of RF fields. *Nuclear Fusion*, 29:1907+, 1989.

[47] M.Brambilla. Quasi-linear ion distribution function during ion cyclotron heating in tokamaks. *Nuclear Fusion*, 34:1121+, 1994.

[48] L.Spitzer. *Physics of Fully Ionized Gases.* Interscience, 1962.

[49] F.L. Hinton and R.D. Hazeltine. Theory of plasma transport in toroidal confinement systems. *Review of Modern Physics*, 48:239+, 1976.

[50] C.S.Chang and P.Colestock. Anisotropic distribution function of minority tail ions generated by strong ion-cyclotron resonance heating. *Physics of Fluids*, 2:310, 1990.

[51] D.Anderson, W.Core, L.-G.Erikkson, H.Hamnen,T.Hellsten, and M.Lisak. Distortion of ion velocity distributions in the presence of ICRH:a semi-analytical analysis. *Nuclear Fusion*, 27:911+, 1987.

[52] T.Morishita, A.Fukuyama, K.Hamamatsu, S.Itoh, and K.Itoh. Analysis of minority velocity distribution and power deposition profile in ICRF heating in a tokamak. *Nuclear Fusion*, 27:1291+, 1987.

[53] C.S.Chang. Radial diffusion of energetic tail ions driven by electromagnetic waves of ion-cyclotron range of frequencies in bumpy torus and tokamak geometry. *Physics of Fluids*, 28:3598, 1985.

[54] H.Weitzner. Geometry effects on ion heating at ion cyclotron frequencies. *Physics of Fluids*, 26:998, 1983.

[55] M.D.Carter *et alia.* Collisional effects on coherent nonlinear wave-particle interactions at cyclotron harmonics. *Physics of Fluids*, 29:100, 1986.

[56] J.D.Callen, J.P.Christiansen, J.G.Cordey, and K.Thomsen. Modelling of temperature profiles and transport scaling in auxiliary heated tokamaks. *Nuclear Fusion*, 27:1857+, 1987.

[57] J.Sheffield. The physics of magnetic fusion reactors. *Reviews of Modern Physics*, 66:1015+, 1994.

[58] R.J.Goldston, D.C.McCune, H.H.Towner, S.L.Davis, R.Hawryluk and G.L.Schmidt. New techniques for calculating heat and particle source rates due

to neutral beam injection in axisymmetric tokamaks. *Journal of Computational Physics*, 43:61+, 1981.